Cellular Senescence induced by RUNX1 and its Fusion Oncoprotein Derivatives as a Barrier to Leukaemogenesis

Gail Anderson

A thesis submitted for the degree of Doctor of Philosophy

UNIVERSITY
of
GLASGOW

Molecular Oncology Laboratory

The MRC Centre for Virus Research

School of Medical, Veterinary and Life Sciences

College of Life Sciences

University of Glasgow

June 2016

Figures and Tables

Acknowledgements

I would first like to thank Professor James Neil, my principle investigator for the opportunity to work on such an exciting project within his group and for his insight and expertise.

I would like to express my gratitude to my supervisor, Dr Anna Kilbey, not only for her expertise and support, but for her patience, melt-down management and pep-talks throughout the completion of this project and thesis.

My thanks also go to Dr Kathryn Gilroy, for help with array analysis and statistics, to Nancy Mackay for imparting her cloning expertise and to Anne Terry and all other past and present members of the Molecular Oncology group for technical advice and encyclopaedic knowledge! A special mention goes to my office-mates, Dr Gillian Borland and Dr Jodie Hay, for friendship, support and top-notch proof-reading abilities (along with biscuits, sweets and the occasional dinner!).

For helpful discussions, advice and thorough assessments, I would like to thank my assessors, Professor Peter Adams and Dr Julia Edgar. Special thanks also go to Dr John Van Tuyn, Dr Dong-Er Zhang and Dr Elizabeth Sloan who kindly gifted plasmids and cells for use in this study.

I would also like to the friends and colleagues I have met during my time at the CVR, especially Professor Iain Morgan, Professor Roger Everett, Dr Mary Donaldson and Dr Delphine Cuchet who encouraged me in my studies.

To my friends and family, I want to thank you for putting up with my eternal student-hood (I will go and get a job now). Special thanks go to Steph, Adele and Katie for always being on my side and cheering me on when I needed it the most.

I would also like to thank my Gran, Helen Smith, for her enthusiastic cheerleading and for always being pleased to see me, even if it has been a bit sporadic.

To Ross, thank you for putting up with me and for loving and encouraging me when even I had grown quite tired of myself.

To my sister, Gillian, thank you for being fierce, generous, loving and hard-working. And thank you to my lovely Mum and Dad for raising me in a liberal, opinionated and affectionate home and for working to give me incredible opportunities.

I would like to dedicate my thesis to my lovely Uncle Gillies who helped me along the way but couldn't be here at the end.

Author's Declaration

I declare that, except where explicit reference is made to the contribution of others, that this thesis is the result of my own work and has not been submitted for any other degree at the University of Glasgow or any other institution.

Gail Anderson

June 2016

Abstract

This thesis explores the ability of RUNX1 and its fusion oncoprotein derivatives to induce senescence-like growth arrest (SLGA) in primary cell cultures. While this phenomenon resembles replicative senescence seen in normal diploid human fibroblasts after extensive passage, it does not involve telomere attrition. From previous studies in the host laboratory it can also be distinguished from Ras oncogene-induced senescence (OIS) as it does not appear to depend on a DNA damage response secondary to hyper-proliferation.

Despite these differences, this study supports the hypothesis that RUNX SLGA is an anti-cancer fail-safe which protects cells against oncogenic transformation. In favour of the fail-safe model, two out of the three RUNX1 fusion oncoproteins examined fail to induce SLGA in a well characterised human fibroblast cell system (Hs68). In the case of TEL-RUNX1 (TR), a fusion which is associated with around 25% of childhood B-cell acute lymphoblastic leukaemias, loss of SLGA activity is due to N—terminal fusion to TEL. SLGA activity is regained by deletion of the HLH dimerisation domain in TEL or by introduction of a single amino acid mutation (K99R). The other major RUNX1 fusion oncoprotein, RUNX1-ETO (RE) which is commonly observed in M2 subtype acute myeloid leukaemia (AML), induces a potent SLGA. However, the RE phenotype differs from that of RUNX1, as RE strongly induces reactive oxygen species (ROS) and a pronounced senescence-associated secretory phenotype (SASP). In human AML, RE is co-expressed with a truncated variant generated by alternative splicing (RE9a), which has been shown to be much more potently leukaemogenic in animal models. This study demonstrates that RE9a also fails to induce SLGA and induces a markedly attenuated SASP. RE is generated by fusion of the N-terminal moiety of RUNX1 to the ETO C-terminus that encompasses a series of repressive nervy homology regions (NHRs), three of which are missing from RE9a. The effect of deleting or mutating NHRs from RE was also examined and show that loss of both NHR3 and NHR4 is necessary for complete ablation of RE SLGA. It was also demonstrated that aspects of RUNX1-induced SLGA are dissociable as, for example, the RUNX1P2 isoform induces profound growth arrest but only a minimal SASP.

This study supports the hypothesis that RUNX1-induced SLGA must be overcome to allow oncogenic transformation, either by intrinsic inactivation (TR, RE9a) or by co-operating mutations (RUNX1, RE). Notably, loss of sensitivity to RUNX1-induced SLGA appears to correlate with mutational loss of $p16^{INK4A}$, and it was shown that growth of the human leukaemia cell line REH is stimulated rather than repressed by the TR K99R mutant. The possibility that the RE-induced SASP has pro-oncogenic effects through effects on cell survival or on bystander cells is also discussed.

Abbreviations

AKAP – A-Kinase Anchoring Proteins

ALL – Acute Lymphoblastic Leukaemia

AML – Acute Myeloid Leukaemia

ATM – Ataxia Telangiectasia Mutated

ATR – Ataxia Telangiectasia and Rad3-related

BCA – Bicinchoninic Acid

BSA – Bovine Serum Albumin

CBF – Core-binding factor

C/EBPß - CCAAT-enhancer-binding protein beta

CDK – Cyclin-Dependent Kinase

CHK2 – Checkpoint kinase 2

CKI – Cyclin-dependent kinase inhibitor

DCFDA - 2',7' –dichlorofluorescin diacetate

DDR – DNA Damage Response

DS – Down's Syndrome

ETO – Eight Twenty-One protein

FCS – Foetal Calf Serum

GLB – Guanidinium Lysis Buffer

GLB1 – Galactosidase, beta 1

HDAC – Histone deacetylase

HF – Human Fibroblasts

HLH – Helix-Loop-Helix

HPV – Human Papillomavirus

HSC – Haematopoietic Stem Cell

hTERT – human Telomerase Reverse Transcriptase

MAPK – Mitogen-Activated Protein Kinase

MDS – Myelodysplastic syndrome

MEF – Murine Embryonic Fibroblast

MKP – MAPK Phosphatase

MLV – Murine Leukaemia Virus

MOI – Multiplicity of Infection

MSK – Mitogen and stress-activated protein kinase

MYND – Myeloid-Nervy-DEAF

NBS1 - Nibrin

NCoR – Nuclear Co-repressor Complex

NFκB - nuclear factor kappa-light-chain-enhancer of activated B cells

NHR – Nervy Homology Region

NK – Natural-killer cells

OIS – Oncogene-Induced Senescence

ORI – Origin of Replication

PCD – Programmed Cell Death

PKCD – Protein Kinase C Delta

PKD1 – Protein Kinase D1

Rb – Retinoblastoma Protein

RE – RUNX1-ETO

RHD – Runt Homology Domain

RIPA – Radioimmunoprecipitation assay

ROS – Reactive Oxygen Species

SA-ß-Gal – Senescence-Associated ß-Galactosidase

SASP – Senescence-Associated Secretory Phenotype

SLGA – Senescence-Like Growth Arrest

SUMO – Small Ubiquitin-like Modifier

SV40 – Simian Virus 40

TAD – Transactivation Domain

TAO – Thousand and one amino acid kinase

TID – Trans-Inhibitory Domain

TLE – Transducin-Like Enhancer of Split

TR – TEL-RUNX1

WCL – Whole-cell lysis

1 Introduction

1.1. RUNX Transcription Factor Family

The RUNX family of transcription factors are closely related to the *Drosophila runt* gene which regulates segmentation, sex determination and some aspects of neurogenesis during *Drosophila* embryogenesis. While *Drosophila* have one *runt* gene, duplication events have resulted in the presence of three conserved mammalian RUNX genes, *RUNX1*, *RUNX2* and *RUNX3* which are located on human chromosomes 21, 6 and 1 respectively [1, 2]. The expression of RUNX proteins is subject to tight regulation meaning that they are only expressed in certain tissues at specific times during development. The three RUNX family members display significant homology and are expressed from two distinct promoters, the P1 or distal promoter and the P2 or proximal promoter, resulting in isoforms of RUNX with distinct N-terminal sequences [3].

The RUNX proteins retain a highly conserved Runt homology domain (RHD) which is a 128 amino acid motif that is essential for the formation of a functional heterodimer with core-binding factor-beta (CBFß), the non-DNA-binding partner of RUNX. The RUNX-CBFß interaction is required to increase the affinity of RUNX for DNA and is essential for the function of RUNX as a transcription factor [1, 2]. Additionally, the RHD is required for DNA binding, ATP binding and nuclear localisation of RUNX [4]. Other regions of the RUNX proteins that display sequence homology are the transactivation/inhibitory domains towards the C-terminal portion of the protein which enable RUNX proteins to execute context-dependent transcriptional activation or repression (**Figure 1.1**).

Figure 1.1 RUNX1 and its functional domains
Schematic representation of the RUNX1 protein indicating its functional domains. The RUNT Homology Domains (RHD) is represented in red and is required for interaction with the RUNX co-factor, CBFß and DNA binding. The Transactivation Domain (TAD) is orange and functions to recruit co-activator complexes to promote transcriptional activation by RUNX1. The Trans-Inhibitory Domain (TID) is green and is required for RUNX1-mediated transcriptional repression through the recruitment of co-repressor complexes. The C-terminal VWRPY domain is represented in brown and is required for CD4 repression during thymocyte development.

The RUNX transcription factors play essential roles in development evidenced by the severe phenotypes associated with their functional disruption. RUNX1 is required for normal definitive haematopoiesis and is often mutated in human leukaemia. Additionally, hemizygosity for *RUNX1* results in a characteristic myeloproliferative disorder with increased risk of acute myeloid leukaemia (AML) [5, 6]. RUNX2 is essential for osteogenesis and hemizygosity for RUNX2 results in cleidocranial dysplasia, a disorder affecting the bones and cartilage [7]. The precise function of RUNX3 is less well characterised but evidence supports a role in aspects of neurogenesis and development of the gastroinstestinal tract and *RUNX3* has been found to be epigenetically silenced in some gastric cancers [7-9].

1.2 RUNX1 Isoforms

RUNX1 expression is controlled by two promoters, the P1 (proximal) promoter and the P2 (distal) promoter separated by approximately 160kb [3]. There are three major isoforms of RUNX1, denoted in the previous nomenclature system as AML1a, AML1b and AML1c [10]. AML1c is transcribed from the P1 or MASDS promoter and will be referred to from this point as RUNX1P1. AML1b is transcribed from the P2 or MRIPV promoter and will be referred to as RUNX1P2. AML1a is also transcribed from the P2 promoter but alternative splicing generates a C-terminally truncated protein lacking the RUNX1 transactivation domain that has the potential to inhibit the activity of full-length RUNX1P2 [11]. RUNX1P1 encodes a 32 amino acid sequence at its N-terminus which is replaced by 5 amino acids in RUNX1P2. The different RUNX1 N-termini may result in altered transcription factor activity by RUNX1P1 and RUNX1P2. RUNX1 binds to the DNA sequence TGTGGNNN (NNN= TTT or TCA) [12-15] where it acts as a context-dependent transcriptional regulator through recruitment of co-activator or co-repressor complexes to the C-terminal trans-activation domain TAD or trans-inhibitory domain (TID) [16, 17].

1.3 Transcriptional Regulation

1.3.1 Transcriptional Activation

RUNX1 is a transactivator of gene expression, including genes required for haematopoiesis. It is a relatively inefficient transcriptional activator in its own

right and commonly cooperates with other transcription factors such as Ets family members that bind adjacent sequence specific recognition sites in RUNX1-dependent gene promoters [18-23]. In addition, the C-terminal TAD recruits co-activators. These include the Aly/LEF1 complex which cooperates with RUNX1 for transcriptional activation of the major histocompatibility complex in T-cells [24] and p300/CREB-binding protein (CBP) that is required for RUNX1 mediated myeloid specific gene expression [25]. Co-activators do not bind to DNA but recruit transcription initiation complexes or modify histones to enable transcriptional activation by RUNX1. RUNX1 transcriptional activity is also modified by post-translational regulation. Examples include GATA-1-associated cyclin-dependent-kinase (CDK) phosphorylation of RUNX1 to directly promote RUNX1 transactivation [23] and protein arginine methyltransferase (PMRT) methylation of arginines 206 and 210 to abrogate recruitment of the mSin3A co-repressor and thereby indirectly activate RUNX1 transactivation [26].

1.3.2 Transcriptional Repression

RUNX1 encodes a TID toward the C-terminus of the protein which directs RUNX1 transcriptional repression through direct recruitment of corepressors such as the histone methyltransferases mSin3A and SUV39H1, and indirect recruitment of histone deacetylases (HDACs) via nuclear hormone co-repressor (NCoR) complexes [27-29]. Although RUNX1 trans-repression is largely attributed to the TID, it can also recruit the transducin-like enhancer of Split (TLE) co-repressor to a conserved VWRPY motif at the extreme C-terminus of the protein [30]. While the VWRPY motif is not required for definitive haematopoiesis, it is critical for efficient repression of CD4 during thymocyte development [31]. TLE recruitment of HDACs enhances the trans-repressor activity of RUNX1 [32].

1.4 RUNX1 and Haematopoiesis

A critical role for RUNX1 in foetal haematopoiesis was implicated in Runx1$^{-/-}$ mouse embryos that die at E11.5-12.5 due to a complete lack of definitive haematopoietic progenitors in the foetal liver and yolk sac and severe haemorrhage [33, 34]. The RUNX1$^{-/-}$ phenotype significantly overlaps with that of CBFβ$^{-/-}$, consistent with a cooperative role for RUNX1/CBFβ in normal haematopoiesis [35-37].

It has been reported that RUNX1P2 is expressed in early haematopoietic stem and progenitor cells (HSPC) and colony-forming units while RUNX1P1 expression is delayed and restricted to definitive colonies. Depletion of the RUNX1P2 isoform, however, was also shown to uniquely oppose definitive haematopoiesis suggesting that RUNX1P1 and RUNX1P2 play critical but non-redundant roles. Mouse models broadly support this conclusion with embryonic survival maintained despite loss of RUNX1P1. However, loss of RUNX1P2 proved to be more catastrophic with pups dying shortly after birth. Loss of RUNX1P1 was associated with perturbations to the white blood cell and platelet counts and increased numbers of multipotent progenitors and $Lin^{-}Sca^{+}c\text{-}Kit^{+}$ haematopoietic stem cell (HSC) populations but the pups still survived. Furthermore a single allele of *RUNX1P2* but not *RUNX1P1* was sufficient to rescue the *RUNX1*-null embryonic lethal phenotype; these data suggest that normal haematopoietic development during embryogenesis is more dependent on the RUNX1P2 isoform than RUNX1P1 [38].

The role of RUNX1 in adult haematopoiesis appears to be less critical. Conditional knock out mouse models revealed that loss of RUNX1 during adult haematopoiesis did not negatively affect haematopoietic progenitors. Indeed, RUNX1-null adult haematopoietic progenitor cells exhibited a growth advantage [39]. However, RUNX1 has also been reported to play a significant role in adult megakaryocyte maturation as well as for T- and B-lymphocyte differentiation in mouse models supporting a critical function for RUNX1 in specific maturation pathways in adult tissue [40].

1.5 Acute Myeloid Leaukaemia and Acute Lymphoblastic Leukaemia

Mutations and translocations affecting RUNX1 are frequently observed in human leukaemias [41]. Leukaemia describes a group of cancers that typically form in the bone marrow and can be characterised by a marked increase in the number of abnormal blood cells. Statistics released by Cancer Research UK (Cancer research UK, http://www.cancerresearchuk.org/health-professional/cancer-statistics/statistics-by-cancer-type/leukaemia, Accessed 02/11/2016) state that in 2013 there were 9,301 new reported cases of leukaemia in the UK causing over 4,500 deaths making it the 11^{th} most common type of cancer in the UK.

Leukaemias can be largely classified as myeloid or lymphoid, according to the cell type affected. Lymphoid leukaemias affect common lymphoid progenitors which go on to form mature lymphocytes [42, 43] while myeloid leukaemias affect common myeloid progenitors which are precursors to red blood cells, platelets and some types of white blood cells [44, 45]. Leukaemias can be further classified as chronic or acute, leading to the identification of four major subtypes of leukaemia; Acute Myeloid Leukaemia (AML), Acute Lymphoid Leukaemia (ALL), Chronic Myeloid Leukaemia (CML) and Chronic Lymphoid Leukaemia (CLL). Chronic leukaemias demonstrate a long-term accumulation of a more mature population of abnormal blood cells(https://bloodwise.org.uk/chronic-myeloid-leukaemia-cml/understanding-cml and https://bloodwise.org.uk/chronic-lymphocytic-leukaemia-cll/understanding-cll Accessed 06/11/2016). while acute leukaemias are identified by a rapid expansion of immature blood cells which compromise the ability of the bone marrow to continue to produce normal blood cells (https://bloodwise.org.uk/acute-myeloid-leukaemia-adult-aml/understanding-acute-myeloid-leukaemia-aml and https://bloodwise.org.uk/acute-lymphoblastic-leukaemia-adult-all/understanding-acute-lymphoblastic-leukaemia-all, Accessed 25/11/2016).

This study focuses on the RUNX1-derived fusion oncoproteins, RUNX1ETO and TEL-RUNX1 that are associated with Acute Myeloid Leukaemia (AML) and Acute Lymphoblastic Leukaemia (ALL) respectively. Acute leukaemias are characterised by a rapid replacement of normal bone marrow with leukaemic cells resulting in increased susceptibility to infections, fatigue, bruising and flu-like symptoms. Without the appropriate treatment, they progress aggressively with death occurring within weeks or months.

AML accounts for approximately 35% of leukaemia cases in the UK (Cancer Research UK, http://www.cancerresearchuk.org/health-professional/cancer-statistics/statistics-by-cancer-type/leukaemia-aml, accessed 02/11/2016) and affects myeloblastic cells which are precursors to mature myeloid cells. AML is preceded by a pre-leukaemic state where myeloblasts accumulate mutations which compromises their ability to differentiate into mature myeloid white blood cells and freezes affected cells in an immature proliferative state. This alone does not constitute AML but renders affected cells vulnerable to additional mutations that are required to promote the full leukaemic state. ALL represents

approximately 1% of leukaemia cases in the UK (Cancer Research UK, http://www.cancerresearchuk.org/health-professional/cancer-statistics/statistics-by-cancer-type/leukaemia-all/incidence#ref-0, Accessed 02/11/2016). Like AML, it results in a proliferating population of immature cells but in this case lymphoblastic rather than myeloblastic cells represent the cell of origin

Risk factors for AML and ALL include chromosomal translocations and abnormalities such as chromosomal inversions, deletions and translocations [46]. Common chromosomal abnormalities identified in AML include the t(8;21) translocation (RUNX1-ETO) [47-49], inv(16) inversion (CBFβ/MYH11) [49, 50] and deletions affecting chromosomes 5 and 7 [51]. The chromosomal translocation that is most commonly associated with ALL is the t(12;21) translocation (TEL-RUNX1) [49, 52, 53]. Other risk factors include genetic conditions such as Down's Syndrome which is associated with increased incidence of leukaemia [54] and exposure to radiation and chemicals which include drugs used in anti-cancer therapies.

Treatment of acute leukaemia has two phases of chemotherapy known as the Remission Induction and Consolidation phases. The Induction phase comprises a period of treatment with a cytotoxic agent such as cytarabine, followed by treatment with an anthracycline such as daunorubicin. This phase of treatment is designed to aggressively clear leukaemic cells and increase the chance of a complete remission [55, 56]. The Consolidation phase is designed to eliminate any potential remaining leukaemic cells and reduce the risk of relapse. This phase may consist of courses of chemotherapy or a haematopoietic stem cell transplant. Although the treatment of AML and ALL is designed to minimise the risk of relapse, patients who do relapse frequently display leukaemias that are refractory to traditional treatments. In the case of relapsed leukaemias, the only available treatment is a haematopoietic stem cell transplant or alternatively patients may participate in a clinical trial.

1.6 RUNX1 and Leukaemia

RUNX1 exhibits dual oncogenic and tumour suppressor functions in cancer development [6, 57-61]. All three RUNX genes were initially identified as

insertional targets for murine leukaemia virus (MLV) in a transgenic Myc model of murine T-cell lymphoma [57, 58]. More recently, recurrent copy number alterations involving the 21q22 amplicon encoding *RUNX1* have been observed in patients with acute lymphoblastic leukaemia (ALL). Increased expression of RUNX1 co-segregated with poorer prognosis and a higher chance of relapse [62, 63]. Furthermore, individuals with Down's syndrome (DS) were reported to display a significantly increased risk of developing acute myeloid leukaemia (AML), ALL and myeloproliferative diseases before the age of 5 compared to the general population and also possess an extra copy of chromosome 21 where *RUNX1* resides. To formally test whether increased expression of non-mutated RUNX1 was responsible in these patients, retroviral acceleration of leukaemogenesis was compared in mice possessing 2 or 3 copies of *Runx1*. In every case, mice overexpressing Runx1 displayed a faster onset of leukaemia compared to littermate controls, supporting the suggestion that increased dosage of RUNX1 plays a significant role in onset of DS-related leukaemia [64].

In contrast to ALL, the role of RUNX1 in certain myeloid and T-cell tumours appears more tumour suppressive with loss of function mutations observed in myeloproliferative disorders with increased risk of AML [65, 66]. Furthermore, RUNX1 loss of function mutations are frequently observed in T-cell precursor ALL and have been associated with poor disease outcome [67-69].

1.7 RUNX1 Leukaemogenic Fusion Proteins

RUNX1 is a frequent target of chromosomal translocations associated with human leukaemia. Approximately 30 partner chromosomes have been identified in fusion with *RUNX1*. The two translocations most frequently observed in leukaemia are t(8;21) resulting in the RUNX1-ETO (RE) fusion and t(12;21) encoding the TEL-RUNX1 protein (**Figure 1.2**).

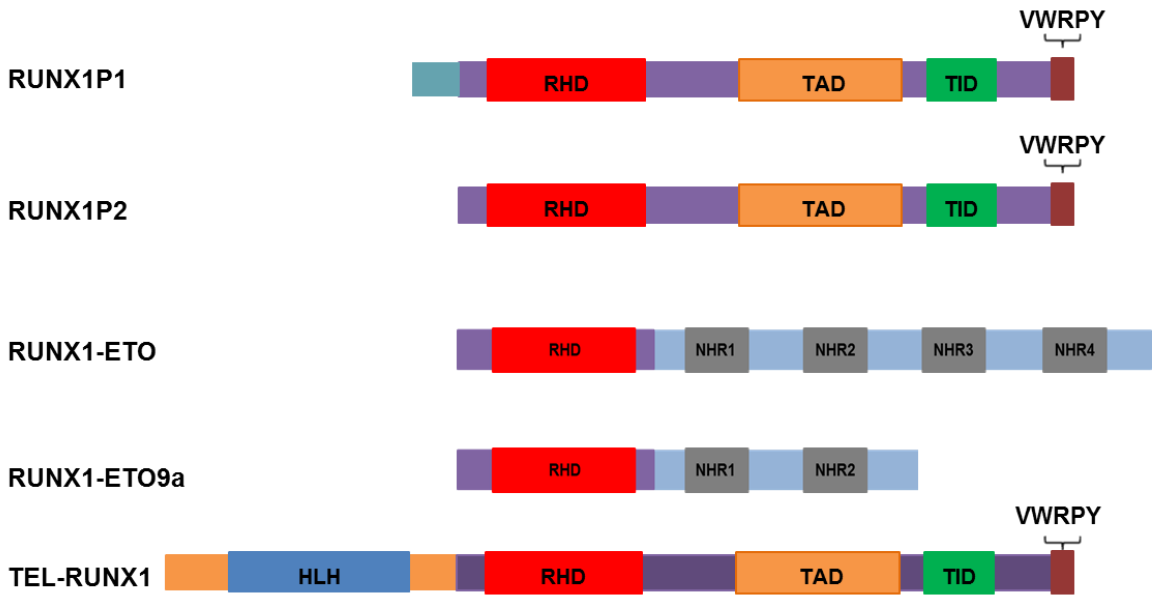

Figure 1.2 RUNX1 isoforms and their fusion derivatives.
Schematic representation of RUNX1P1, RUNX1P2, RE, RE9a and TEL-RUNX1 proteins. RUNX1P1 is approximately 32 amino-acids longer than RUNX1P2 (Turquoise) and is transcribed from the distal promoter. RUNX1P2 is transcribed from the proximal promoter. The t(8;21) chromosomal translocation results in expression of the RUNX1-ETO (RE) fusion protein. The RHD of RUNX1 is fused to four nervy homology regions (NHR) of ETO which are represented in grey. RE9a is a C-terminally truncated splice variant of RE which lacks NHR3 and NHR4. The t(12;21) translocation results in the TEL-RUNX1 fusion protein which retains most of the RUNX1P1 protein sequence and gains the HLH domain of TEL which is depicted in blue.

1.7.1 RUNX1-ETO (t(8;21))

The t(8;21) translocation was the first chromosomal translocation identified in AML [47, 48] and is associated with approximately 40% of M2 subtype AML [49]. The RE fusion protein results from the fusion of exons 1-5 of *RUNX1* to exons 2-11 of the *Eight-Twenty-One* (ETO) gene and has been described as a transcriptional repressor [70].

RE knock-in mice display an embryonic lethal phenotype identical to that observed in RUNX1 knock-out mice [71, 72] suggesting that RE functions as a dominant-negative regulator of RUNX1. Transient transfection assays support this prediction demonstrating that RE can antagonise transactivation by RUNX1 [73, 74]. A direct comparison of RE and RUNX1-mediated gene transcription in 3T3 fibroblasts confirmed that a proportion of RUNX1-upregulated targets were opposed by RE but also revealed a population of RUNX1-repressed genes that were markedly derepressed suggesting that RE may possess additional functions such as disruption of RUNX1-recruited co-repressor complexes [75]. Several RE

transgenic mouse models have been developed to avoid embryonic lethality. In murine models expressing RE under control of tetracycline induction [76], an MRP8 promoter [77] or Cre-mediated recombination [78, 79], the mice remained healthy throughout their lifespan showing normal haematopoiesis in the presence of RE. These data suggest that although RE is strongly associated with AML, it is insufficient to induce leukaemia in isolation. In this respect it is notable that RE was capable of inducing leukaemia in a retroviral transduction model of leukaemia where an alkylating agent was used to generate secondary mutations [80]. Moreover, Sca-1-mediated expression of RE specifically within the haematopoietic stem cell compartment generated a spontaneous myeloproliferative disorder after a period of normal haematopoiesis suggesting that stem cell-specific factors may cooperate with RE to enhance its leukaemogenicity [81].

In human $CD34^+$ cells, ectopic expression of RE induced an early proliferative arrest that was gradually replaced over 4-5 weeks with a population of pluripotent stem cells with enhanced self-renewal and committed progenitors with impaired differentiation [82]. It is notable that this phenotype resembles AML M2 leukaemia with sustained $CD34^+$ expression, a lack of cellular differentiation and enhanced self-renewal [82]. However, despite this, RE failed to transform $CD34^+$ cells, strongly supporting a requirement for secondary cooperating mutations. A frequent mutation identified in t(8;21) patient samples expressing RE is mutated RAS. Co-expression of RE and $N\text{-}RAS^{G12D}$ in human haematopoietic cells enhanced their replating and colony formation ability relative to RE alone but was not sufficient to drive immortalisation, suggesting that further mutations were still required [83].

While RE retains the RHD of RUNX1 and therefore its ability to bind to RUNX1 targets, the fusion replaces the TAD and TID of RUNX1 with four nervy-homology region (NHR1, 2, 3 and 4) domains from ETO that effectively recruit co-repressors to RUNX1 target genes. NHR1 is referred to as TATA-box-associated factor homology domain (TAFH) as it shares sequence homology with *Drosophila* TAF-110. It has been demonstrated to interact with E-proteins and also with NCoR which can recruit HDACs to assist with transcriptional repression [84, 85]. NHR2 is an α-helical tetramer [86] that is predicted to interact with corepressors such as mSin3A, NCoR/SMRT and HDACs [86-91]. NHR2 is also essential for

oligomerisation of ETO and RE [86]. Disruption of the NHR2 domain by mutation or targeting with cell-penetrating peptides resulted in enhanced apoptotic activity, decreased proliferation and attenuation of the enhanced self-renewal capacity conferred by RE [92]. NHR3 has a predicted coiled-coil structure and has been reported to interact with the N-terminus of the regulatory subunit of type II cyclic AMP-dependent protein kinase A (PKA RIIα). PKARIIα binds subcellular structures such as the Golgi apparatus and the endoplasmic reticulum via A-Kinase Anchoring Proteins (AKAPs) leading to speculation that ETO NHR3 is a type of AKAP. Abrogation of the interaction between NHR3 and PKA RIIα failed to eliminate the RE-mediated block on differentiation or the enhanced self-renewal of RE-expressing haematopoietic progenitor cells [93] suggesting that NHR3 plays only a minor role in leukaemia development but this has yet to be determined *in vivo*. NHR4 is also known as the Myeloid-Nervy-DEAF (MYND) domain and contains conserved zinc-chelating motifs [86, 94]. Deletion of NHR4 reversed RE-mediated proliferative arrest and opposed RE-mediated repression of granulocyte differentiation [95]. Furthermore, NHR4 deletion prevented recruitment of the NCoR/SMRT co-repressor complex and thence HDACs to RE, thereby attenuating its function as a transcription factor. NHR4 has also been reported to interact with SON, a large splicing co-factor protein which exhibits both DNA and RNA binding capabilities and is thought to contribute to cell cycle progression by enhancing the efficiency of mRNA splicing [95, 96]. Prevention of this interaction enhanced leukaemia development in mouse models suggesting a critical role for SON in leukaemia restraint [95, 97]. It is notable that, while the contribution of NHR3 to RE-induced leukaemogenesis is unclear, studies have suggested it may cooperate with NHR4 to recruit both NCoR/SMRT [90] and SON to RE [97] which indicates that NHR3 may be required to potentiate the effects of NHR4 on gene repression and leukaemic restraint *in vivo*. Indeed a cloning artefact resulting in a 200 amino acid C-terminal deletion of RE devoid of NHR3 and NHR4 domains induced spontaneous leukaemia development in a retroviral transduction transplantation mouse model [98]. From these results it was concluded that the RUNX1 RHD in combination with the NHR1 and NHR2 domains of ETO were sufficient to promote leukaemogenesis while NHR3 and NHR4 functioned to oppose these effects. Supporting evidence for this assumption was generated by a naturally occurring splice variant of RE, RE9a, that introduces the small exon 9a and its encoded stop codon into the RE transcript. The

resulting RE9a protein lacks NHR3 and NHR4 domains and, in contrast to RE, was reported to spontaneously induce leukaemogenesis in retroviral transduction transplantation mouse models with no additional mutagens within a matter of weeks [80]. Moreover, RE9a was detected in approximately 90% of t(8;21)-positive AML patients at varying levels. Patients with higher levels of RE9a expression displayed a more primitive, blast-like population of cells and a poorer disease outcome supporting suggestions that loss of NHR3 and NHR4 promoted leukaemogenesis *in vivo* [80].

1.7.2 TEL-RUNX1 t(12;21)

The TEL-RUNX1 (TR) fusion results from the t(12;21) chromosomal translocation between the P1 isoform of *RUNX1* and the Ets family transcription factor, *TEL*. TR is associated with approximately 25% of childhood B-cell ALL but is extremely rare in adult onset ALL [99]. Evidence indicates that the t(12;21) translocation occurs *in utero* as an initiating mutation driving the existence of pre-leukaemic clones that then undergo secondary mutations during childhood to generate the fully transformed ALL phenotype [52, 100].

Several transgenic mouse models have been developed to investigate the role of TR in the evolution of ALL. Transgenic mice expressing TR in lymphoid cells were observed for over two years but failed to display leukaemogenesis [101]. Murine bone marrow transplantation mouse models displayed impaired differentiation in the pro-B-cell compartment with an accumulation of early progenitor cells very similar to the t(12;21) phenotype observed in ALL patients but no leukaemia was observed for over a year post-transplantation [102]. Models that have attempted to enhance the potential for secondary cooperating mutations have been marginally more successful. A retroviral mouse model revealed cooperation between TR and loss of $p16^{INK4a}$ for leukaemia development [103] and co-expression of TR with the sleeping beauty transposon as an additional insertional mutagen developed a B-cell precursor ALL in approximately 20% of the mice [104]. The requirement for secondary events is supported by the aetiology of the disease *in vivo*. Indeed, in the context of human ALL, the occurrence of the TR fusion far exceeds the incidence of TR-related leukaemia suggesting that TR alone is insufficient to induce spontaneous leukaemia. One mutation that is frequently found in human TR positive ALL cells is deletion or inactivation of the

unrearranged allele of TEL. This is observed in approximately 65%-80% of established ALL although its biological significance has not yet been determined [105-108].

The TR fusion retains all of the functional domains of RUNX1 and the N-terminal helix-loop-helix (HLH) domain of TEL [99, 109]. Despite retention of the RUNX1 TAD, TR is compromised in its ability to activate RUNX1 target gene expression and has been shown to recruit co-repressors such as HDACs and mSin3A to RUNX1-specific gene promoters [110, 111]. From these results, it has been suggested that TR functions as a dominant-negative repressor of RUNX1 activity, but results from another study showing upregulation of a subset of RUNX1 targets in the presence of TR suggests that the reality may be more complicated [75]. What has been clearly established is that the HLH domain of TEL is critical for TR-mediated pre-leukaemic activity. The HLH domain regulates TEL localisation and oligomerisation, suggesting that these functions play an essential role [112]. Specifically, the TEL HLH domain has been reported as a target for SUMOylation [113-115]. SUMOylation is a form of post-translational modification involving covalent attachment of small ubiquitin-like modifiers (SUMO) at specific amino acid sequences and regulates several cellular processes including cell cycle progression, apoptosis and subcellular localisation of target proteins [116]. It seems likely that any of these processes could directly contribute to TR-mediated leukaemogenicity or provide a more indirect effect through antagonism of RUNX1 functions.

1.8 Anti-Cancer Fail-Safes

Cellular senescence and apoptosis are cellular fail-safe mechanisms that are activated in response to potentially harmful cellular events including viral infections, pro-oncogenic mutations and hypoxia that can result in altered tissue homeostasis. Senescence and apoptosis regulate genetic programmes that share some common signalling components such as p53, p38MAPK and reactive oxygen signalling. Most importantly, both senescence and apoptosis are considered to be primary anti-cancer cell defences which must be overcome for cellular transformation to occur.

1.8.1 Apoptosis

Apoptosis represents a mechanism of programmed cell death (PCD) that results in the regulated destruction of cell organelles and structures in response to intrinsic and extrinsic cellular signals [117]. Apoptotic cell death is induced by caspases which are a family of cysteine proteases ubiquitously expressed in the form of zymogens. Initiator caspases (caspase 2, 8, 9 and 10) become activated upon cleavage at conserved aspartate residues. Activated initiator caspases then proceed to cleave effector caspases (Caspase 3, 6 and 7) which cleave other target proteins within the cell to trigger apoptosis [118].

Apoptosis is initiated through one of two pathways, the intrinsic pathway or the extrinsic pathway. The intrinsic pathway is initiated by stress signals such as activated oncogenes that promote mitochondrial swelling and membrane permeabilisation. Cytochrome C is released from the mitochondria into the cytoplasm where it forms an apoptosome with apoptosis protease activating factor 1 (Apaf1), ATP and procaspase 9 [119] that subsequently forms the site of procaspase cleavage to form activated caspase 9 [120]. The extrinsic pathway is triggered by cytokines such as tumour necrosis factor α (TNFα) and Fas which bind to receptors and form death domains that activate initiator caspases and thence effector caspases to promote apoptosis [121, 122].

1.8.2 Cellular Senescence

Cellular senescence is characterised as a stable growth arrest undergone by normal cells after a finite number of population doublings. Senescence was initially described by Hayflick and Moorhead in 1961 [123] who demonstrated that primary human fibroblasts have a finite replicative life-span, displaying arrested growth after approximately 50-70 population doublings due to progressive telomere attrition. Senescent cells have a complex phenotype including a flattened and enlarged cell morphology [124], senescence-associated β-galactosidase (SA-β-Gal) activity at pH6.0 [125], activation of tumour suppressor pathways [126], accumulation of reactive oxygen species and changes in gene expression resulting in increased levels of growth factors and inflammatory cytokines associated with the senescence-associated secretory phenotype (SASP) [127].

Normal human cells undergo senescence in response to telomere attrition that occurs over the life span of the cell as DNA replication takes place [128]. At a critical length the shortened telomere is detected as irreparable DNA damage and the cell undergoes a form of growth arrest termed replicative senescence [129]. Premature senescence is physiologically and morphologically indistinguishable from replicative senescence but occurs more rapidly in early passage cells in response to diverse stress stimuli, including oxidative stress, DNA damage or oncogene activation, that activate common tumour suppressor pathways such as p53 and $p16^{INK4a}$ to execute a cell cycle arrest [126]. Oncogene-Induced Senescence (OIS) is an example of premature senescence that represents an important failsafe mechanism protecting cells against cancer development. OIS was first observed in response to oncogenic RAS. The downstream pathways included activation of RAS-RAF-MEK signalling to induce a p53 and $p16^{INK4a}$-dependent cell cycle arrest [130]. OIS has now been identified as a response to multiple oncogenes and invariably engages tumour suppressor pathways that must be overcome for cancer progression to occur [131-137].

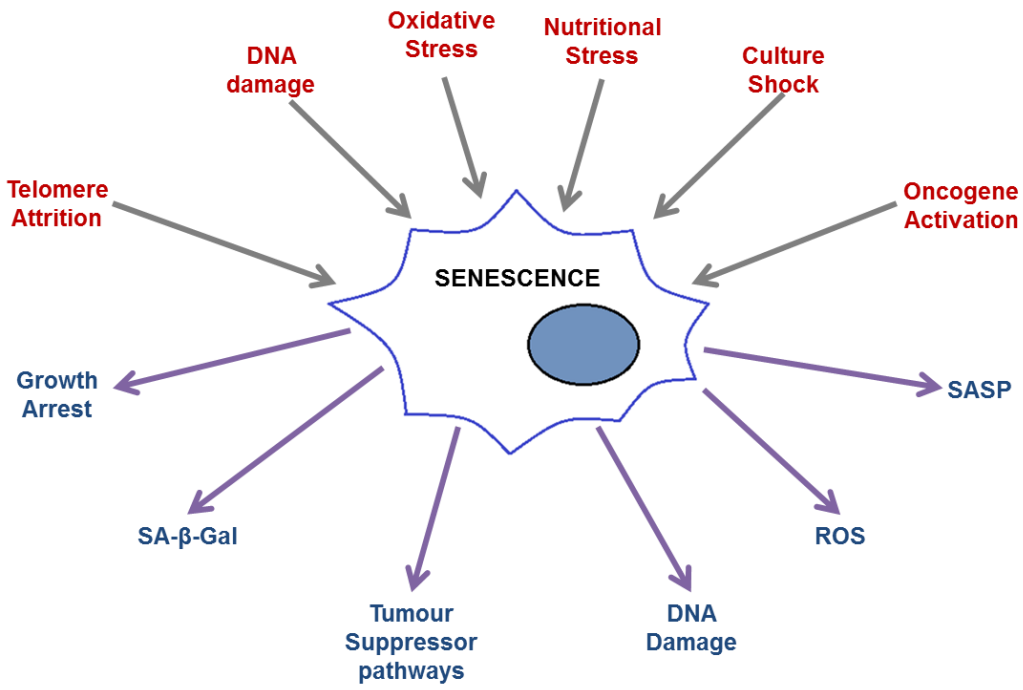

Figure 1.3. Causes and consequences of cellular senescence.
Cellular senescence can be triggered by a wide range of stimuli including telomere attrition, which is related to aging and replicative senescence, and cellular stresses which result in premature senescence. The resulting senescence phenotype comprises a plethora of hallmarks which can include growth arrest, activation of tumour suppressor pathways and induction of a SASP.

1.9 Defining Senescence

Senescence is defined by a plethora of "hallmarks" including growth arrest, SA-β-Gal activity, engagement of tumour suppressor pathways and DNA damage [125, 126, 138] (**Figure 1.3**). Individually, these characteristics are not necessarily indicative of cellular senescence and elements must be observed in combination to generate the complex phenotype that is defined as senescence. Furthermore, several pro-senescence hallmarks have also been implicated in oncogenesis suggesting that senescence induction requires a delicate balance to prevent oncogenic progression [139].

1.9.1 Growth arrest

Growth arrest is a major hallmark of senescence and is considered indispensable for the phenotype. The irreversibility of senescence-like growth-arrest (SLGA), however, is somewhat more controversial. Previous reports have identified a

permanent growth arrest in primary human fibroblasts in response to RAF1, $p16^{INK4A}$, and HDAC inhibitors [140-142]. However, more recent results suggest that escape from senescence is possible under certain circumstances. Inactivation of p53 may be a key event [127, 143-145] but studies also implicate expression levels of $p16^{INK4a}$ as an important determining factor. Cells with low levels of $p16^{INK4a}$ at the point of senescence were permissive for growth when p53 was inactivated but those expressing high levels of $p16^{INK4a}$ failed to restore proliferation [143].

1.9.2 Cell Morphology

Cells that undergo senescence often assume a flattened and enlarged morphology compared to their proliferating counterparts. In an attempt to identify the signalling components responsible, HPV16 E6 or E7 proteins have been exploited since they disable the p53 or $p16^{INK4a}$ tumour suppressor pathways respectively. Upregulation of actin stress fibres and sporadic redistribution of focal adhesion proteins associated with the flattened and enlarged senescent morphology of a population of senescent cells was opposed in the presence of E7 but not E6. Since E7 directly degrades the Rb protein, it was concluded that the senescent morphology was dependent on an intact $p16^{INK4a}$/pRb signalling pathway [124]. It is unclear whether this represents a cell-type dependent effect or a more widespread phenomenon.

1.9.3 Senescence-Associated β-Galactosidase

One of the most common assays used to distinguish senescent and non-senescent cells is the detection of SA-β-Gal activity at pH6.0 [125]. SA-β-Gal is expressed from the *GLB1* locus and is typically detected as a lysosomal enzyme activated at pH4.0-4.5. The activity at pH6.0 is novel and restricted to senescent cells. Although SA-β-Gal activity represents a useful marker of senescence, it is not considered to be an inducer and indeed, in some cases its appearance can be somewhat inconsistent. An shRNA targeted to *GLB1* failed to abrogate replicative senescence in late passage human fibroblasts [146] and SA-β-Gal activity has been observed in non-senescent cells under stress conditions, all indicating that while SA-β-Gal is a common marker of senescence, it is not essential for senescence to occur and is not necessarily indicative of the phenotype [146].

However, with these caveats in mind and in conjunction with other factors, SA-ß-Gal activity can provide a useful marker of senescence.

1.9.4 Tumour Suppressor Pathways

The stimuli that induce cellular senescence are multiple and diverse but ultimately converge on two important tumour suppressor pathways controlled by p53 and $p16^{INK4a}$ that function as key regulators of senescence [126]. Their importance in senescence is inferred from the frequency at which they are inactivated in human cancers [147]. The p53 tumour suppressor protein has been described as the "guardian of the genome" [148]. In the absence of stress, p53 has a short half-life and is maintained at low levels as an inactive transcription factor in normally proliferating cells. In response to cellular stresses such as DNA damage and oncogene expression the pattern is reversed [149-153]. The levels of p53 dramatically increase and the protein is activated to regulate expression of a plethora of genes targeting major functional pathways such as cell cycle progression and DNA repair [154, 155]. $p21^{CIP1}$ represents one of the primary p53-regulated targets controlling cell cycle progression. It functions as a CDK inhibitor (CKI) complexing with CDK4/6 and CDK2 to prevent cyclin A/E-mediated cell cycle progression [156]. $p16^{INK4a}$ represents another CKI associated with SLGA. $p16^{INK4a}$ opposes cell cycle progression by binding to CDK 4/6 and preventing their association with D-type cyclins. Cyclin-CDK complexes phosphorylate pRb, triggering its release from E2F and the subsequent expression of E2F-regulated genes required for cell cycle progression. In the presence of CKIs, cyclin-CDK activity is opposed and E2F is retained in an inactive state by unphosphorylated pRb [157] (**Figure 1.4**).

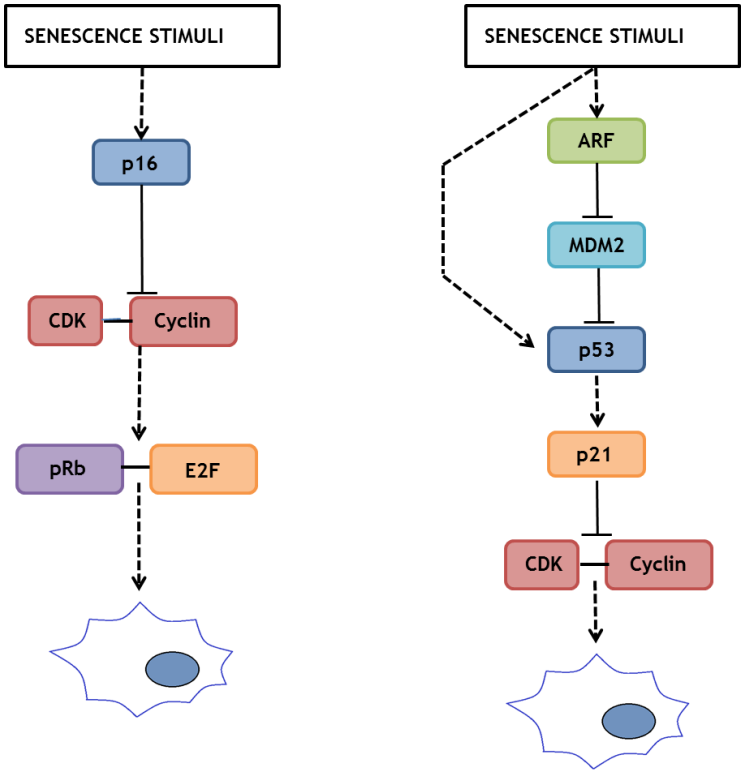

Figure 1.4 Tumour suppressor pathways
Senescence is induced in response to a wide range of stimuli, senescence signalling ultimately converges on two major tumour suppressor pathways, the $p16^{INK4A}$ pathway and the p53 pathway.

Inactivation of p53 signalling is sufficient to abrogate RAS-induced senescence in primary MEFs [130]. Parallel experiments in $p16^{INK4a}$-null MEFs resulted in a premature senescence response that was indistinguishable from wild type MEFs, suggesting that $p16^{INK4a}$ is not absolutely required in this system [158]. However, the reality may be more complicated since inactivation of pRb or pRb family members was also sufficient to oppose senescence in primary MEFs [159, 160]. With such contrasting evidence, it seems likely that p53 provides the dominant senescence signal in primary MEFs but that both tumour suppressor pathways have a role to play [130, 161]. A requirement for p53 and $p16^{INK4a}$ is also described in human senescence but in this case a dominant role is emerging for $p16^{INK4a}$ since $p16^{INK4a}$-null human cells displayed resistance to RAS-induced premature senescence [143].

1.9.5 DNA Damage

Double-stranded DNA breaks are induced by multiple stress signals and are targeted by cellular complexes for DNA repair. The Mre11/Rad50/Nbs1 (MRN) complex recruits the ataxia telangiectasia mutated (ATM) and ataxia

telangiectasia and Rad3-related (ATR) DDR factors to sites of double-stranded breaks. There they phosphorylate H2AX which serves both as a marker of the damage (γH2AX) and as a recruitment factor for further ATM molecules and repair factors, establishing a positive feedback loop necessary to ultimately remove the break and repair the DNA [162, 163]. Although ATM and ATR are sufficient to mediate the cell cycle arrest required for low level DNA repair, in the event of irreparable DNA damage ATM phosphorylates and stabilises the p53 tumour suppressor to induce senescence or apoptosis [164, 165].

Replicative senescence is considered to represent a response to persistent DDR signalling due to the critical shortening of telomeres sensed as double-stranded DNA breaks or irreparable DNA damage [129]. DDR signalling has subsequently been implicated in various types of premature senescence including OIS. Expression of oncogenic RAS is associated with a hyper-proliferative phase that drives replicative stress, oxidative DNA damage and the appearance of stalled DNA replication forks. The ensuing DNA damage foci activate a persistent DDR which blunts the hyper-replicative phase and induces OIS [166]. Similar observations have been made for other oncogenes including BRAF [167]. It is of note that, despite representing an important factor for the establishment and maintenance of senescence, impairment of the DDR can also act as a driving force for oncogenesis, promoting genomic instability and increased DNA damage. It is perhaps not surprising then that while the DDR can represent a barrier to *in vivo* transformation, mutations and epigenetic silencing affecting DDR components are commonly observed in cancer cells [168-172].

1.9.6 Reactive Oxygen Species

ROS are normal bi-products of cellular metabolism with functions in cell signalling and growth. Several organelles and enzymes have been identified as producers of intracellular ROS [173]. In the mitochondrial the electron-transport chain passes electrons via a series of proteins through a progression of oxidation/reduction reactions. The terminal electron acceptor on this chain is molecular oxygen which is most commonly reduced to form water. However, in a very small percentage of cases, the acceptor oxygen molecule undergoes incomplete reduction which results in the formation of superoxide [174]. Other organelles including the endoplasmic reticulum and peroxisomes have also been

identified as sources of intracellular ROS [173]. In addition numerous enzyme systems have been established as ROS producers. A notable example of a ROS producing family of enzymes is the NADPH oxidase (NOX) family of enzymes which transfer electrons from NADPH in the cytoplasm to molecular oxygen to produce superoxide. ROS production by NOX family enzymes can be induced by soluble factors including TNF, PDGF and EGF [175] and is thought to have a role in the immune response to pathogens [176] as evidenced by the finding that patients with mutations affecting NOX function displayed granulomatous disease associated with recurrent bacterial and fungal infections [177].

Several strategies for the detection of intracellular ROS have been developed including the use of redox dependent fluorescent dyes and protein probes. The most frequently used means of measuring intracellular ROS is DCF-DA, a membrane permeable dye which is cleaved by intracellular esterases and retained within the cell where it can be oxidised, resulting in fluorescence that can be measured by flow cytometry [178]. However, more recently, fluorescent protein-based probes have been developed, enabling cells to be transduced to express redox-sensitive chimeric proteins [179]. For example, HyPer is a protein probe which consists of a YFP protein transcript inserted into the regulatory domain of the prokaryotic OxyR gene which is sensitive to hydrogen peroxide. The use of these probes may enable detection of ROS generated in specific subcellular organelles [179].

Although ROS have important functions in cell signalling and the cellular response to pathogens, in particular contexts ROS can also activate senescence [180, 181]. MEFs undergo rapid premature senescence when grown under standard tissue culture conditions (20% oxygen) but this is delayed or even prevented when the cells are propagated in physiological oxygen (3% oxygen) where ROS levels are reduced [181-183]. The replicative life span of primary human fibroblasts can also be extended in physiological oxygen conditions [183]. In addition, expression of oncogenes such as RAS^{V12} have been reported to induce marked increases in ROS that initially had mitogenic effects on the cells, resulting in hyperproliferation but ultimately inducing an accumulation of DNA damage and OIS due to replicative stress [166]. ROS was also reported to induce senescence through direct damage to cellular DNA and proteins via oxidative reactions.

Complementing its role as an inducer of premature senescence, accumulated levels of ROS have also been implicated in the maintenance of senescence. Senescent human fibroblasts expressing conditionally active SV40 large-T-antigen were susceptible to large-T-antigen mediated inactivation of p53 and recommenced proliferation but only under conditions of low ROS generation. When growth conditions were adapted to increase ROS production, senescence persisted unless N-Acetyl-cysteine was included in the growth medium as an antioxidant, thus providing evidence of ROS as a critical senescence maintenance factor [184].

The signalling pathways downstream of ROS responsible for SLGA include p53 and $p16^{INK4a}$. ROS engages the p53 axis through persistent DNA damage signalling and activation of the DDR and downstream targets including p53. Accumulation of ROS can also induce $p16^{INK4a}$ expression through the stress-induced p38MAPK protein [185]. Furthermore, oncogene-induced ROS has been associated with induction of the SASP which plays an important role in the maintenance of senescence [186].Together, these data indicate an important role for ROS in both the induction of SLGA and establishment of the senescence response.

1.9.7 p38 Mitogen Activated Protein Kinase

The p38 Mitogen Activated Protein Kinase (p38MAPK) is a member of the MAPK family of stress-induced protein kinases that play important roles in inflammation and the cellular response to a wide range of stress stimuli including UV irradiation, exposure to heat, osmotic shock, oxidative stress, inflammation and oncogene expression [187, 188]. p38MAPK has also been identified as a key inducer of cellular senescence and may provide a common link between pro-senescence stimuli and key tumour suppressor pathways as it can activate both the p53 and $p16^{INK4a}$ pathways [189].

1.9.7.1 p38MAPK Can Be Activated Downstream of Reactive Oxygen Species

Many stimuli that induce ROS subsequently activate p38MAPK suggesting that they lie on a linear pathway. Treatment of cells with hydrogen peroxide (H_2O_2) as a source of oxidative stress promotes p38MAPK activation whereas the use of ROS scavengers opposes p38MAPK activation [188, 190-192]. The signalling

pathways between ROS and p38MAPK are poorly understood and somewhat context-dependent. MAPK proteins themselves are susceptible to oxidative stress. ASK1, for example, is a MAPK family member that associates with thioredoxin under normal cellular conditions. In the presence of oxidative stress, thioredoxin is oxidised and dissociates from ASK1, thereby facilitating ASK1 oligomerisation and the subsequent activation of p38MAPK [193, 194]. Oxidative stress is also reported to promote growth factor-mediated activation of p38MAPK. Specifically, oxidative modification of key amino acids such as cysteine, in response to H_2O_2, was sufficient to activate p38MAPK. Finally oxidative stress can perturb the activity of MAPK phosphatases (MKPs) which are required to maintain the MAPK pathway in an inactive state. Oxidation of specific cysteines in the catalytic domain attenuates their activity, permitting constitutive MAPK activation [195].

1.9.7.2 p38MAPK Activation in Response to DNA damage

p38MAPK activation represents a stress response to genotoxic stimuli including X-irradiation and oxidative DNA damage. Thousand and one amino acid (TAO) kinases are MAP3Ks that have been reported to activate p38MAPK in response to oxidative stress and DNA damage [196]. TAOs are potently activated by ATM in response to DNA damage. The use of dominant-negative mutants or specific TAO knockdown assays to reduce kinase activity abrogates p38MAPK activation in response to genotoxic stress [196]. Furthermore, cells derived from ataxia telangiectasia mutated (ATM) patients display severely compromised TAO and p38MAPK activation, strongly suggesting that p38MAPK lies downstream of ATM and represents a crucial signalling component of the DDR.

1.9.7.3 p38MAPK is a Key Regulator of Oncogene-Induced Senescence

ROS and DDR signalling pathways are induced by oncogenes such as H-RAS^{V12} that are also associated with senescence [166, 169]. It is perhaps no surprise then, that p38MAPK activation, which has been linked to oxidative stress and DNA damage, is also induced in response to sustained oncogene expression [197-199]. The hyperproliferative phase associated with RAS-induced senescence is partially driven by constitutive activation of RAF-MEK-ERK signalling that also directs phosphorylation of p38MAPK. The significance of this for cellular senescence is illustrated by the opposition of SLGA in the presence of p38MAPK inhibitors

[198]. A similar finding was observed when Wip1 was overexpressed with oncogenic Ras in murine models. Wip1 is a p38MAPK phosphatase which dephosphorylates and inactivates p38MAPK [200].

p38MAPK activates SLGA through direct engagement of the p53 and $p16^{INK4a}$ tumour suppressors. p38MAPK phosphorylates p53 in response to cellular stress on key serine residues (Ser 15, 33 and 46) that are associated with p53 mediated senescence and apoptosis [201]. Activation of $p16^{INK4a}$ in response to p38MAPK is more indirect and a consequence of p38MAPK-mediated activation of ETS transcription factors Ets1, Ets2 and ESE-3 which then transactivate $p16^{INK4a}$ expression [202-204]. In addition, p38MAPK has been implicated in the maintenance of senescence through downstream signalling pathways such as nuclear factor kappa-light-chain-enhancer of activated B cells (NFκB) that promotes development of the SASP. The SASP sustains OIS through inflammatory cytokine signalling and chemotaxis [185].

1.9.8 The Senescence-Associated Secretory Phenotype

Although senescent cells are no longer proliferating, they remain metabolically active and are frequently found to produce a characteristic secretory profile of cytokines, growth factors and proteases termed the SASP [205]. The SASP signals in an autocrine and paracrine fashion to consolidate SLGA in cells that have already undergone senescence and induce senescence in adjacent non-senescent populations [206]. Furthermore, numerous SASP components act as attractants for the immune system to clear damaged cells, suggesting that the SASP is not simply a downstream consequence of senescence but an integral tumour suppressor component. In this respect it is notable that autophagy may facilitate development of a SASP. Autophagy represents a survival mechanism that is engaged in response to cellular starvation [207] but autophagy-related genes also display similar patterns of induction to SASP markers and their expression appears to be related. Furthermore, it has been reported that knockdown of autophagy related genes resulted in late expression of some SASP components which can act to further promote senescence [208]. Opposed to these growth suppressive functions, the SASP also supports pro-oncogenic effects including the proliferation of malignant and pre-malignant cells and the maintenance of tissue microenvironments permissive for oncogenesis [127, 209]. From these studies it

has been proposed that senescence-associated secretion is “antagonistically pleiotropic” exhibiting tumour suppressor and oncogenic activities to both support and resist the senescent phenotype.

1.9.8.1 SASP Initiation and Regulation

The upstream signalling pathways associated with the appearance of a SASP are varied and somewhat context-dependent. Early studies demonstrated a clear association between a persistent DNA damage signal and the initiation of a SASP. DDR mediators such as ATM, Nibrin (NBS1) and checkpoint kinase 2 (CHK2) were identified as essential components and assumed to signal the SASP downstream of the damage [210]. These conclusions were challenged by observations that neither p53 nor $p16^{INK4A}$ were absolutely required and that a transient DDR failed to induce the response suggesting that while the DDR may be important for SASP induction, it is not sufficient [210]. More recent reports suggest that the active phosphorylated form of p38MAPK can induce a potent SASP independently of the DDR and that inhibition of p38MAPK activity results in attenuated cytokine secretion [185]. Studies have also demonstrated the importance of ROS as a potential initiator of the SASP. ROS was previously reported to activate p38MAPK in response to oxidative stress [193, 194] but in the context of RAS-induced senescence has also been shown to activate NFκB through the activation of protein kinase D1 (PKD1) [186]. The PKD1 pathway is independent of DNA damage or p38MAPK phosphorylation, suggesting that multiple pathways are capable of activating a SASP and that cellular context is an important determinant of pathway selection.

The SASP is controlled by pro-inflammatory “master regulators” NFκB and CCAAT-enhancer-binding protein beta (C/EBP-β), the binding-sites for which are frequently found adjacent to each other in the promoters of SASP-associated genes such as IL8 and CXCL1 [211]. More recent studies indicate that NFκB may be the critical determinant [212-214]. NFκB is an important sensor of cellular stress. It is maintained in the cytoplasm as large precursor proteins, NFκB1 (p105) and NFκB2 (p100) that dimerise with REL family members to form inactive complexes. In response to stress, these precursor complexes are rapidly processed to form the mature p50 and p52 NFκB subunits. Stress signalling is

mediated through canonical and non-canonical pathways that exhibit distinct and overlapping features and ultimately regulate the nuclear localisation of the NFκB transcription factor. The canonical pathway promotes dissociation of NFκB from the inhibitory IκB subunit whereas the non-canonical pathway regulates the phosphorylation and activation of the NFκB p100 precursor protein [215].

NFκB signalling is activated by multiple stimuli including the DDR, ROS and p38MAPK. Signalling through ATM or the ROS-PKD1 pathway activates the canonical pathway whereas the non-canonical pathway is activated by p38MAPK via MAPK signalling components, Mitogen and stress activated kinase (MSK)1 and 2 [185, 216, 217]. In addition, p38MAPK can phosphorylate histone H3 located within the promoters of specific subsets of cytokine and growth factor genes thereby increasing the affinity of NFκB for the promoter region [218]. Activation of NFκB is accompanied by a transcriptional response that regulates multiple genes associated with the SASP.

1.9.8.2 Pleiotropic Consequences of the SASP

The secretory phenotype is pleiotropic, mediating both tumour suppressor and oncogenic effects in cells and tissues. The acute response serves to reinforce the senescent phenotype. Specific inflammatory factors such as IL-6 and IL-8 directly mediate these effects. Knock-down of the IL-8 receptor (CXCR2) was reported to attenuate OIS induced by oncogenic RAS signalling [211] while opposition to IL-6 expression completely abrogated BRAF600-induced senescence [145]. SASP mediators have also been reported to extend the senescent phenotype to surrounding cells via paracrine signalling. In this respect $p16^{INK4a}$ activation has been observed in normal cells surrounding malignant lesions [219] and IL1-β was demonstrated to induce premature senescence in normal proliferating cells in mouse models [206]. Finally numerous SASP components have been identified as chemo-attractants that recruit innate immune cells to clear damaged cells. For example, reactivation of p53 in a p53 depleted mouse liver carcinoma model resulted in the induction of a SASP that was accompanied by extensive tumour regression. The effect was attributed to an infiltration of natural killer (NK) cells, neutrophils and macrophages due to the release of inflammatory cytokines from the senescent cells [220]. Infiltrates of innate immune cells have also been

reported to clear senescent cells. In mouse models this resulted in an increased healthy lifespan with reduced incidence of tumours and age-related pathologies [221, 222]. This self-regulatory mechanism presumably reduces the negative effects of chronic inflammation on aging cells and could be considered tumour suppressive.

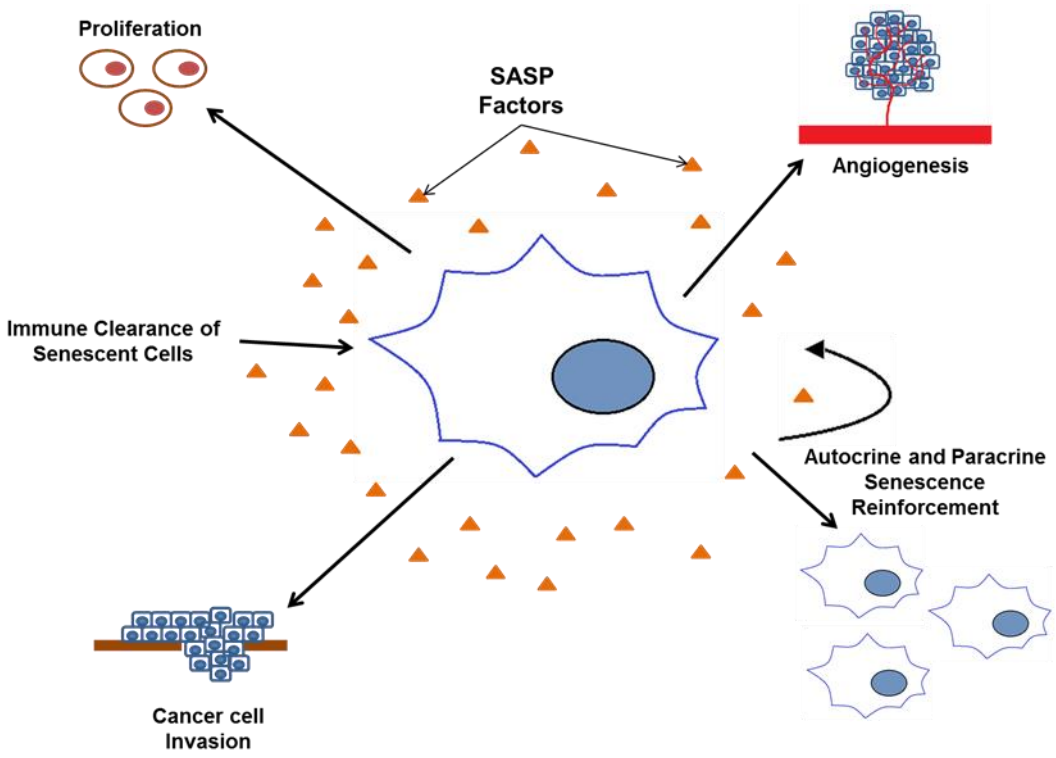

Figure 1.5 Antagonistic Pleiotropy of the SASP
The SASP produced by senescent cells has effects that can promote transformation and oncogenesis as well as senescence and tumour suppression. Although the SASP can promote cellular senescence through autocrine and paracrine routes, it is also considered to have pro-oncogenic activities including promotion of tumour angiogenesis, enhancing cancer cell invasiveness and promoting cellular proliferation in certain contexts.

SASP signalling is required to maintain and extend the senescent phenotype but a large number of SASP factors also display pro-oncogenic effects supporting a role for the SASP in tumour promotion (**Figure 1.5**). GROα, is secreted by senescent fibroblasts but has also been demonstrated to stimulate proliferation of pre-malignant mammary epithelial cells, and IL-6, IL-8, bFGF and VEGF support cellular migration and invasion to promote a metastatic phenotype [127, 205, 223]. Chronic inflammatory stimulation may be required for tumour promotion since the effects are generally associated with the persistence of senescent cells. This is in contrast to the more acute consequences of a SASP for

tumour suppression and may provide one explanation for the antagonistic pleiotropy associated with the secretory phenotype.

1.10 RUNX1 and Oncogene Induced Senescence

In primary murine fibroblasts, all three *Runx* genes exhibit a profound SLGA that is dependent on an intact $p19^{ARF}$/p53 pathway [224]. Moreover all three genes collaborate with c-Myc in retroviral mouse models of murine lymphoma supporting an oncogenic role *in vivo* [57]. Extending these observations to human fibroblasts it was shown that RUNX1P2 induced a profound SLGA in Hs68 fibroblasts that required the RUNX1 RHD and TAD and was dependent on expression of the $p16^{INK4a}$ tumour suppressor [59]. Moreover, RUNX1-induced senescence in contrast to other oncogenes was independent of a DDR or hyperproliferation in this cell background lending weight to the existence of alternative senescence inducing pathways. The pathway responsible for RUNX1-induced senescence remains to be elucidated but DDR-independent premature senescence has become more widely reported, invoking signalling modules downstream of PI3K, p38MAPK and ATR in for a number of oncogenes including AKT, RUNX1-ETO, BCR-ABL and CBFß-MYH1[59, 225, 226] .

1.10.1 RUNX1-ETO Induces Oncogene-Induced Senescence in Hs68 Cells

The RUNX1 t(8;21) fusion oncoprotein, RE, is expressed in approximately 40% of M2 AML and is the most common abnormality in childhood AML [227]. Despite these statistics RE is insufficient to induce leukaemia in mouse models [80]. Furthermore, RE expression results in OIS *in vitro,* supporting a requirement for secondary collaborating mutations to overcome RE-mediated growth suppression [59, 80, 225]. The p53 and $p16^{INK4A}$ tumour suppressors were previously identified as critical mediators of RE-induced senescence, with their relative contributions depending on the cell background studied, but the most defining phenotype was a virtual absence of replicative stress [59]. Few or no γH2AX foci marking sites of double-stranded DNA damage were observed in either human primary fibroblasts or murine haematopoietic progenitors compared to cultures expressing $H\text{-}Ras^{V12}$. Higher levels of γH2AX foci have been observed in other studies where RE was ectopically expressed in primary MEFs or human U937 lymphoma cells [228]. It is possible that the exquisite sensitivity of MEFs to oxidative stress or specific secondary mutations in U937 cells present more susceptible cell backgrounds for

DNA damage but the phenotype in this study was also absolutely dependent on $p21^{CIP1}$ suggesting that an alternative senescence pathway was responsible [228]. The absence of DNA damage in RE-induced senescence in Hs68 fibroblasts was accompanied by an accumulation of ROS [59]. ROS is reported to activate pro-senescence stress response pathways [59] but has also been associated with an induction of DNA damage [166]. In this study, it seems likely that the complete absence of hyperproliferation in Hs68 human fibroblasts had attenuated the potential for ROS-induced DNA damage in response to RE. A requirement for ROS was not directly investigated but it was notable that p38MAPK was activated in response to RE in human fibroblasts and murine haematopoietic progenitors and that multiple studies indicate that this stress kinase lies downstream of ROS. Moreover SLGA was opposed by p38MAPK inhibition demonstrating a critical requirement for p38MAPK signalling for the induction of RE senescence.

While RE alone is insufficient to induce leukaemia in murine models, RE9a, a C-terminally truncated splice variant of RE induces rapid leukaemogenesis in a retroviral transduction-transplantation model in mice [80]. As the reduced leukaemogenic potential of RE appears to correlate with its ability to induce SLGA, it might be predicted that the increased leukaemogenic potential of RE9a will correlate with escape from OIS.

1.10.2 TEL-RUNX1 Fails to Induce Cellular Senescence in Hs68 Cells

The t(12;21) translocation drives expression of the TR fusion oncoprotein associated with childhood B-ALL. TR was insufficient to induce leukaemia in murine models [101] but retroviral expression in primary murine haematopoietic progenitors enriched for a population of proliferating early B cells, suggesting that TR expression was capable of supporting cell growth in this background [103]. Ectopic expression of TR in primary human fibroblasts was also compatible with cellular proliferation. Growth promotion was not actually observed but the cells expanded with similar kinetics to the parental controls and exhibited no visible markers of premature senescence [59]. It has been suggested that persistent proliferation may be a pre-requisite for the acquisition of secondary mutations necessary for cancer development. In this respect it is notable that TR-positive murine pre-B cells displayed reduced sensitivity to growth inhibitory

signalling by TGF-β [229] suggesting that TR-mediated leukaemogenesis may be attributable to a failure to engage the senescence failsafe.

The observation that TR fails to induce SLGA in human primary fibroblasts is somewhat surprising given that the fusion protein retains a virtually intact *RUNX1* sequence and RUNX1 readily induces senescence in this cell background [59]. The pre-leukaemic activity of TR in pre-B cells was shown to require the RUNX1 RHD and the HLH domain of TEL [112]. The HLH domain is the only functional domain retained by the TEL portion of the fusion and has been associated with oligomerisation and subcellular distribution [112]. It is conceivable that either or both functions disrupt the ability of RUNX1 to induce senescence thereby permitting a proliferating phenotype vulnerable to the acquisition of secondary mutations necessary for leukaemia development.

1.11 Project Aims

1. Studies have demonstrated that, while RE is insufficient to induce leukaemogenesis in murine models, RE9a is a potent inducer of leukaemia. The low leukaemogenic potential of RE has been related to its ability to induce robust cellular senescence in primary cells *in vitro*. This project aims to determine whether the increased leukaemogenic potential of RE9a correlates with impaired induction of cellular senescence in primary cells.
2. RE9a is a C-terminally truncated splice variant of RE which lacks the repressive NHR3 and NHR4 domains. If RE9a is indeed demonstrated to evade senescence, it would be interesting to identify whether disruption of one of these domains is sufficient to promote senescence evasion.
3. The SASP has been identified as a promoter of cellular senescence. However, a chronic or persistent SASP has been found to have pro-oncogenic effects in certain context. This study aims to compare the Secretory profiles observed in cells expressing wild-type RUNX1 to those observed in cells expressing RE and RE9a to further elucidate the mechanisms of enhanced leukaemogenicity induced by RE9a expression.
4. Previous studies have demonstrated that the TR fusion protein fails to induce cellular senescence in primary cells despite its retention of almost

full length RUNX1, a known senescence inducer. This study aims to identify the critical domains required for TR to evade senescence .

2 Materials and Methods

2.1 Mammalian Cell Culture

Mammalian cell culture was performed in a sterile class II laminar flow hood using standard aseptic procedures.

All media and supplements were purchased from Invitrogen Life Technologies as sterile solutions unless stated otherwise.

2.1.1 Cell lines

293T cells (ATCC) are a highly transfectable cell line derived from 293 human embryonic kidney (HEK) cells that have been transformed using adenovirus E1a. The "T" refers to the expression of the SV40 T-antigen which allows replication of plasmids containing an SV40 origin of replication to a high copy number.

Phoenix (Eco) cells are an ecotropic retroviral packaging cell line derived from the 293T cell line. The Phoenix line was created by transfecting 293T cells with constructs expressing a retroviral gag-pol under hygromycin selection and the ecotropic envelope protein under diphtheria toxin selection.

Hs68 primary human foreskin fibroblasts (Sigma-Aldrich) isolated from a newborn Caucasian male were purchased from Sigma-Aldrich. Hs68 cells were expanded to passage 22 and frozen for use. Hs68 cells expressing a MLV ecotropic receptor were provided by Professor Gordon Peters.

Murine Embryonic Fibroblasts (MEFs) were isolated from E13.5 mouse embryos [230]. The head and red organs were removed and the body minced and treated with 0.5% trypsin to disperse the cells which were then expanded for culture.

Leiden cells are $p16^{INK4a}$ null human diploid fibroblasts isolated from a male who developed multiple naevi from a young age which had become atypical.

NIH3T3 cells are a line of MEFs established by 3T3 passage culture protocol [231].

REH cells are a suspension cell line derived from a patient with ALL.

HepaRG cells are terminally differentiated hepatic cells. The HepaRG cells used in this study have been transduced using lentiviruses (pLKO) to express his-tagged SUMO1, SUMO-2 or SUMO-3. Expression was maintained using continuous

puromycin selection. These cells were kindly gifted by Dr Elizabeth Sloan and Professor Roger Everett.

2.1.2 Maintenance of Mammalian Cells

Mammalian cells were cultured at 37°C in humidified incubators maintained at 5% CO_2 and 20% or 3% oxygen. Cells were maintained in complete medium (10% foetal-calf serum (FCS), 2mM L-glutamine and 100 units each of penicillin and streptomycin). All cells were maintained in DMEM with the exception of HepaRG cells which were cultured in WME and REH cells which were maintained in RPMI 1640. Cells were passaged at 80%-90% confluence every 3-4 days.

2.1.3 Making Cell Pellets

Adherent cells were trypsinised using a 0.05% trypsin-EDTA solution. Trypsinised or suspension cells were harvested and centrifuged at 172g for 5 minutes. The supernatant was discarded and cells washed with cold PBS and centrifuged at 172g for 5 minutes. Cells were resuspended in PBS and transferred into cold Eppendorf tubes which were centrifuged at 3823g for 2 minutes before the supernatant was discarded and pellets stored at -80°C.

2.1.4 Cell Cryopreservation and Recovery

To make liquid nitrogen stocks, cells were trypsinised and pelleted as described above and resuspended in freezing medium (10% DMSO in FCS) at 3-5x10^6 cells/ml; 1ml aliquots were transferred into cryovials. Vials were frozen overnight at -80°C in an isopropanol freezing chamber before being transferred to liquid nitrogen for long-term storage.

Cell stocks were thawed rapidly at 37°C prior to use. The outside of the cryovial was decontaminated using 70% ethanol and the contents diluted in 7ml pre-warmed complete medium. Cells were centrifuged for 5 minutes at 172g or 10 minutes at 62g for 293T and Phoenix cells. Supernatant was discarded and cells resuspended in complete medium and transferred into a tissue culture flask.

2.1.5 Cell Viability Counts

Trypsinised cells were suspended in media or PBS. 20µl of the cell suspension were diluted 1:1 with 0.4% trypan blue and incubated at room temperature for 1 minute to stain dead cells. The mixture was introduced into the haemocytometer and cell counts made by counting the cells in each of the four sets of 16 corner squares. Cells lying on the top and bottom perimeters of the large squares were included in the counts while those lying on the left of right perimeters were excluded. Cells/ml was calculated using the equation;

$$Number\ of\ cells\ x\ (1x10^4)\ x\ dilution\ factor$$

2.1.6 Growth Curves

Cells were plated at $2.5x10^4$/well in 12 well plates in selection medium containing 2µg/ml puromycin (Sigma Aldrich). Each cell type was plated out in triplicate. Cell viability counts were performed every 2-3 days and cells were re-fed with fresh selection medium.

2.1.7 SA-β-Gal Staining

Cells were plated in triplicate at $2.5x10^4$ per well in a 12 well plate for 6 days. SA-ß-Gal activity was detected as previously described [130]. Briefly, cells were washed with PBS then fixed with 0.5% glutaraldehyde in PBS for 10 minutes at room temperature. Cells were washed with PBS supplemented with 1mM $MgCl_2$ before staining overnight at 37°C in 0.22µm filtered X-Gal solution (1mg/ml X-Gal, 0.12mM $K_3Fe[CN]_6$ and $K_4[Fe]CN_6$, 1mM $MgCl_2$ in PBS pH6.0. Cells were washed with pH6.0 PBS.

2.1.8 3T3 Passage Culture

3T3 passage culture was performed on MEFs according to the protocol used by Todaro and Green [231]. Three independent cultures per retroviral construct were harvested and re-plated at $3x10^5$ cells per T25 flask. This was repeated every 3 days over 14 passages. Cumulative gains were calculated and plotted.

2.1.9 ROS analysis

Trypsinised cells were suspended in PBS with 15µM 2',7' –dichlorofluorescein diacetate (DCF-DA) (Calbiochem) and incubated at 37°C for 20 minutes. Cells

were centrifuged at 172g for 5 minutes and the supernatant discarded. Cell pellets were resuspended in PBS and the centrifugation step repeated. Cells were resuspended in PBS and DCF fluorescence (maximum excitation 495nm; maximum emission 530nm) measured on an Accuri C6 flow cytometer (BD Biosciences) using a 488nm blue laser and detecting fluorescence using the FL1 channel with a 533/30 filter. The cell population was gated on a forward scatter/side scatter plot to exclude debris and the mean DCF fluorescence of the gated population was measured.

2.1.10 Drug Treatments

2.1.10.1 Sodium Pyruvate

Sodium pyruvate was diluted in ddH_2O and added to cell culture medium at 250μM. Treatment of cells commenced on the day of antibiotic selection and medium was changed every 2-3 days.

2.1.10.2 SB203580

SB203580 was diluted in DMSO and added to cell culture medium at a final concentration of 8μM. Treatment of cells commenced on the day of antibiotic selection and medium with inhibitor was changed every 2-3 days.

2.2 DNA and Viruses

2.2.1 Plasmids

2.2.1.1 pBabe

The pBabePURO vector was derived from the Moloney Murine Leukaemia Virus (MMLV) and encodes a viral packaging signal in addition to the MMLV LTR which promotes expression of inserted genes. The vector also contains a puromycin resistance gene to enable selection of infected cells post-transduction. To enable propagation in bacterial cells, pBabePURO also contains the bacterial origin of replication (ORI) and an ampicillin resistance gene [232].

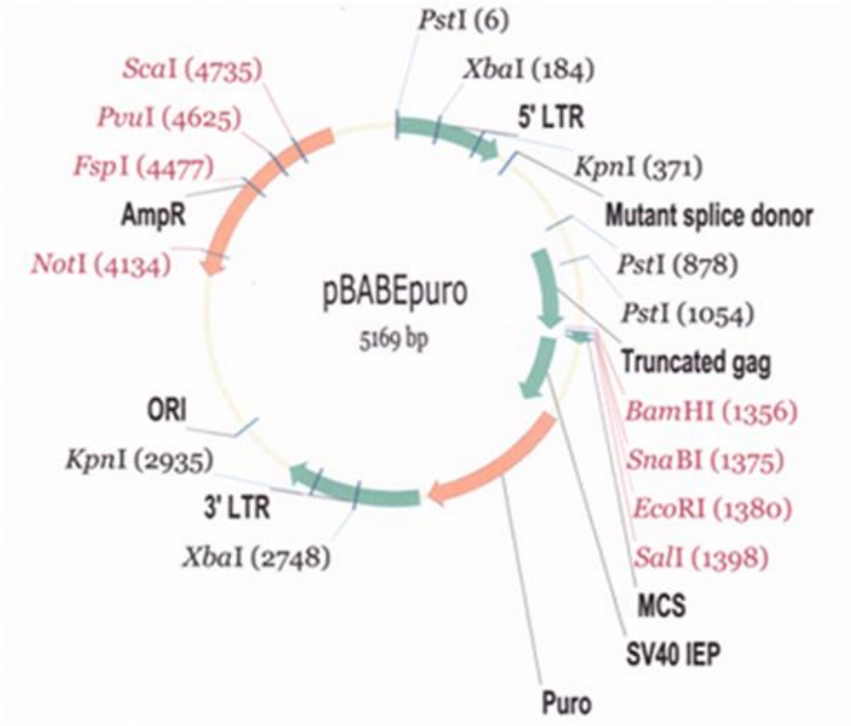

Figure 2.1 pBabe PURO Plasmid Map

2.2.1.2 pLenti6

The pLenti6 vectors are lentiviral expression vectors (a kind gift from Dr John Van Tuyn). pLenti6 vectors promote expression from a CMV promoter and contain puromycin or neomycin resistance genes to enable selection of infected cells post-transduction. To enable propagation of the vectors in bacterial cells, pLenti6 vectors also contain a bacterial origin of replication (ORI) and an ampicillin resistance gene.

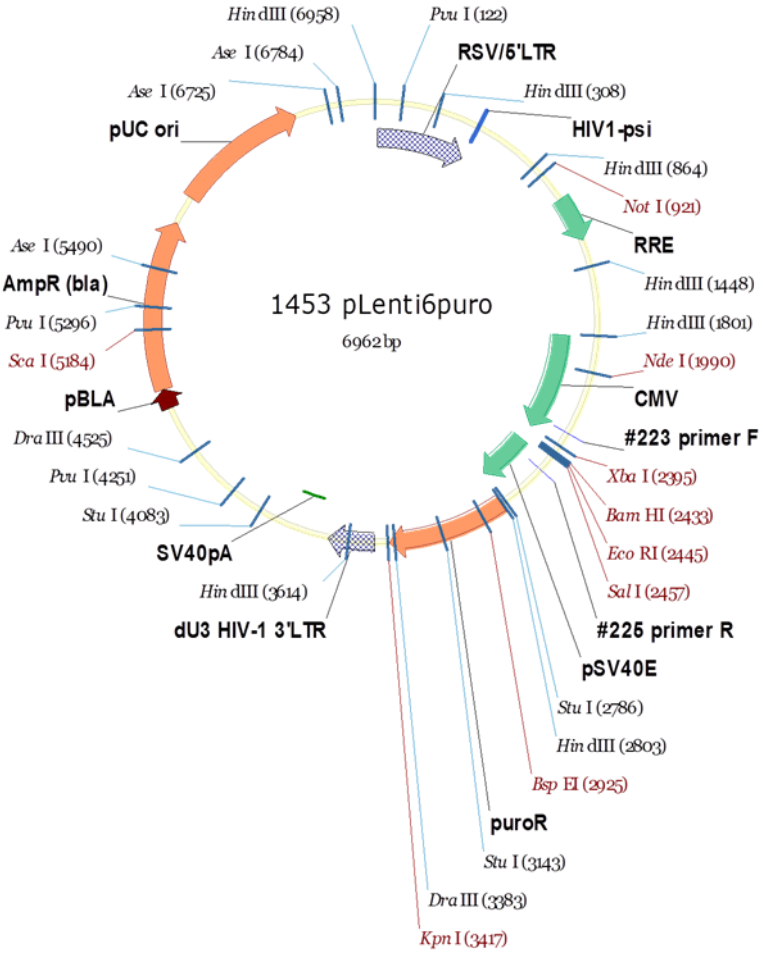

Figure 2.2 pLenti6PURO Plasmid Map

2.2.1.3 psPAX2

psPAX2 is a lentiviral helper plasmid expressing the HIV gag, pol, tat and rev genes. Gag, pol and env encode viral structural proteins required to assemble a functional virus while rev is involved in the regulation of viral protein expression.

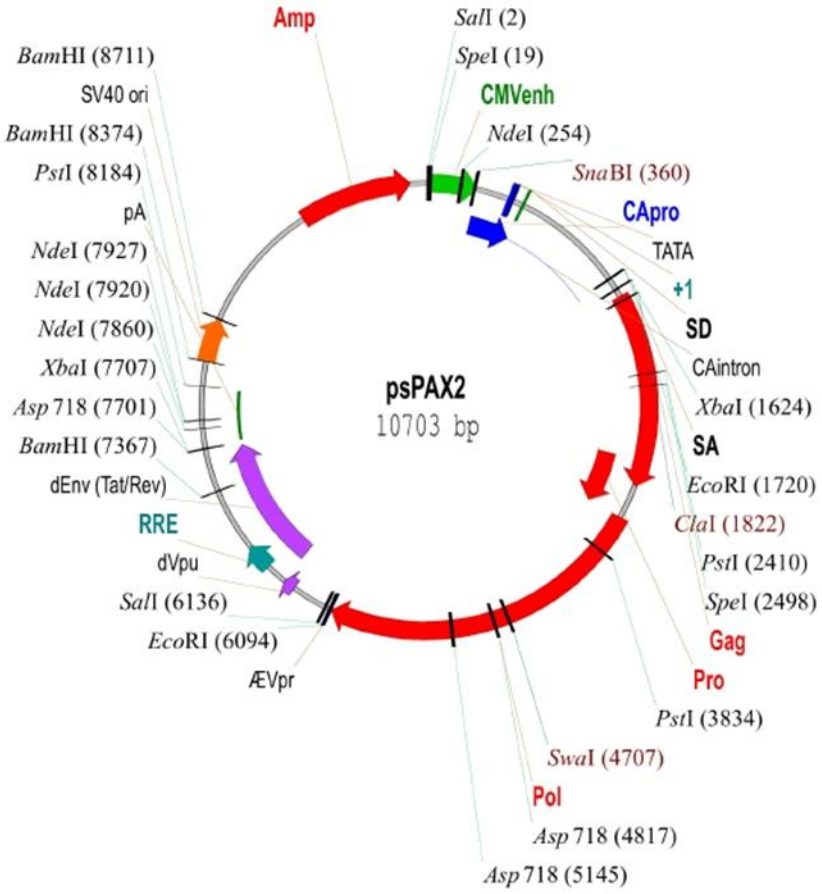

Figure 2.3 psPAX2 Plasmid Map

2.2.1.4 pCMV-VSVG

pCMV-VSVG is a lentiviral helper plasmid expressing the G-glycoprotein of vesicular stomatitis virus (VSV-G) under the control of a CMV promoter. The VSV-G protein facilitates the fusion of viral and cellular membranes by interacting with phospholipids on the surface of the target cell.

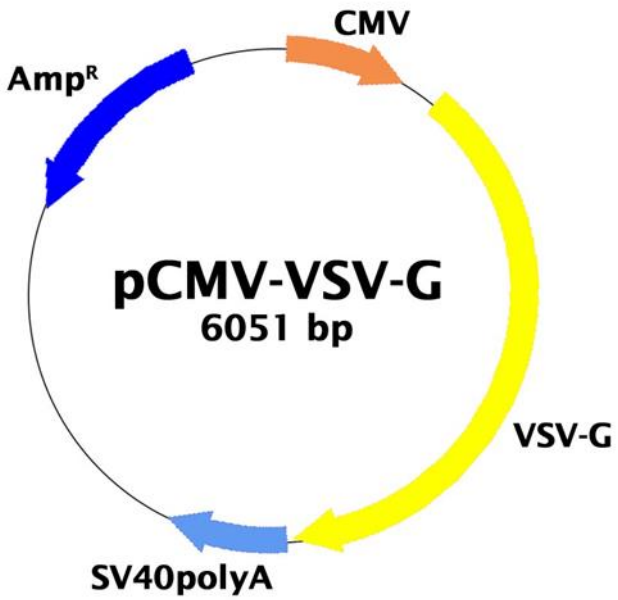

Figure 2.4 pCMV-VSVG Plasmid Map

2.2.2 Bacterial Work

2.2.2.1 Bacterial strains

Bacteria were cultured in LB broth or on LB agar plates supplemented with ampicillin (100µg/ml) as described in Table 1.

Bacteria	Culture Conditions	Plasmid
Top10 Chemically Competent *E.coli* (Invitrogen)	37°C for 16 hours	pBabePURO, psPAX2, pCMV-VSVG
JM110 Chemically Competent *E.coli* (Agilent)	37°C for 16 hours	pLentiPURO/pLentiNEO for XbaI cloning
Stbl2 Chemically Competent *E.coli* (Invitrogen)	30°C for 48 hours	Cloned pLentiPURO/pLentiNEO

Table 1.1 Chemically Competent *E.coli*

2.2.2.2 Bacterial Transformation

Chemically competent *E.coli* were transformed with 1-10ng of plasmid DNA in accordance with the manufacturers protocols. 50µl of transformed cultures were spread on LB agar plates supplemented with ampicillin (100µg/ml).

2.2.2.3 Glycerol Stocks

Glycerol stocks were prepared by mixing 200µl glycerol with 800µl of culture with ampicillin to make a 20% glycerol mixture for storage at -80°C.

2.2.3 DNA

2.2.3.1 Miniprep

Sterile bijoux tubes with 2ml lysogeny broth (LB) with 100µg/ml ampicillin were inoculated with bacteria using a sterile pipette tip. Cultures were incubated with shaking as described in Table1. 1.5ml of each culture was harvested by centrifugation and DNA was extracted using the Qiaprep Miniprep kit (Qiagen) according to the manufacturer's instructions.

2.2.3.2 Maxiprep

200ml LB media supplemented with 100µg/ml ampicillin were inoculated with 500µl of miniprep culture or a sterile loop dipped in glycerol stock. Cultures were incubated with shaking as described in Table 1. Bacteria were pelleted by centrifugation at 4°C at 4000g for 20 minutes. DNA isolation was performed using the EndoFree Plasmid Maxi Kit (Qiagen) in accordance with the manufacturer's protocol.

2.2.3.3 Determining DNA Concentration

DNA concentration was determined using the Nanodrop 2000 Spectrophotometer (Thermo Scientific). TE buffer or ddH_2O were used as a blank where appropriate.

2.2.3.4 Gel Electrophoresis of DNA

Agarose powder was melted in 1xTAE buffer (40mM Tris, 20mM acetic acid and 1mM EDTA) to give a 1% or 1.5% agarose gel which was set and submerged in 1xTAE buffer. DNA samples were diluted with distilled water or TE buffer (Qiagen) to give 1µg of DNA in a final volume of 20µl to which 5ul of sample loading buffer was added. Samples were loaded alongside a DNA ladder (1kb or 10kb) and gels run at 100 volts for 60-90 minutes. The gel was removed to a container, submerged in 1xTAE supplemented with ethidium bromide (0.5µg/ml) and incubated at room temperature with shaking for 20 minutes. The gel was de-stained for 10-20 minutes in ddH_2O and visualised on a transilluminator.

2.2.3.5 DNA Purification from Gel

A long-wave UV light source was used to identify the desired DNA fragment which was excised from the gel using a clean scalpel and purified using the

QiaQuick Gel Extraction kit (Qiagen) in accordance with the manufacturer's instructions.

2.2.3.6 DNA Sequencing

DNA sequencing was performed by Source Bioscience. Plasmid solutions were diluted with ddH_2O to give a concentration of 100ng/µl and primers were diluted to a concentration of 3.2pmol/µl. A minimum of 5µl each of sample and primer were included per reaction. DNA sequencing was subsequently analysed using CLC workbench to confirm that the correct sequence was present.

2.2.4 Viral Vectors

2.2.4.1 Cloning

Inserts encoding RUNX1P1, RUNX1P2, RE, RE9a, DNHR3, DNHR4, mNHR3, TR and TR K99R were subcloned into lentivirus vectors. The inserts encoding RUNX1P1, RUNX1P2, TR and TR K99R were excised from the pBabePURO retroviral vector by restriction digest with *EcoRI*. RE was excised from a pCMV vector (a kind gift from Professor Scott Heibert) by restriction digest by *XbaI*. DNHR3, DNHR4 and mNHR3 were inserted into Topo subcloning vectors and excised using a *SalI* restriction enzyme.

Digested fragments were separated by gel electrophoresis, purified using the QiaQuick Gel Extraction Kit (Qiagen) and resuspended in 20µl TE buffer. The pLenti vectors were simultaneously digested using appropriate restriction enzymes (New England Biolabs) and purified as described. The cut vector was treated with Antarctic phosphatase (New England Biolabs) to prevent religation, according to the manufacturer's instructions. The excised inserts were ligated into the pLenti backbones using the Quick Ligation Kit (New England Biolabs) in accordance with the manufacturer's protocol. Transformation of competent bacteria was performed as described. Up to 12 colonies of the transformed bacteria were picked and inoculated into LB broth for miniprep. Minipreps were screened for successful clones by diagnostic restriction digest, confirmed by sequencing and maxipreps performed.

2.2.4.2 Lentiviruses

2.2.4.2.1 Production of a Concentrated Lentivirus Stock

293T cells were plated at $11x10^6$ cells in T150 flasks and incubated overnight. 293T cells were transfected with lentiviral plasmids (20 µg pLenti6PURO, 8µg psPAX2 and 5µg pCMV-VSVG) using Lipofectamine 2000 (Invitrogen) according to the manufacturer's instructions. Viral supernatants were collected 48 hours and 72 hours post-transfection and filtered through 0.45µm filters. Supernatants were concentrated by ultracentrifugation for 2 hours at 166880g. Supernatant was discarded and the pelleted virus resuspended in PBS overnight at 4°C with shaking. Virus was frozen rapidly on dry ice and stored at -80°C in 20µl aliquots.

2.2.4.2.2 Calculating Lentivirus Concentration

NIH 3T3 cells were seeded at $8x10^3$ per well in 12-well plates, incubated overnight, then the cells were fed with 1ml complete media supplemented with polybrene (4µg/ml). Virus was thawed rapidly at 37°C and agitated to resuspend particles. 11µl of virus stock were added to one well and mixed. A series of 1:5 serial dilutions were performed over 6 wells and plates were incubated for 48 hours at 37°C. The virus/polybrene mixture was replaced with complete media supplemented with 2µg/ml puromycin (Sigma) and incubated for 8 days. Cells were fixed with 100% methanol for 10 minutes then washed with PBS (pH6.8) and stained with 10% Giemsa in PBS (pH6.8) for 30 minutes. The plates were washed with water and discreet colonies counted. Plaque-forming units (pfu)/µl was calculated using the following equation;

Number of Plaques x Dilution Factor

2.2.4.2.3 Lentiviral Transduction

Target cells were plated at $8x10^5$ per 10cm dish and incubated overnight at 37°C in 3% oxygen, 5% CO_2 conditions. Cells were infected with enough virus to give a mulitiplicity of infection (MOI) of 1 which indicates that there should be roughly one virus particle for every cell. Infection medium was supplemented with polybrene (4µg/ml) to improve transduction efficiency. The cells were incubated with the virus/polybrene mixture for 8-10 hours at 37°C then re-fed with complete media overnight. Cells were selected with puromycin (2µg/ml) for 5

days. Non-transduced cells died under selection, confirming successful selection. Transduced cells were plated for experimental purposes.

2.2.4.3 Retroviruses

2.2.4.3.1 Retrovirus Production

Phoenix Eco cells were plated at $5x10^6$ cells in 10cm dishes and incubated at 37°C overnight. Phoenix cells were transfected with pBabePURO expression vectors using Superfect Transfection Reagent (Qiagen) in accordance with the manufacturer's instructions. Viral supernatants were harvested after 48 hours and 72 hours and filtered through a 0.45µm filter.

2.2.4.3.2 Retroviral Transduction

Target cells were plated at $8x10^5$ cells in 10cm dishes and incubated overnight. Cells were infected using harvested (48 hour) viral supernatant supplemented with polybrene (4µg/ml) for 24 hours and then with the 72 hour supernatant for 8 hours. Supernatants were replaced with complete medium overnight then re-fed with selection medium with puromycin (2µg/ml). After 5 days, puromycin resistant cells were counted and re-plated for experimental work.

2.3 Protein Analysis

2.3.1 Protein Extraction

2.3.1.1 Whole Cell Lysis

Cell pellets were lysed in 100µl lysis buffer per 10^6 cells. Buffers used were whole cell lysis (WCL) buffer (Section 2.7.1.1), immunoprecipitation lysis buffer or radioimmunoprecipitation assay (RIPA) buffer (Section 2.7.1.2). Lysates were incubated at 4°C with rotation for 10 minutes and centrifuged for 30 minutes at 20000g. Supernatants were transferred to a fresh, cold eppendorf. Protein concentrations were determined (See Section 2.3.2) and lysates stored at -80°C.

2.3.1.2 Whole Cell Fractionation

Cell pellets were lysed using lysis buffer 1 (Section 2.7.2.1) and homogenised using a 21G needle to ensure cells were lysed but nuclei remained intact. Samples were then transferred to clean eppendorf tubes. Nuclei were pelleted by centrifugation at 3000g for 10 minutes. The supernatants were retained and

transferred to clean tubes. Nuclei were washed again in lysis buffer 1 and pelleted by centrifugation at 3000g for 10 minutes. The supernatant was again retained and combined with supernatant from the previous step. The pelleted nuclei were washed with 500µl nuclear lysis buffer 1 (Section 2.7.2.3) and centrifuged for 5 minutes at 370g. This was repeated twice before the nuclear pellet was resuspended in Nuclear Lysis Buffer 2 (Section 2.7.2.4) and labelled as the "Nuclear Fraction". The supernatants retained after cell lysis were centrifuged at 5000g for 15 minutes and then ultracentrifuged for 1 hour at 100,000g to pellet membrane-associated proteins. Supernatants were retained and labelled as the "cytoplasmic fraction". Pelleted membrane proteins were washed with 0.5mM Tris-HCL then dissolved in 500µl of membrane lysis buffer (Section 2.7.2.2) and centrifuged at 20000g for 15 minutes. Supernatants were stored in fresh tubes and labelled as the "membrane fraction". All centrifuge spins were performed at 4°C.

2.3.1.3 His-Affinity Purification

Cell pellets were lysed with 1ml of guanidinium lysis buffer (GLB) (Section 2.7.3.1) per $1x10^8$ cells. Samples were kept on ice and sonicated on 10% amplitude for one minute (Branson Digital). This was repeated four times for each sample. Lysed samples were centrifuged for 7 minutes at 3800g and filtered through a 0.45µm syringe filter. 20µl Nickel NTA agarose beads were washed twice in 500µl GLB and centrifuged for 2 minutes at 955g to pellet the beads. Samples were then added to the washed beads and the mixture rotated at 4°C for 16 hours, centrifuged for 5 minutes at 955g and the supernatant discarded. Beads were washed as follows, once with 500µl GLB, twice with pH8 Wash Buffer (Section 2.7.3.2, twice with pH6.3 wash buffer (2.7.3.3) and once with pH8 wash buffer with centrifugation as before. Residual buffer was removed from the beads before they were resuspended in 40µl of elution buffer (Section 2.7.4.1). The tubes were agitated for 10 minutes at room temperature before the samples were boiled at 100°C for 2 minutes. Boiled samples were stored at -20°C.

2.3.2 Determining Protein Concentration

Bovine serum albumin (BSA) protein standard was diluted using ddH_2O to give a standard curve (0.2mg/ml to 1.4 mg/ml). The Bicinchoninic Acid (BCA) Protein Assay Dye Concentrate (Bio-Rad) was diluted 1:5 with dH_2O and filtered through 1mm filter paper (Whatman). Samples were diluted 1/500 in the prepared dye and incubated in sterile cuvettes for 5 minutes at room temperature. OD_{595} was determined against a blank of ddH_2O with diluted Protein Assay Dye Concentrate. Concentrations were determined using a standard curve produced from the BSA standards.

2.3.3 Western Blot

Whole cell lysates were diluted with ddH_2O to 30µg protein per 20µl. Samples were supplemented with 2µl Sample Reducing Agent (Invitrogen) and 5µl Sample Buffer (Invitrogen) and denatured at 70°C for 10 minutes. Samples were loaded into pre-cast NuPAGE™ Novex™ 4-12% Bis-Tris Gels (Life Technologies) which were run at 35mA in MOPs SDS running buffer (NP0001, Life Technologies) diluted to 1x concentration with ddH_2O until the dye front reached the bottom of the gel.

Protein transfer was performed by wet-blotting of gels onto a nitrocellulose membrane (Amersham). The transfer was set up in a cassette as described in **Figure 2.5,** submerged in transfer buffer (Section 2.7.4.1) and performed for 1 hour at 100 volts. The nitrocellulose membrane was blocked in 1xTBST (Section 2.7.4.2) with 5% fat-free milk powder (Marvel) for 1 hour at room temperature or 4°C overnight.

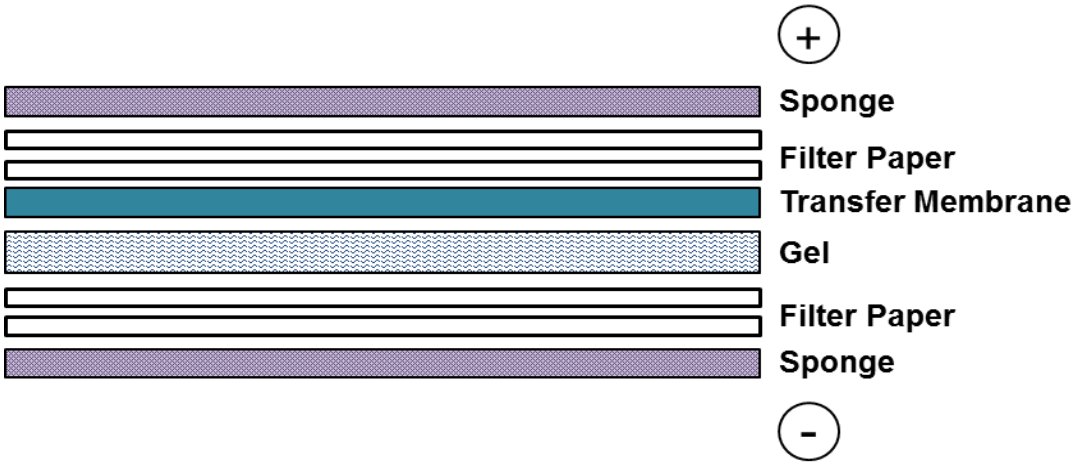

Figure 2.5 Western Blotting Transfer Sandwich

2.3.4 Protein Detection

Blocked membranes were washed 3 x 10 minutes in 1xTBST with shaking. Primary antibodies were diluted in 1xTBST with 5% milk powder or 5% BSA as specified in **Section 2.8**. Membranes were incubated in the primary antibody with shaking for 1-2 hours at room temperature or overnight at 4°C. The membrane was washed as above then incubated with the appropriate HRP-linked secondary antibody for 1 hour at room temperature with shaking. The membrane was washed as previously specified prior to using ECL chemiluminescent substrate (Pierce) to detect HRP-linked secondary. Western blots were subsequently developed in a dark room using ECL film. Band densitometry was determined using ImageJ software.

2.3.5 Membrane Stripping

Membranes were submerged in a mild stripping buffer (Section 2.7.4.3) and incubated at room temperature with shaking for 1 hour. Membranes were then washed 3 x 10 minutes with 1xTBST and blocked with 1xTBST with 5% milk powder.

2.4 Immunofluorescence

Glass coverslips or chamber slides were covered with 13.3µg/ml poly-L-lysine in ddH_2O and incubated overnight at 37°C before the mixture was decanted and the slides dried in a sterile laminar flow hood before being washed with PBS.

Cells were plated on the poly-L-lysine coated glass chamber slides or coverslips and incubated for 1-6 days. Cells were fixed with 4% paraformaldehyde in PBS for 15 minutes at room temperature then washed three times with PBS and permeabilised with 3 x 10 minute incubations with 0.1% Triton-X-100 in PBS. Cells were blocked for an hour with blocking buffer (10% FCS and 0.1% Triton-X-100 in PBS) and incubated overnight at 4°C with the appropriate primary antibody diluted in blocking buffer (Section 2.8.1). Slides were washed 2 x 5 minutes with 0.1% Triton-X-100 in PBS and 1 x 5 minutes in blocking buffer. Slides were incubated with a secondary antibody (Section 2.8.2) diluted in blocking buffer (1:100) at room temperature in the dark for 1 hour. Slides were mounted using Vectashield hard-set mounting medium with DAPI (Vector Laboratories) and imaged using an LSM Confocal 710 (Zeiss).

2.5 Cytokine Detection

2.5.1 ELISA

Cells were plated out at $2.5x10^4$ in 12-well plates and fed with fresh media every 3 days. On day 6 post-selection, the cell culture medium was harvested and stored at -80°C and the cells were counted. Harvested media was thawed rapidly at 37°C. A Quantikine IL-6 ELISA (R & D Systems) was performed in accordance with the manufacturer's protocol. Plates were analysed at 450nm using an ELISA plate reader. Plates were additionally read at 540nm to remove background fluorescence. The values were normalised to cell count and final values were normalised to the empty vector control.

2.5.2 Cytokine Array

Cells were plated out at $2.5x10^4$ in 12 well plates. At 4 days post-selection, complete DMEM was replaced with DMEM supplemented with 0.2% FCS. At 6 days post selection, the cell culture medium was harvested and stored at -80°C. Harvested supernatant was thawed rapidly at 37°C. Supernatants were diluted to control for cell-number using DMEM with 0.2% FCS and applied to a human cytokine array chip (RayBiotech) and treated as specified in the manufacturer's guidelines. Slide reading and was performed by RayBiotech using a 532nm laser. Fluorescence was normalised to remove background fluorescence.

The following cytokines were measured using this array;

Acrp30	Fractalkine	IL-16	MIP-3beta
AgRP	GCP-2	IL-17	MSP-alpha
Amphiregulin	GCSF	IL-1alpha	NAP-2
Angiogenin	GDNF	IL-1beta	NT-3
Angiopoietin-2	GITR	IL-1ra	NT-4
Axl	GITR-Ligand	IL-2	Oncostatin M
BDNF	GM-CSF	IL-2 Rapha	Osteoprotegerin
bFGF	GRO	IL-3	PARC
BLC	GRO-alpha	IL-4	PDGF-BB
BMP-4	HCC-4	IL-5	PIGF
BMP-6	HGF	IL-6	RANTES
b-NGF	I-309	IL-6 R	SCF
BTC	ICAM-1	IL-7	SDF-1
CCL-28	ICAM-3	IL-8	sgp130
CK beta 8-1	IFN-gamma	I-TAC	sTNF RII
CNTF	IGFBP-1	Leptin	sTNF-RI
CTACK	IGFBP-2	LIGHT	TARC
Dtk	IGFBP-3	Lymphotactin	TECK
EGF	IGFBP-4	MCP-1	TGF-beta 1
EGF-R	IGFBP-6	MCP-2	TGF-beta 3
ENA-78	IGF-I	MCP-3	Thrombopoietin
Eotaxin	IGF-I SR	MCP-4	TIMP-1
Eotaxin-2	IL-1 R4/ST2	M-CSF	TIMP-2
Eotaxin-3	IL-1 RI	MDC	TNF-alpha
Fas/TNFRSF6	IL-10	MIF	TNF-beta
FGF-4	IL-11	MIG	TRAIL R3
FGF-6	IL-12 p40	MIP-1alpha	TRAIL R4
FGF-7	IL-12 p70	MIP-1beta	uPAR
FGF-9	IL-13	MIP-1-delta	VEGF
Flt-3 Ligand	IL-15	MIP-3-alpha	VEGF-D

2.6 Statistical Tests

Charts and graphs display the mean of at least 3 independent replicates ± Standard Deviation (SD). Statistical significance in histograms was calculated using the analysis of variance (ANOVA) statistical test to analyse the difference between transduced cells relative to the empty vector control (PURO) cultures. P-values are denoted using asterisks (* $p<0.05$, ** $p<0.01$, *** $p<0.001$).

2.7 Buffers and Solutions

2.7.1 Cell Lysis Buffers

2.7.1.1 Whole Cell Lysis Buffer (WCL)

20mM Hepes (pH 7.0), 5mM EDTA, 10mM EGTA, 5mM NaF, 1mM DTT, 0.4% Triton-X-100, 10% Glycerol. WCL was aliquoted and stored at -20°C. It was supplemented immediately prior to use with 0.1µg/ml okadaic acid (OA) and protease inhibitors as follows; 5µg/ml aprotinin, 5µg/ml leupeptin, 5µg/ml pepstatin-A, 1mM benzamidine, 50µg/ml PMSF.

2.7.1.2 Radioimmunoprecipitation Assay Buffer (RIPA)

150mM NaCl, 1% NP40, 0.5% DOC, 0.1% SDS, 50mM Tris (pH8.0). Aliquoted and stored at -20°C. Supplemented immediately prior to use with 0.1µg/ml OA and protease inhibitors as follows; 5µg/ml aprotinin, 5µg/ml leupeptin, 5µg/ml pepstatin-A, 1mM benzamidine, 50µg/ml PMSF.

2.7.1.3 Immunoprecipitation Lysis Buffer

150mM NaCl, 50mM Tris (pH8.0), 5mM EDTA, 0.5% NP40. Aliquoted and stored at -20°C. Immediately prior to use, ILB was supplemented with 1mM DTT, 0.2mM sodium orthovanadate (Na_3VO_4), 10µg/ml leupeptin, 2.5µg/ml pepstatin-A, 1mM PMSF, 10µg/ml aprotinin, 10mM ß-glycerophosphate.

2.7.2 Cell Fractionation Buffers

2.7.2.1 Lysis Buffer 1

10mM Tris/HCl (pH7.5), 0.5mM EDTA, 0.3M sucrose. Aliquoted and stored at -20°C. Supplemented prior to use with 1mM Na_3VO_4, 50µg/ml PMSF

2.7.2.2 Membrane Lysis Buffer

20mM HEPES (pH7.0), 150mM NaCl, 0.5% NP40. Aliquoted and stored at -20°C Supplemented prior to use with 1mM Na_3VO_4, 50µg/ml PMSF, 5µg/ml pepstatin-A, 5µg/ml leupeptin, 1mM benzamidine, 5µg/ml aprotinin, 0.1µg/ml OA.

2.7.2.3 Nuclear Lysis Buffer 1

10mM HEPES (pH7.0), 60mM KCl, 1mM EDTA.

2.7.2.4 Nuclear Lysis Buffer 2

10mM Hepes (pH7.0), 60mM KCl, 1mM EDTA, 1% NP40.

2.7.3 Nickel Affinity Purification Buffers

2.7.3.1 Guanidinium Lysis Buffer

6M guanidinium hydrochloride, 94.7mM Na_2HPO_4, 5.3mM NaH_2PO_4, 10mM Tris/HCl (pH8.0), 20mM imidazole, 5mM ß-mercaptoethanol, EDTA-free protease inhibitor cocktail (Roche).

2.7.3.2 Wash Buffer (pH 8.0)

8M urea, 94.7mM Na_2HPO_4, 5.3mM NaH_2PO_4, 10mM Tris/HCl (pH8.0), 5mM ß-mercaptoethanol, EDTA-free protease inhibitor cocktail (Roche).

2.7.3.3 Wash Buffer (pH 6.3)

8M urea, 22.5mM Na_2HPO_4, 77.5mM NaH_2PO_4, 10mM Tris/HCl (pH8.0), 5mM ß-mercaptoethanol, EDTA-free protease inhibitor cocktail (ensure pH6.3, adjust if necessary).

2.7.3.4 Elution Buffer

200mM Imidazole, 2x LDS (Invitrogen), 1x reducing agent (Invitrogen).

2.7.4 Western Blot Buffers

2.7.4.1 Transfer Buffer

Transfer buffer was made as a 10x solution (1.92M glycine and 250mM Tris) and diluted using ddH_2O and methanol to give a 1x solution containing 20% methanol.

2.7.4.2 TBST

TBST was made as a 10 x solution (0.1M Tris-Base, 1.5M NaCl, 0.5% Tween-20). It was adjusted to pH8.0 and diluted using ddH_2O to make a 1x solution prior to use.

2.7.4.3 Membrane Stripping Buffer

0.2M glycine (pH2.5), 1% SDS. Made fresh prior to use.

2.8 Antibodies

Antibodies were diluted in TBST with 5% skimmed milk powder unless stated otherwise.

2.8.1 Primary Antibodies

2.8.1.1 Santa Cruz Biotechnology., Inc

Anti-Actin, sc1616 (1:1000)

Anti-p53, sc-126 (1:1000)

Anti-p16, sc-468 (1:1000)

2.8.1.2 Medical and Biological Laboratories Co., Ltd

Anti-RUNX, D207-3 (1:1000)

2.8.1.3 Cell Signalling Technology

Anti-p38P, 9211 (1:1000 in 5% BSA)

Anti-p38 (Total), 9212 (1:1000)

Anti-HA, C29F4 (1:100 in 10% FCS and 0.1% Triton-X-100 in PBS for confocal).

2.8.1.4 Abcam

Anti-Calnexin, ab22595 (1:1000)

Anti-His, ab18184 (1:1000 for western blot and 1:200 in 10% FCS and 0.1% Triton-X-100 in PBS for confocal).

2.8.1.5 MerckMillipore

Anti-ϒH2AX, JBW301 (1:200 in 10% FCS and 0.1% Triton-X-100 in PBS for confocal)

2.8.2 Secondary Antibodies

2.8.2.1 DAKO Ltd

Polyclonal Swine anti-rabbit Immunoglobulins/HRP (1:3000)

Polyclonal rabbit anti-mouse immunoglobulins/HRP (1:1000)

Polyclonal rabbit anti-goat immunoglobulins/HRP (1:2000)

2.8.2.2 Stratech Scientific Ltd

FITC-conjugated Sheep anti-mouse IgG (1:200 in 10% FCS and 0.1% Triton-X-100 in PBS for confocal).

2.9 General Chemicals

General chemicals were molecular grade quality and were supplied by Sigma, Thermo-Fisher, Invitrogen or VWR Prolabo unless stated otherwise.

3 RUNX1-ETO9a Fails to Induce Premature Senescence in Primary Cells

3.1 Introduction

The RE fusion protein generated by the t(8;21) chromosomal translocation is associated with 40% of AML (M2 subtype) [233]. Despite this strong association with AML in humans, expression of RE is insufficient to induce leukaemia in retroviral transduction/transplantation mouse models [76]. Furthermore, It has been suggested that the t(8;21) fusion is an early event and that it persists for a long period of time before leukaemia develops. Indeed, studies in CD34+ cells have demonstrated that retroviral expression of RE results in a growth arrest that is eventually overcome by a more primitive population of cells. However, this cell population is not transformed, further supporting the suggestion that RE itself is insufficient for leukaemogenesis to occur [82]. A study of a RE retroviral transduction/transplantation model found that the only mouse in the study to develop leukaemia was expressing a spontaneous truncated RE mutant [98]. Moreover, an alternatively spliced variant of RE, RE9a has since been identified and is commonly co-expressed with RE in t(8;21) leukaemias [80]. In contrast to RE, RE9a is a potent inducer of leukaemia in mouse model systems with RE9a-expressing mice developing leukaemia within weeks [80]. This may indicate that expression of RE9a is a key leukaemia promoting factor in RE-associated disease.

RE has been identified as a potent inducer of premature SLGA in primary human fibroblasts. As studies have identified premature senescence as a potent tumour-suppressor mechanism, the finding that RE induces a robust SLGA may correlate with its lack of leukaemogenic potential in murine models [59]. To determine whether the increased leukaemogenic potential of RE9a is linked to an evasion of this anti-cancer failsafe mechanism, RE9a was introduced into human and murine primary fibroblasts and the cells examined for markers of premature senescence.

Aims and Objectives

- To examine whether primary cells transduced to express RE9a undergo premature senescence.
- To compare the phenotype of RE9a and RE-expressing cells with respect to markers of premature senescence. These will include cellular proliferation, SA-β-Gal staining activity and activation of the p53 and $p16^{INK4a}$ tumour suppressor pathways.

3.2 Results

3.2.1 RUNX1-ETO9a Fails to Induce Premature Senescence in Primary Cells

Lentiviral vector constructs containing RE or RE9a were used to transduce primary human foreskin fibroblasts (Hs68 cells). The empty vector expressing a puromycin resistance gene was included as a control and will be referred to as PURO. Following selection, puromycin resistant cells were replated for a further 6-10 days and the cells monitored for growth, morphology and the appearance of senescence markers. Day 0 refers to the day of replating after the selection period.

To determine the ectopic expression levels of RE and RE9a, western blots were performed on samples collected on day 0. Expression of RE was lower than RE9a but exceeded that of endogenous RUNX1 in Hs68 cells (**Figure 3.1 a**). As previously reported, expression of RE was associated with a rapid and profound growth arrest. In contrast, RE9a-expressing cells continued to proliferate at a comparable rate to the PURO controls (**Figure 3.1 b**). RE-induced SLGA was accompanied by a characteristic flat and enlarged cellular morphology frequently associated with cellular senescence, and positive staining for SA-β-Gal. PURO and RE9a cultures retained a spindle-shaped fibroblastoid morphology and displayed very little SA-β-Gal staining (**Figure 3.1 c**). Together, these data suggest that expression of RE9a failed to induce premature senescence *in vitro*.

The p53 and $p16^{INK4a}$ tumour suppressor pathways have previously been identified as key drivers of premature senescence in primary human fibroblasts [126]. To determine whether RE9a-mediated evasion of senescence is accompanied by inactivation of either of these pathways, western blots were performed on samples collected 6 days after puromycin selection, when visible

signs of senescence such as altered morphology and SA-ß-Gal staining were apparent. In contrast to a previous study using a retroviral expression system [59], $p16^{INK4a}$ was highly expressed in the presence of RE (**Figure 3.1 d (i) and (ii)**) while p53 expression was only modestly induced (**Figure 3.1 e (i) and (ii)**). Neither $p16^{INK4a}$ nor p53 were upregulated by RE9a, suggesting that failure to activate these key pathways underlies bypass or escape from premature senescence in RE9a-expressing Hs68s.

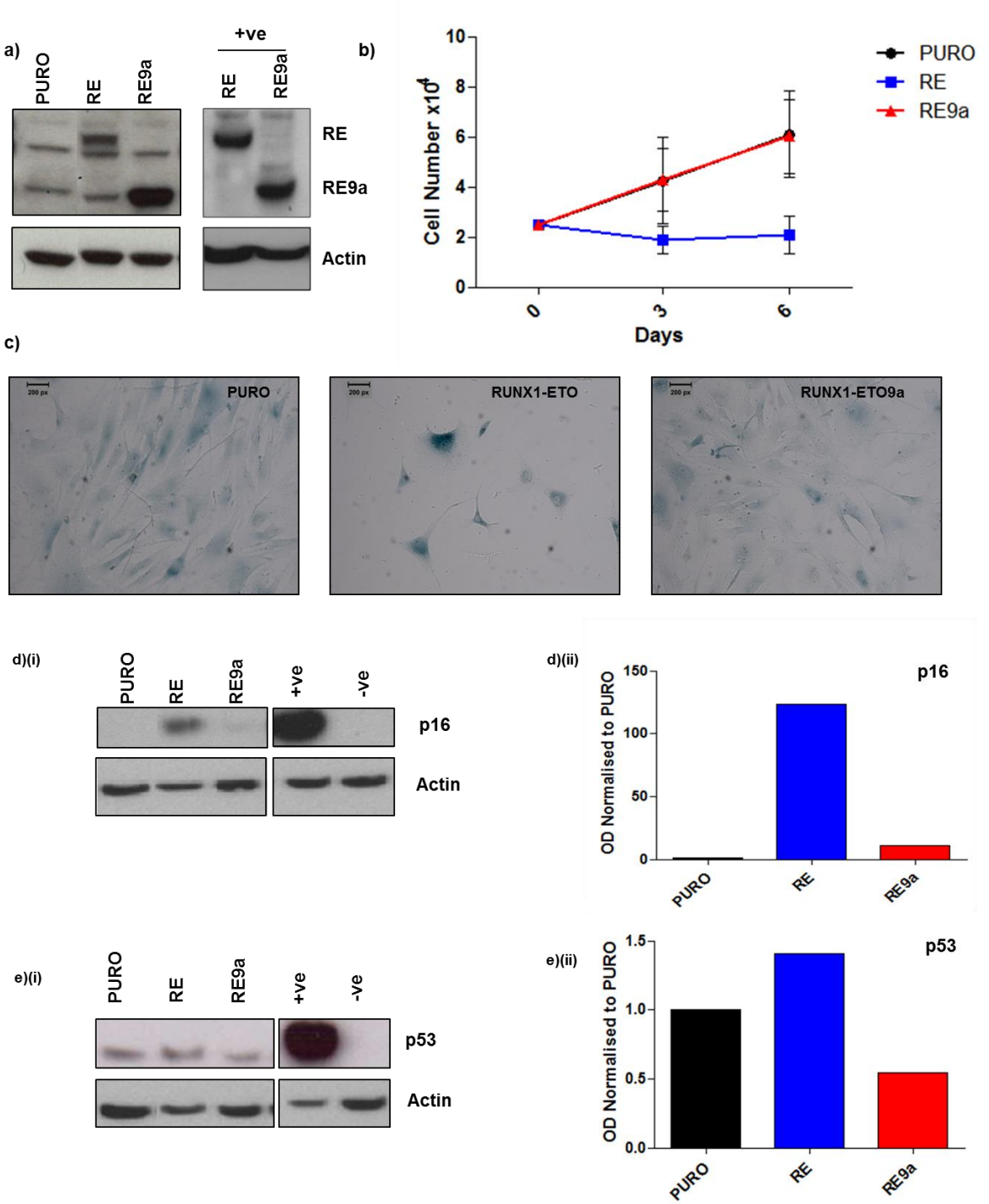
a)
PURO
RE
RE9a
+ve
RE
RE9a
RE
RE9a
Actin
b)
Cell Number x10^4
Days
PURO
RE
RE9a
c)
PURO
RUNX1-ETO
RUNX1-ETO9a
d)(i)
PURO
RE
RE9a
+ve
-ve
p16
Actin
d)(ii)
p16
OD Normalised to PURO
PURO
RE
RE9a
e)(i)
PURO
RE
RE9a
+ve
-ve
p53
Actin
e)(ii)
p53
OD Normalised to PURO
PURO
RE
RE9a

Figure 3.1 RUNX1-ETO9a fails to induce premature senescence in primary human fibroblasts

Hs68 human fibroblasts were transduced with lentiviral vectors containing RE or RE9a. The empty vector (PURO) was included as a negative control. Transduced cells were selected using Puromycin. The results shown are representative of three biological replicates. (a) Western blot analysis of ectopic RE (83 kDa) and RE9a (62 kDa) in transduced Hs68 cells using an anti-RUNX antibody (D207-3, MBL Ltd). GP86 cells transduced to express RE and RE9a were included as positive controls. (b) Representative growth curves showing cell proliferation measured over 6 days. Plots show the mean of three independent replicates and error bars show standard deviation. (c) Images captured after staining cells 6 days post-transduction for SA-β-Gal activity at pH6.0. Images were captured with a 20x magnification. Western blot analysis of expression of (d(i)) $p16^{INK4a}$ (sc-468, Santa Cruz Biotechnology Inc) and (e(i)) p53 (sc-126, Santa Cruz Biotechnology Inc) in transduced Hs68 cells 6 days post-selection. Quantification of (d(ii)) $p16^{INK4a}$ and (e(ii)) p53 as determined by measuring the densitometry of bands on the adjacent western blots using ImageJ software and normalising the optical densitometry (OD) values to those obtained for the actin loading control.

3.2.2 RUNX1-ETO9a fails to induce a sustained growth arrest in primary MEFs

Murine embryonic fibroblasts (MEFs) senesce more rapidly than their human counterparts due to their relatively high sensitivity to cellular stresses such oxidative stress and DNA damage [183]. However, they also have a greater capacity to escape cellular senescence due to inactivation of tumour suppressor pathways. To determine how RE9a affects senescence, primary MEFs were transduced with retroviral vectors containing RE and RE9a. An empty vector conferring resistance to puromycin was included as a negative control and will be referred to as PURO.

Equivalent expression of RE and RE9a was confirmed by western blot analysis on day 0 samples (**Figure 3.2 a**). Expression of RE was accompanied by a profound growth arrest while RE9a cultures continued to proliferate albeit at a slightly reduced rate compared to PURO (**Figure 3.2 b**). In addition, RE9a-expressing cultures displayed distinct areas of flattened, enlarged cells that appeared senescent along with clear outgrowths of fibroblastoid non-senescent cells (**Figure 3.2 c**) suggesting that RE9a is a weaker inducer of senescence in primary MEFs. To examine effects on growth in more detail, 3T3 passage culture was performed to facilitate the outgrowth of cells with secondary mutations that can immortalise primary MEFs *in vitro*[231]. To this end, 3 parallel cultures of MEFs expressing PURO, RE and RE9a were passaged every 3 days at a fixed cell density and cumulative gains in cell number calculated over 14 passages. The Puro and RE9a cultures displayed accelerated growth from passage 4 with the RE9a cultures demonstrating a higher growth rate at later time points. The RE cultures failed to show accelerated growth until after passage 8, however, after this point, cumulative gain in cell number increased at a rate equivalent to RE9a (**Figure 3.2 d**). These data suggest that MEFs expressing RE9a are more prone to accumulating secondary mutations that favour immortalisation and that this may promote escape from senescence *in vitro*.

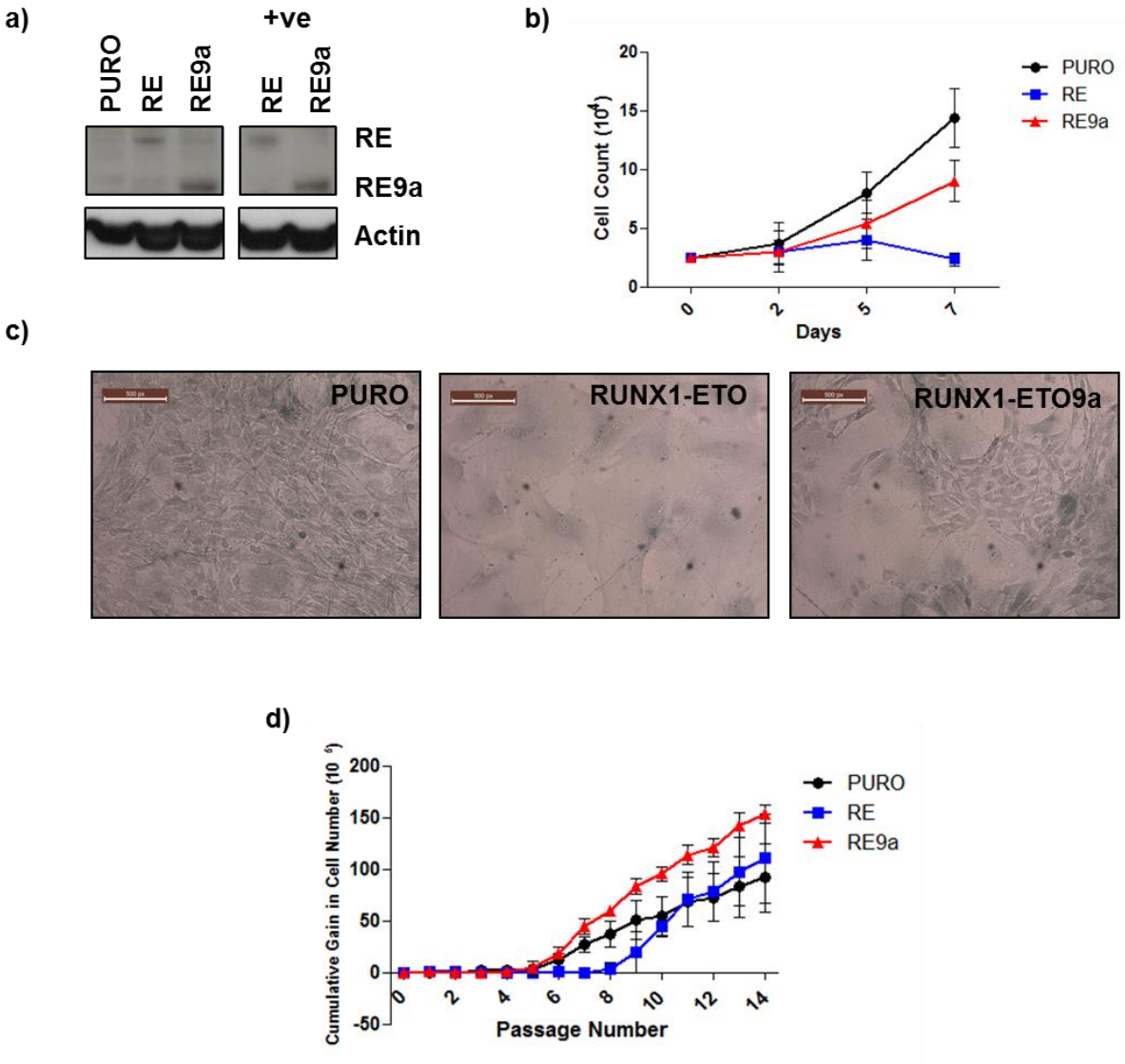

Figure 3.2 RUNX1-ETO9a induces a weak senescent phenotype in Murine Embryonic Fibroblasts (MEFs)

Murine embryonic fibroblasts (MEFs) were transduced with lentiviral vectors expressing RE or RE9a. The empty vector (PURO) was included as a negative or normal cell control. Transduced cells were selected using puromycin. Results shown are representative of three biological replicates. (a) Western blot analysis of ectopic RE (83 kDa) and RE9a (62 kDa) expression in transduced MEFs using anti-RUNX (D207-3, MBL Ltd). GP86 cells transduced to express RE and RE9a were included as positive controls. (b) Representative growth curves of transduced MEFs recorded over the 7 days following selection. Plots show the mean of three independent replicates and error bars show standard deviation. (c) Images of transduced MEFs captured 6 days post-selection showing proliferating and senescent cell populations. Images were captured using 20x magnification. (d) Plots showing cumulative gain in cell number over 14 passages in transduced MEFs subjected to 3T3 passage culture as described by Todaro and Green [231]. Plots show the mean of three independent replicates and error bars show standard deviation.

3.3 Discussion

In this study, ectopic expression of the RE9a splice variant of RE failed to induce premature senescence in primary human Hs68 fibroblasts. The cells did not display arrested growth and retained a fibroblastoid morphology with no evidence of SA-ß-Gal staining, all of which are characteristic of the senescence phenotype. Since premature senescence is a fail-safe mechanism engaged in response to certain oncogenes, the ability to overcome it may account for the greater leukaemogenic potential of RE9a *in vivo*.

Arrested growth and SA-ß-Gal staining are important hallmarks of senescence, but other factors including activation of key tumour suppressor pathways such as the p53 and $p16^{INK4a}$ axes have important roles in senescence activation and maintenance. While a previous study identified p53 as the primary effector of RE-induced SLGA in primary human fibroblasts [59], only modest induction was observed in this study. Instead, a strong induction of $p16^{INK4a}$ was observed which corroborated findings from another study, demonstrating $p16^{INK4a}$ upregulation in response to RE expression [225].

It has previously been reported that human fibroblasts lacking $p16^{INK4a}$ are resistant to RAS-induced senescence suggesting that $p16^{INK4a}$ has a more significant role in human cell senescence than p53 [234]. In contrast, it was also reported that $p16^{INK4a}$ null human fibroblasts are sensitive to RE-induced SLGA when expression is driven from a retroviral vector [59]. The disparity between this study and our own might be explained by the use of different vector delivery systems. Wolyniec et al, [59] used an ecotropic murine retroviral vector to transduce Hs68 fibroblasts while this study relied on a lentiviral transduction system. It has previously been reported that p53 induction in response to reactive oxygen species comprises part of an anti-retroviral response in murine astrocytes [235]. Lentiviral vectors, in contrast, encode factors that significantly abrogate antiviral mechanisms and may effectively blunt the p53 response [236, 237]. In addition, Wolyniec et al used Hs68 cells that have been engineered to express an ecotropic receptor [59]. It is possible that this extra level of genetic manipulation had altered their response to RE compared to the parental Hs68 cells. More importantly, however, RE9a failed to induce either p53 or $p16^{INK4a}$ suggesting that failure to fully activate one or both of these tumour suppressor

pathways is critical for escape from RE-induced SLGA and may contribute to the leukaemogenicity of this protein in vivo.

Early studies led to the assumption that senescence is an irreversible process [140-142], but more recent data clearly show that escape from senescence can occur as a result of inactivation of key tumour suppressor pathways including p53 and $p16^{INK4a}$ and can contribute to cellular transformation *in vitro* and *in vivo* [127, 143-145]. This interpretation is supported by evidence from studies in primary MEFs [183, 238]. Premature senescence is engaged in response to a wide range of oncogenes but cells can escape this failsafe mechanism when passaged routinely to facilitate the accumulation of secondary mutations commonly manifested by loss of $p16^{INK4a}$ or p53. When RE9a was introduced into primary MEFs, both fibroblastoid and flat, enlarged senescent cells were observed and the overall growth rate was intermediate between RE-expressing and control cultures. Moreover, growth was accelerated when the cells were subjected to 3T3 passage culture [231]. Significantly, although RE-expressing MEFs displayed a later onset accelerated proliferation, the rate was equivalent to that observed in RE9a suggesting that RE has the potential to support secondary mutations but that this effect is delayed relative to RE9a-expressing MEFs. It is not known whether the earlier onset of accelerated growth represents the ability of RE9a to suppress premature senescence or to stimulate growth leading to secondary mutations and a further selective advantage for fibroblastoid cells. Since primary MEFs represent a heterogeneous cell population derived from a whole mouse embryo, it is possible that RE9a induces senescence in a subpopulation that affects the overall growth rate of the culture while other more resistant cells grow out when the cells are passaged *in vitro*. This hypothesis could be tested in future studies by following the fates of individual cells expressing RE9a.

I suggest that the increased leukaemogenicity of RE9a is at least in part due to its failure to engage tumour suppressors including $p16^{INK4a}$ which might induce SLGA in RE9a-expressing cells. This allows RE9a-expressing cells to evade cellular senescence which may render the cells vulnerable to additional cancer-causing mutations.

4 RUNX1-ETO9a Fails to Engage Pro-Senescence p38MAPK-ROS Signalling in Hs68 cells

4.1 Introduction

Ectopic expression of oncogenic RAS was previously reported to promote mitochondrial reactive oxygen species (ROS) in primary human fibroblasts [239]. Consequences of ROS accumulation include hyper-replication and oxidative DNA damage that together induce a rapid DNA damage response [166] and the downstream activation of major tumour suppressor pathways such as p53 and $p16^{INK4A}$ required for senescence [169].

Previous work identified RE as a potent inducer of ROS in human fibroblasts [59]. Interestingly previous studies have shown that RE-induced SLGA occurs in the absence of hyper-replication and significant DNA damage [59, 225]. This phenotype has subsequently been reported for other oncogenes such as BCR-ABL and AKT suggesting that the DDR is not absolutely essential for OIS and that alternative pathways exist [225, 226]. Although RE-induced senescence occurs in the absence of a significant DDR, previous studies have identified p38MAPK activation as a critical factor in RE-induced senescence [59, 225]. Furthermore, p38MAPK activation has been identified downstream of ROS. Specifically, ROS induces the oxidative dissociation of Thioredoxin and ASK1, thereby releasing ASK1 to phosphorylate and activate p38MAPK [194, 240]. AS RE has been reported to be a potent inducer of intracellular ROS, the ROS-p38MAPK signalling axis presents a possible mechanism for RE-induced cellular senescence which may be lacking in cells expressing RE9a.

To address whether the enhanced leukaemogenic potential of RE9a is associated with failure to engage the ROS/p38MAPK tumour suppressor axes, DNA damage, ROS production and p38MAPK activation were compared in primary human fibroblasts expressing RE and RE9a.

4.1.1 Aims and Objectives

- Determine whether RE9a-expressing cells display γH2AX foci which are indicative of DNA double-stranded breaks.

- Examine whether elevated ROS and p38MAPK activation are features of the RE9a phenotype by measuring DCF fluorescence in transduced cells.

- Determine whether elevated ROS production in RE-expressing cells is an essential pro-senescence factor by scavenging ROS using sodium pyruvate.

- Determine whether p38MAPK activation is essential for RE-induced senescence using the p38MAPK inhibitor, SB203580, to inhibit signalling through this axis.

4.2 Results

4.2.1 RUNX1-ETO9a Fails to Induce DNA Damage in Hs68 Cells

Phosphorylated γH2AX foci at sites of double-stranded DNA breaks were visualised by indirect immunofluorescence in Hs68 cells transduced with a lentiviral vector expressing PURO, RE or RE9a. RUNX1P2 and $HRAS^{V12}$ were included as negative and positive controls respectively for DNA damage. As expected, expression of $HRAS^{V12}$ was accompanied by a substantial increase in the number of FITC-labelled γH2AX foci indicative of a strong DNA damage response whereas RUNX1P2 failed to induce DNA damage relative to the PURO control as previously reported [59]. RE9a also failed to induce the appearance of γH2AX foci consistent with the absence of SLGA in these cultures. RE also failed to induce the appearance of γH2AX foci (**Figure 4.1 a**) despite a robust SLGA in these cells. These data contrast with others describing modest levels of DNA damage in primary human fibroblasts in response to RE [59, 225]. This disparity may simply reflect intrinsic differences between lentiviral and retroviral expression of RE and strongly suggests that the DDR is not absolutely critical for RE-induced SLGA in primary human fibroblasts.

AKT has been reported to induce premature senescence in human fibroblasts in the absence of a DNA damage signal [226]. To determine whether phosphorylated AKT signals downstream of RE to induce senescence, day 6 protein extracts were analysed by western blot. Phosphorylated AKT was detected in extracts from RE-expressing cells but at a lower intensity relative to cells expressing ectopic RUNX1P2 where the signal was strong. AKT was completely undetectable in RE9a expressing cells (**Figure 4.1 b**). These data suggest that, while AKT signalling may play a role in RUNX1P2-induced SLGA, it is less significant for senescence induction by RE.

a)

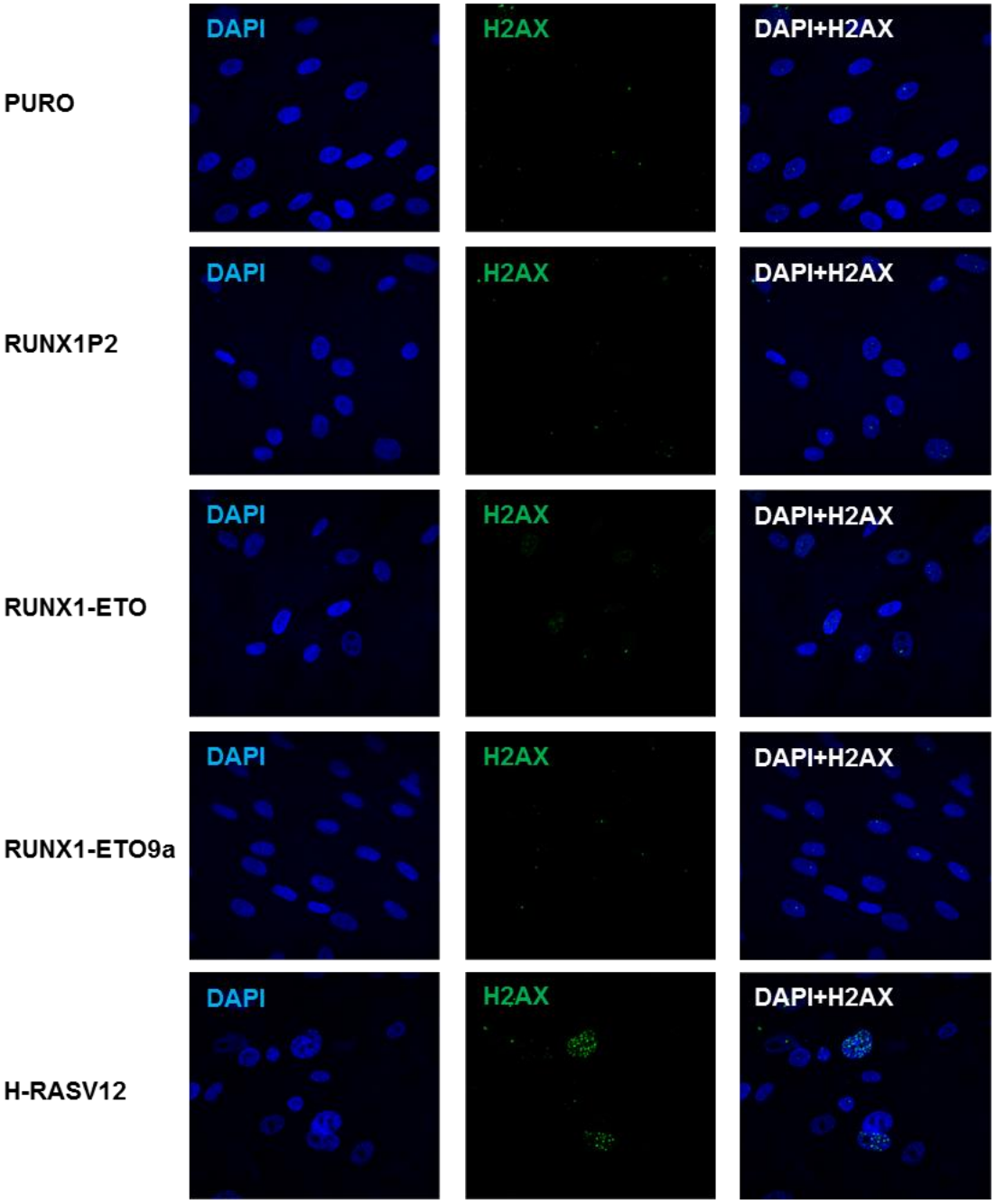
DAPI
H2AX
DAPI+H2AX
PURO
RUNX1P2
RUNX1-ETO
RUNX1-ETO9a
H-RASV12

b)

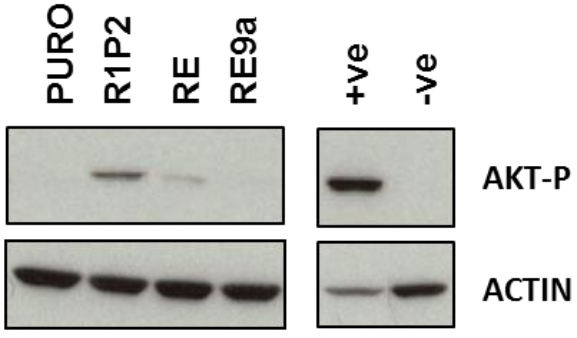
PURO
R1P2
RE
RE9a
+ve
-ve
AKT-P
ACTIN

Figure 4.1 RUNX1-ETO9a fails to induce DNA damage in Hs68s
Analysis of double-stranded DNA breaks in Hs68 cells transduced with lentiviruses containing RUNX1P2, RE and RE9a 6 days after puromycin selection. Vectors containing the control (PURO) or H-RASV12 were included as negative and positive controls respectively (a) Nuclei were stained using DAPI (left hand column). Immunodetection of DNA double-stranded breaks was performed using an anti-γH2AX antibody (JBW301, MerckMillipore) and a FITC conjugated secondary antibody (Stratech Scientific Ltd.) (Middle column). The right hand column shows the γH2AX (FITC) and nuclei (DAPI) overlaid. Images were captured using 40x magnification (b) Western blot analysis of phosphorylated AKT (60kDa) in Hs68 fibroblasts expressing the control vector (PURO), RUNX1P2, RE or RE9a 6 days after puromycin selection. 293T cells were used as a positive control for AKT phosphorylation and Jurkat cells were used as a negative control. Results shown are representative of three biological replicates.

4.2.2 RUNX1-ETO9a Fails to Induce Reactive Oxygen Species

While replicative stress and DNA damage were not features of RE-induced SLGA, induction of ROS was previously reported in RE-expressing Hs68 fibroblasts [59]. To determine whether RE9a senescence escape is associated with a failure to accumulate intracellular ROS, a FACs-based detection of fluorescence emitted by a peroxide-sensitive fluorophore, DCF-DA, was used to measure intracellular ROS 6 days after selection. In support of previous observations, RE but not RUNX1P2 induced significant levels of intracellular ROS relative to the PURO control [59]. RE9a, in contrast, failed to accumulate intracellular ROS supporting previous evidence that ROS correlates with and is causally involved in RE-induced SLGA (**Figure 4.2 a**). To address this question, cultures were treated at the initiation of selection with 250μM sodium pyruvate and again at 2-3 days intervals to suppress intracellular ROS. Successful scavenging was confirmed 6 days post selection by DCF-DA detection. Although scavenging was observed in all cultures, RE-expressing cells showed the most significant decrease in mean fluorescence with intracellular ROS levels restored to background levels (**Figure 4.2 b**). The reduction in ROS in RE-expressing cultures was accompanied by an increase in proliferation which was not observed in RE9a or PURO control cells in response to sodium pyruvate treatment. Indeed, PURO control cells appeared to be negatively affected by sodium pyruvate treatment, with cultures exhibiting slower growth rates throughout the time course (**Figure 4.2 c**). The increased proliferation of RE-expressing cells was accompanied by a shift to more fibroblastoid cell morphology and a reduced SA-β-Gal staining pattern. RE9a cultures, in contrast, retained a fibroblastoid non-senescent morphology in the presence and absence of sodium pyruvate (**Figure 4.3 d**). Together these data demonstrate that ROS accumulation is critical for RE-induced SLGA and likely to be dependent on the NHR3 and NHR4 ETO repressor domains that are absent from RE9a.

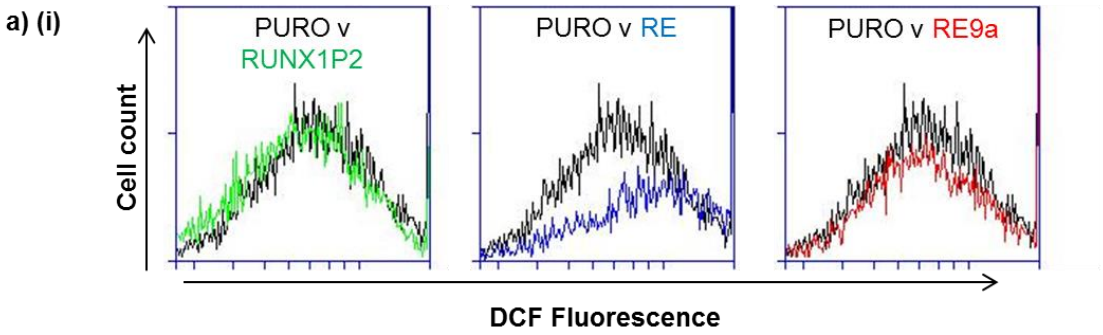
a) (i)
PURO v RUNX1P2
PURO v RE
PURO v RE9a
Cell count
DCF Fluorescence

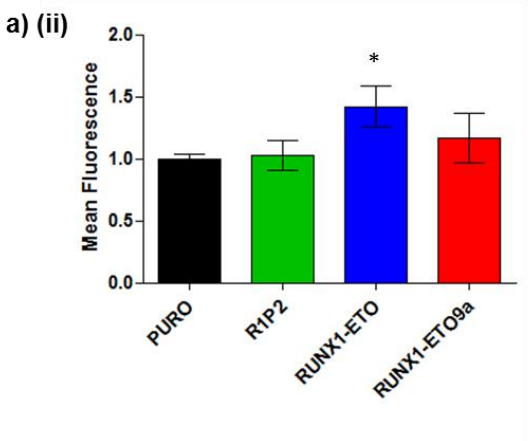
a) (ii)
Mean Fluorescence
2.0
1.5
1.0
0.5
0.0
*
PURO
R1P2
RUNX1-ETO
RUNX1-ETO9a

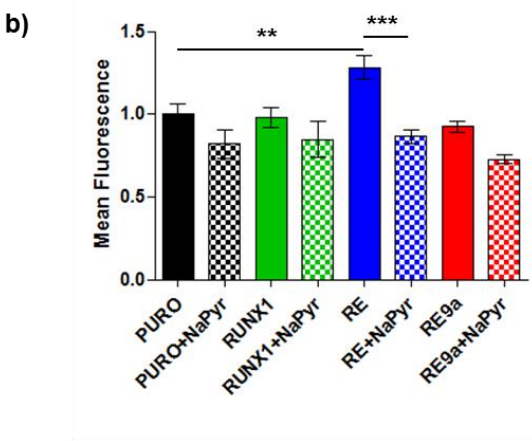
b)
Mean Fluorescence
1.5
1.0
0.5
0.0
**
***
PURO
PURO+NaPyr
RUNX1
RUNX1+NaPyr
RE
RE+NaPyr
RE9a
RE9a+NaPyr

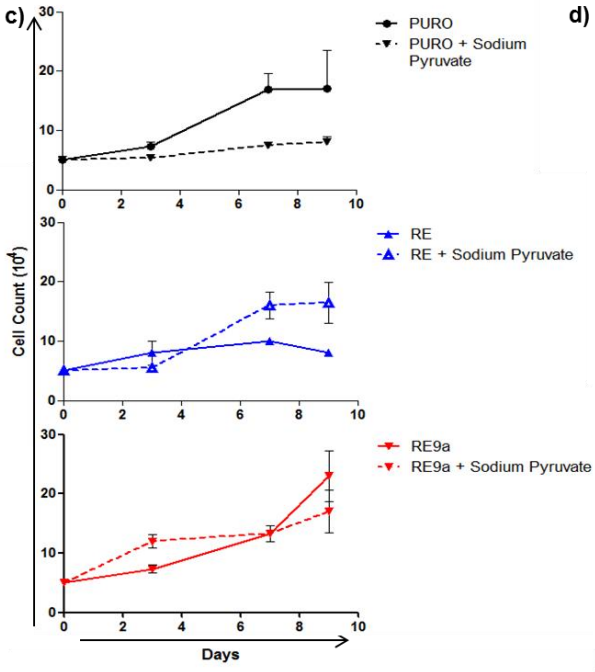
c)
Cell Count (10⁴)
PURO
PURO + Sodium Pyruvate
RE
RE + Sodium Pyruvate
RE9a
RE9a + Sodium Pyruvate
Days

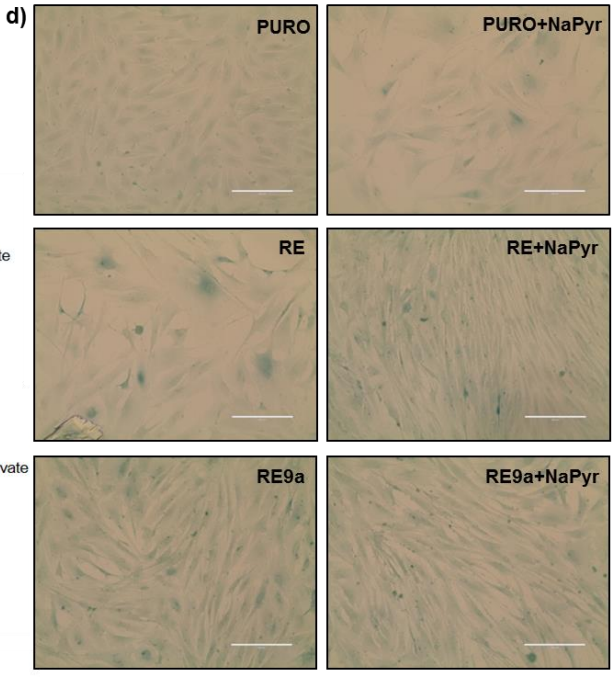
d)
PURO
PURO+NaPyr
RE
RE+NaPyr
RE9a
RE9a+NaPyr

Figure 4.2 RUNX1-ETO9a fails to induce ROS in Hs68s
Hs68 cells were transduced with a lentivirus encoding RE, RE9a or a control lentivirus (PURO) and intracellular ROS levels measured using a flow cytometer to detect DCF-DA fluorescence 6 days after puromycin selection. The data shown are respresentative of 3 independent biological replicates. (a(i)) Representative flow cytometric histograms showing DCF-DA fluorescence against cell count in cells transduced with the PURO control vector overlaid with histograms generated bycells expressing RUNX1P2, RE or RE9a. (a(ii)) Bar chart showing fold change ± SD in mean fluorescence intensity compared with PURO control. Significance was determined using a one-way ANOVA comparing all pairs of columns. (b) Bar chart showing fold change in DCF-DA mean fluorescence measured 6 days post-transduction in cells transduced as above and treated with 250μM sodium pyruvate from the point of transduction compared with untreated cells. Data was collected using a flow cytometer and analysed as in (a (ii). (c) Growth curves from cells transduced and treated with or without 250 μM sodium pyruvate as a scavenger of intracellular ROS as in (b). Plots show the mean of three independent cell counts ±SD. (d) Images of cells stained for SA-β-Gal activity at pH6.0 in cells treated with or without sodium pyruvate on day 6 post-selection. Images were captured using 20x magnification.

4.2.3 RUNX1-ETO9a Fails to Induce p38MAPK Activation

P38MAPK was previously identified as an essential driver of RE-induced SLGA [59, 225] and has been identified as a downstream effector of ROS signalling. To examine whether the failure of RE9a to induce ROS is supported by an inability to activate p38MAPK, the phosphorylation status of p38MAPK was examined by western blotting. As shown in **Figure 4.3 a**, phosphorylated p38MAPK was completely undetectable in Hs68 fibroblasts expressing RE9a on day 0 after puromycin selection (**Figure 4.3 a)**. Moreover, RE9a-expressing cells were also refractory to growth stimulation by a p38MAPK inhibitor (SB203580) which reversed SLGA (**Figure 4.3 b**) and senescence morphology (**Figure 4.3 c**) of RE-expressing cells. In contrast, phosphorylated p38MAPK was readily detectable in the presence of RE but not in vector control cultures or those expressing RUNX1P2 (**Figure 4.3 a**) which also failed to accumulate ROS, consistent with previous reports [59]. To examine the relationship between ROS and p38MAPK, a ROS scavenger, sodium pyruvate, was included in the growth media at the point of selection and p38MAPK phosphorylation re-examined in response to RE. As shown in **Figure 4.3 d**, p38MAPK phosphorylation was suppressed by sodium pyruvate in the presence of RE, confirming dependence on ROS for p38MAPK activation (**Figure 4.3d**). $p16^{INK4A}$ expression was also examined since it has been reported to be downstream of ROS-p38MAPK signalling. However, in this case induction was diminished but not abolished in the presence of sodium pyruvate, suggesting that RE can activate $p16^{INK4A}$ expression through alternative signalling pathways or that this is a more sensitive marker of incomplete ROS removal (**Figure 4.4 e**). Together these data suggest that ROS-p38MAPK signalling is required for RE-induced SLGA and that failure of RE9a to induce senescence may in part reflect its inability to accumulate ROS and activate p38MAPK.

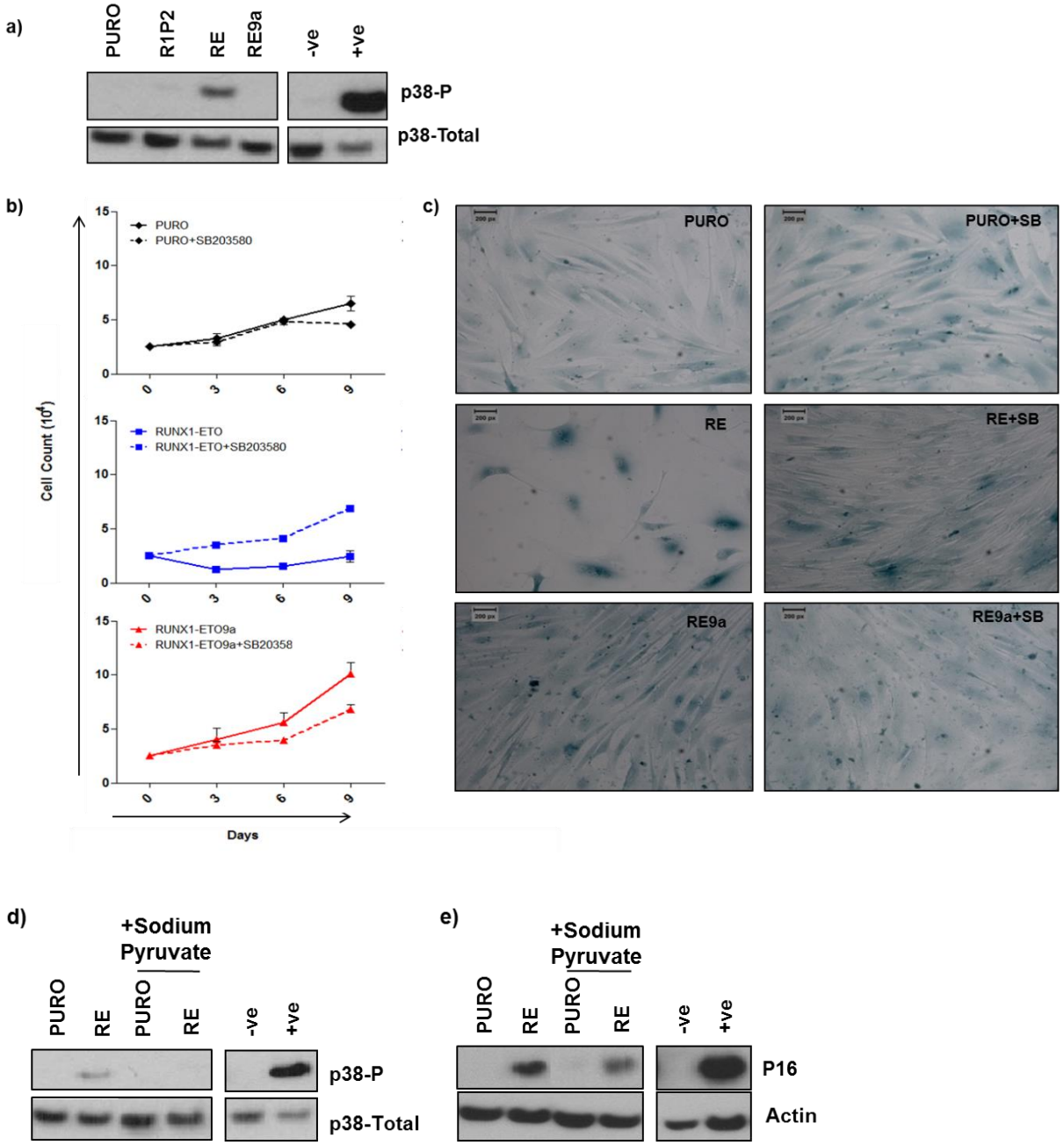
a)
PURO
R1P2
RE
RE9a
-ve
+ve
p38-P
p38-Total
b)
Cell Count (10^4)
PURO
PURO+SB203580
RUNX1-ETO
RUNX1-ETO+SB203580
RUNX1-ETO9a
RUNX1-ETO9a+SB20358
Days
c)
PURO
PURO+SB
RE
RE+SB
RE9a
RE9a+SB
d)
+Sodium Pyruvate
PURO
RE
PURO
RE
-ve
+ve
p38-P
p38-Total
e)
+Sodium Pyruvate
PURO
RE
PURO
RE
-ve
+ve
P16
Actin

Figure 4.3 RUNX1-ETO9a fails to induce p38-P activation of Hs68s
Hs68 cells were transduced with a lentivirus vector encoding RE, RE9a or the PURO empty vector. (a) Western blot analysis of phospho-p38MAPK (9211 Cell Signalling Technology) expression in cells harvested on day 1 post-selection. Total p38MAPK was used as a control (9212 Cell Signalling Technology) to show that all cell types examined displayed similar p38MAPK expression levels. (b) Growth curves showing proliferation of transduced cells over 9 days in the presence or absence of 8μM SB203580. Plots show the mean of three independent cell counts ±SD. (c) SA-β-Gal staining of day 6 Hs68 cells transduced and treated as in (b).Images were captured using 20x magnification. (d) Western blot analysis of phospho-p38MAPK and total p38MAPK expression (9211 and 9212, Cell Signalling Technology) immediately after puromycin selection in Hs68 cells transduced with RE and cultured in the presence or absence of 250μM sodium pyruvate. (e) Western blot analysis of $p16^{INK4A}$ (sc-468, Santa Cruz Biotechnology Ltd) expression measured 6 days post-selection in Hs68 cells transduced and treated with sodium pyruvate as in D.

4.3 Discussion

This study establishes the failure to engage the ROS-p38MAPK stress response pathway as a key feature of the RE9a expression phenotype. This study shows that, in contrast to RE, neither ROS accumulation nor p38MAPK activation is induced by RE9a. Furthermore, inclusion of sodium pyruvate in the growth media to scavenge ROS or direct inhibition of p38MAPK activity is sufficient to attenuate RE-induced SLGA but has only a slight repressive effect on the growth of RE9a-expressing cells, confirming the importance of these signalling factors for RE-induced SLGA and their evasion by RE9a.

Excessive ROS was initially reported to be associated with $HRAS^{V12}$-induced senescence where it induced DNA damage in the form of replicative and oxidative stress [241]. Knock-down of key DDR components such as ATM, Chk2 and p53 resulted in abrogation of RAS-induced senescence, confirming the importance of this pathway in OIS [169]. Indeed, DNA damage has also been described in response to the RE fusion protein. Sustained proliferation of human CD34+ cells was attributed to expression of RE-mediated DNA damage and repression of DNA repair genes and RE-induced SLGA was characterised by a weak DDR in primary human fibroblasts and haematopoietic progenitor cells [228]. In contrast to these reports, no DNA damage was observed in this study in the presence of RE. Indeed, in line with a previous report in Hs68 fibroblasts [59], RE induced a rapid and profound growth arrest that was associated with little or no DNA damage. The disparity between these studies may simply reflect the use of different cell types and viral transduction systems or the fact that $CD34^{+}$ cells were selected for survival after long term culture rather than after the initial stress of RE transduction. Evidence of premature senescence in the absence of proliferative and genotoxic stress is becoming more prevalent with reports that leukaemic fusion oncoproteins such as BCR-ABL and CBFß-MYH11 induce senescence in the absence of DNA damage [225]. Together they corroborate the findings from this study and support the existence of DDR-independent pathways to RE-induced SLGA.

The PI3K/AKT signalling pathway represents a DDR independent senescence signalling pathway that can be activated through oxidative stress [226]. Strong accumulation of ROS was observed in response to ectopic RE but activation of

AKT was modest compared to RUNX1P2 suggesting that PI3K/AKT signalling may be more important for RUNX1P2-induced SLGA than for SLGA induced by RE. An alternative pathway downstream of ROS also implicated in premature senescence involves the redox-dependent phosphorylation of p38MAPK by ASK1 [194]. Activation of p38MAPK has been widely associated with premature senescence [189] where it has been identified as an upstream activator of $p16^{INK4A}$ [188, 242]. The potential significance of this pathway for RE-induced SLGA is evidenced by data from this and another study showing induction of $p16^{INK4A}$ in response to RE and reversal of the senescence phenotype when RE expressing cultures were grown in the presence of a p38MAPK inhibitor SB203580 [59]. Furthermore, it was demonstrated that RE-expressing cells grown in the presence of sodium pyruvate, a scavenger of ROS, continued to proliferate and failed to phosphorylate p38MAPK further implicating ROS-p38MAPK signalling in RE-induced SLGA and the absolute requirement for p38MAPK activity.

Involvement of ROS-p38MAPK signalling in premature senescence is not without precedent. It has previously been reported that oncogenic $HRAS^{V12}$ induces premature senescence that is associated with persistent ROS-p38MAPK-$p16^{INK4A}$ signalling [188, 242]. Moreover, leukaemogenic fusions including BCR-ABL and CBFβ-MYH11 induce p38MAPK and cellular senescence in the absence of DNA damage which supports the existence of DNA-damage independent pathways to cellular senescence. Although intracellular ROS was not assayed in the presence of these fusions, it has also been reported that ROS accumulation can occur in the absence of DNA damage [186].

The data presented in this study demonstrated a transient activation of p38MAPK activity in the presence of RE. Indeed, reversal of the RE-induced growth arrest was restricted to cells exposed to ROS scavengers immediately after viral transduction suggesting that p38MAPK signalling is required for induction of RE senescence but may be dispensable for maintenance of the response. Transient induction of p38MAPK is commonly observed in response to cellular stress [243] but persistent activation has been identified as an inducer of cellular senescence in human fibroblast cells [185]. In this respect it is notable that expression of RE from a retroviral vector in Hs68 fibroblasts was associated with a more sustained activation of p38MAPK and significantly higher levels of ROS [59]. Furthermore somewhat intermediate levels of ROS were observed in response to RE9a that

appeared insufficient to induce SLGA, suggesting that a threshold level of ROS is required for p38MAPK activation and senescence induction *in vitro*. Although activation of p38MAPK was transient in response to RE it was undoubtedly required for SLGA as evidenced by the phenotypic reversal with sodium pyruvate and SB203580. The signalling pathways downstream of p38MAPK associated with premature senescence include activation of $p16^{INK4A}$ and p53 [244]. p53 was previously described as a critical mediator of RE-induced SLGA [59] but was only modestly induced in this study. In contrast a significant induction of $p16^{INK4A}$ was observed in response to RE which was conspicuously absent in the presence of RE9a. Moreover, RE9a failed to induce p38MAPK or premature senescence, supporting a causal link between p38MAPK, $p16^{INK4A}$ and senescence. However, the incomplete suppression of $p16^{INK4A}$ induction by RE in the presence of sodium pyruvate shows that low level induction is insufficient to drive the senescence response. Whether this reflects incomplete scavenging or ROS-independent $p16^{INK4A}$ activation pathways has not been determined.

From the evidence presented here it may be predicted that opposition of ROS-p38MAPK signalling represents a mechanism by which RE9a evades premature senescence. Furthermore persistent proliferation may contribute to the increased leukaemogenicity of the RE9a fusion oncoprotein *in vivo*.

5 Mutation of NHR3 and NHR4 is Necessary for Complete Abrogation of RE-Induced SLGA

5.1 Introduction

Previous studies have shown that the RE fusion oncoprotein behaves as a constitutive transcriptional repressor of RUNX1 gene targets due to the presence of Nervy Homology Regions (NHR) in the ETO protein [70]. The four NHR domains are effective recruiters of co-repressor complexes including NCoR, mSin3A, SON and SMRT which interact with histone deacetylases (HDACs) to repress gene transcription [70]. NHR1 and NHR2 are also important for RE/ETO oligomerisation and are essential for RE9a oncogenic activity [89, 92, 245].

This study demonstrates that the C-terminal portion of ETO encoding the NHR3 and NHR4 domains is critical for RE-induced SGLA Since premature senescence is an important failsafe mechanism that restricts transformation *in vitro* and *in vivo* [246] and RE9a, unlike RE, evades senescence and is capable of inducing leukaemogenesis in murine models [80], it was important to determine whether loss of NHR3 or NHR4 was responsible. Previous studies have demonstrated that deletion or disruption of RE NHR4 results in an enhanced leukaemogenic phenotype in murine models [95, 97]. However other studies indicate that mutations affecting NHR4 rarely occur in human leukaemias [247] arguing against the significance of this single domain for leukaemia development. Similarly disruption of the NHR3 domain was shown to have minimal impact on the leukaemogenic potential of RE [93, 95] suggesting that the loss of both domains in the RE9a spliced variant is required – a finding also supported by the identification of the RE9a spliced variant in over 70% of t(8;21) patient samples [80]. To determine whether loss of both the NHR3 and NHR4 domains was similarly required for senescence evasion by RE9a, a series of RE deletion and point mutants specifically targeting the NHR3 and NHR4 domains (**Figure 5.1** and kindly gifted by Prof. Dong Er Zhang) were subcloned into pLenti PURO and introduced into Hs68 cells to monitor for hallmarks of premature senescence.

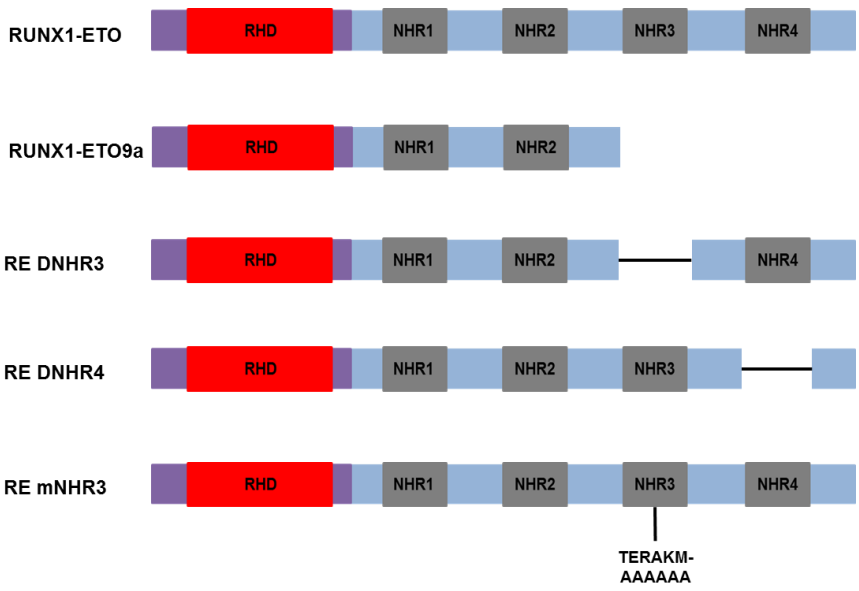

Figure 5.1 RE, RE9a and the NHR mutants
Schematic representation of RE, RE9a, DNHR3 (Deleted NHR3), DNHR4 (Deleted NHR4) or mNHR3 (6 amino-acid alaninisation in NHR3 (TERAKM-AAAAAA)).

5.1.1 Aims and Objectives

- Determine the effect of loss or disruption of NHR3 or NHR4 for RE induced growth arrest of Hs68 primary fibroblasts.

- Explore the consequences of disruption of the NHR3 and NHR4 domains for RE-induced premature senescence staining and morphology in Hs68 fibroblasts.
- Determine whether ROS/p38MAPK signalling is retained or compromised in Hs68 fibroblasts expressing RE NHR mutants.

- Explore the relationship between $p16^{INK4a}$ expression and RE induced senescence in the presence and absence of NHR3 and NHR4.

5.2 Results

5.2.1 NHR3 is Critical for a RUNX1-ETO-Induced Growth Arrest.

Expression levels of RE, RE9a, DNHR3, DNHR4 and mNHR3 were assayed in Hs68 cells by western blotting. The mutants were expressed at high and approximately equivalent levels compared to RE (**Figure 5.2 a**). As reported previously, RE expression in Hs68 cells was accompanied by a profound growth arrest whereas proliferation of RE9a transduced cells was essentially indistinguishable from that of the controls. The growth of Hs68 cells was similarly unaffected by expression of DNHR3 and mNHR3 although an initial growth delay was observed in the presence of mNHR3 from which the cells recovered after 9 days in culture. In contrast, ectopic expression of DNHR4 restricted the growth of Hs68 cells over the time course of the experiment. Slow growth was maintained compared to RE-expressing cells but the restriction was severe with approximately three fold lower cell numbers at the end of the experiment compared to the control and NHR3 mutants (**Figure 5.2 b**). The reduced growth was accompanied by the appearance of senescent cells and positive staining for SA-β-Gal activity (**Figure 5.2 c;** red arrowhead). In contrast to RE, fibroblastoid like cells were also observed in the DNHR4 cultures (**Figure 5.2 c;** blue arrowhead) but these were much fewer in number than in the control cells or cultures expressing DNHR3 or mNHR3. Together these data suggest that NHR3 is absolutely required for induction of a senescence like growth arrest by RE but that NHR4 may contribute additional functions to drive the complete response.

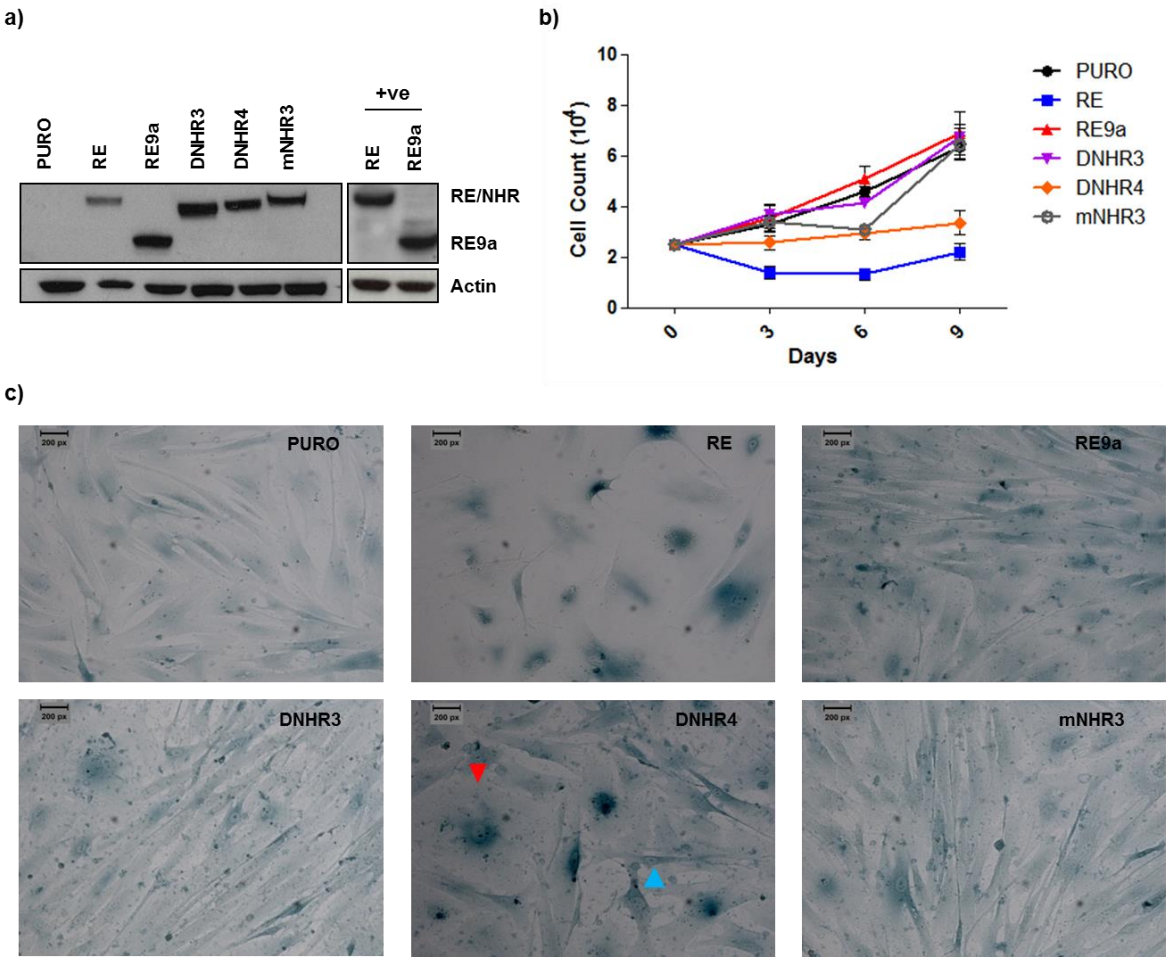

Figure 5.2 The NHR3 domain is essential for the senescence-inducing activity of RE

Hs68 cells were transduced with lentiviral vectors expressing RE, RE9a, DNHR3, DNHR4 or mNHR3. The empty pLenti vector (PURO) was included as a control. (a) Western blot analysis of ectopic RE, RE9a, DNHR3, DNHR4 and mNHR3 expression levels in transduced Hs68 fibroblasts using an anti-RUNX antibody (D207-3, MBL Ltd) immediately after puromycin selection. (b) Representative growth curves measuring proliferation of transduced cells over 9 days. Plots show the mean of three independent replicates ±SD. (c) SA-β-Gal staining (pH6.0) of Hs68 cells expressing PURO, RE, RE9a, DNHR3, DNHR4 or mNHR3 at day 6 post-selection. The red arrow indicates a cell displaying senescent morphology and characteristic SA-β-Gal perinuclear staining while the blue indicates a spindle-shaped fibroblastoid cell. Images were captured using 20x magnification.

5.2.2 Disruption of Either NHR3 or NHR4 is Insufficient to Completely Oppose Induction of ROS and p38MAPK Activation.

We have previously demonstrated that accumulation of intracellular ROS is essential for RE-induced SLGA and is conspicuously absent from RE9a-expressing cells which also fail to senesce. To determine whether the NHR3 domain is sufficient for ROS accumulation by RE or if the NHR4 domain is also required, intracellular ROS was assayed by FACS-based detection of DCF-DA fluorescence in Hs68 cells expressing DNHR3, DNHR4 and mNHR3 6 days after puromycin selection and the levels compared to those achieved by cells expressing RE or RE9a. As shown in **Figure 5.3a,** ROS accumulation was elevated by all three mutants to levels approximately equivalent to RE expressing cultures and exceeding those achieved in the presence of RE9a or the control vector. To determine whether downstream signalling pathways were activated differentially by ROS in the presence of the NHR mutants, day 0 protein lysates were prepared and analysed for phospho-p38MAPK expression which depends on ROS accumulation (**Figure 4.4a**). As reported previously RE expression resulted in p38MAPK phosphorylation whereas the protein remained unphosphorylated in the presence of RE9a. Modest but equivalent levels of phospho-p38MAPK were recorded in Hs68 cells expressing DNHR3 and DNHR4 despite their differential senescence responses suggesting that p38MAPK activity contributes to, but is not sufficient for, RE-induced SLGA in the absence of NHR3 or NHR4 and that deletion of both NHR domains is required to avoid p38MAPK activation. In support of this interpretation, cells expressing mNHR3 which differs from RE by only 6 amino acids displayed the highest levels of phosphorylated p38MAPK yet failed to senesce (**Figure 5.3b**). Comparing the levels of ROS accumulation with phosphorylated p38MAPK for the NHR mutants yielded no immediate correlation suggesting that ROS was not rate-limiting under these conditions and that loss of a single functional NHR domain is insufficient to completely restore the effects of the C terminal deletion in RE9a. To determine the functional consequences of p38MAPK activation for cell growth in the presence of the NHR mutants the experiment was repeated in the presence and absence of a p38MAPK inhibitor, SB203580, and growth monitored for 12 days. As shown in **Figure 5.3c** the inhibitor had an early positive effect on the growth of all the mutants particularly DNHR3 that was not observed in control cultures. The early

proliferative response was sustained in cultures expressing DNHR3 and accompanied by the appearance of very fibroblastoid looking cells (**Figure 5.3d**). More modest shifts to a fibroblastoid morphology were also observed in cells expressing mNHR3 and even DNHR4 (**Figure 5.3d;** blue arrowhead) despite the persistence of senescent cells within the DNHR4 cultures (**Figure 5.3d;** red arrowhead). Since SB203580 was added at the point of puromycin selection before senescence was visually apparent these data suggest that p38MAPK activity is not absolutely required for senescence induction by RE but does continue to be restrictive for cellular growth. Additional functions residing in the NHR3 domain and to a lesser extent the NHR4 domain must be required for a complete response.

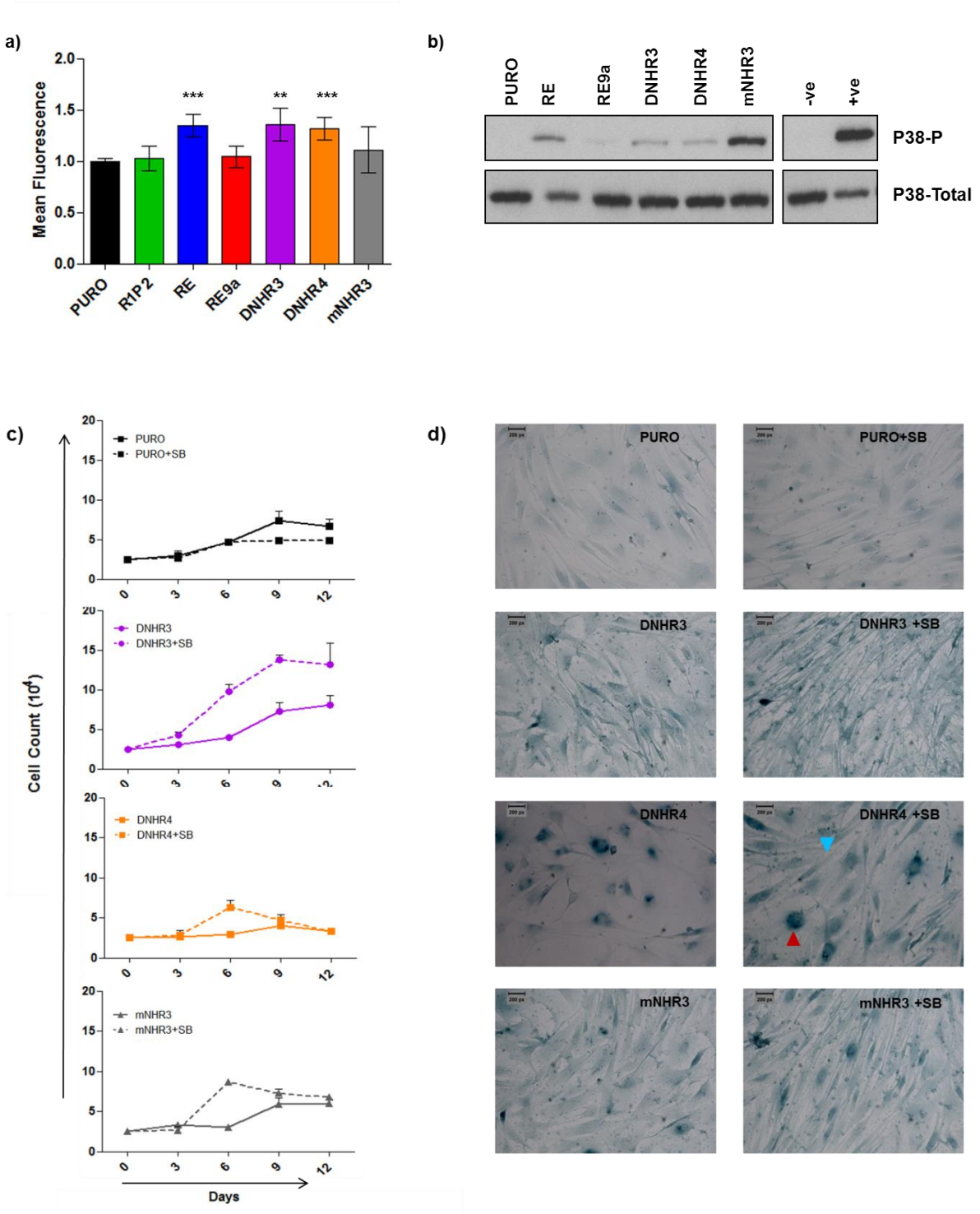
a)
Mean Fluorescence
2.0
1.5
1.0
0.5
0.0
***
**
***
PURO
R1P2
RE
RE9a
DNHR3
DNHR4
mNHR3
b)
PURO
RE
RE9a
DNHR3
DNHR4
mNHR3
-ve
+ve
P38-P
P38-Total
c)
Cell Count (10^4)
PURO
PURO+SB
DNHR3
DNHR3+SB
DNHR4
DNHR4+SB
mNHR3
mNHR3+SB
0
3
6
9
12
Days
d)
PURO
PURO+SB
DNHR3
DNHR3 +SB
DNHR4
DNHR4 +SB
mNHR3
mNHR3 +SB

Figure 5.3 Disruption of the NHR domains of RE affect ROS production and activation of p38-P

Hs68 human fibroblasts were infected with a lentivirus encoding RE, RE9a, DNHR3, DNHR4, mNHR3 or a control lentivirus (PURO), and ROS measured with DCF-DA 6 days after puromycin selection. (a) Bar chart showing fold change ± SD in mean fluorescence intensity compared with PURO control. (b) Western blot analysis of phospho-p38MAPK and total p38MAPK expression (9211 and 9212, Cell Signalling Technology) on day 1 post-selection in transduced Hs68 fibroblasts. (c) Growth curves showing viable cell numbers in Hs68 cell populations expressing either a control vector (PURO), DNHR3, DNHR4 or mNHR3 and grown over 12 days in the presence or absence of 8μM SB203580. Plots show the mean of three independent replicates ±SD. (d) SA-ß-Gal staining of Hs68 cells expressing PURO, RE, RE9a, DNHR3, DNHR4 or mNHR3 in the presence or absence of 8μM SB203580 on day 6 post-selection. Red arrowhead indicates a senescent cell and the blue arrow indicates a spindle-shaped fibroblast cell. Images were captured using 20x magnification.

5.2.3 p16^{INK4a} Signalling is not Required for DNHR4-Induced SLGA

Activation of p16^{INK4a} transcription is a major feature of human cellular senescence both *in vitro* and *in vivo* [126, 143, 234]. Multiple signalling pathways including p38MAPK have been associated with p16^{INK4a} activation and its downstream growth arrest and cellular senescence phenotypes [242]. This study previously showed that p16^{INK4a} was induced by RE but not RE9a in Hs68 fibroblasts and correlated with induction of premature senescence (**Figure 3.1a-c**). To determine whether p16^{INK4a} was induced by the NHR mutants western blot analysis was performed on samples 6 days after puromycin selection when visible signs of senescence were apparent. RE was included as a positive control for p16^{INK4a} induction and as before gave a readily detected band which was not observed in the presence of RE9a. None of the NHR single mutants induced detectable p16^{INK4a} despite activation of the p38MAPK signalling pathway suggesting that this pathway alone was not responsible for p16^{INK4A} induction. Most significantly p16^{INK4a} was not induced in cells expressing DNHR4 despite the appearance of senescent cells in these cultures (**Figure 5.4a**). To address the absolute requirement for p16^{INK4a} RE, RE9a and DNHR4 were introduced into p16^{INK4a}-null primary diploid human foreskin fibroblasts (Leiden cells) and the cultures examined for cell growth. As shown in **Figure 5.4 b,** Leiden cells expressing RE failed to senesce and grew more rapidly than the control cultures suggesting that p16^{INK4A} is absolutely required for RE senescence and opposes the growth promoting activities of RE. It must be presumed that these additional growth promoting functions are absent in RE9a since the growth of these cells was comparable to control cultures. In contrast Leiden cells expressing DNHR4 remained growth-arrested for the duration of the experiment suggesting that growth restriction by RE in the absence of an intact NHR4 domain is independent of p16^{INK4a} signalling (**Figure 5.4b**). Together these data confirm the existence of additional senescence inducing pathways encoded by the NHR3 domain that are revealed in the absence of NHR4 and may contribute to the strength of the RE-induced senescence response.

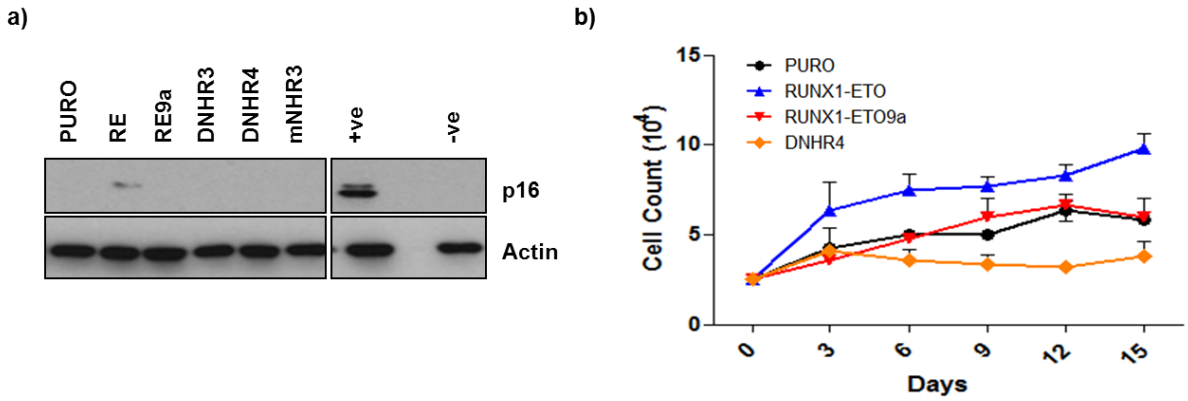

Figure 5.4 DNHR4-induced senescence is refractory to p16^{INK4a} expression.
(a) Western blot analysis of p16^{INK4a} expression (sc-468, Santa Cruz Biotechnology) in transduced Hs68 fibroblasts infected with a lentivirus encoding RE, RE9a, DNHR3, DNHR4, mNHR3 or control lentivirus (PURO). Actin () was used as a loading control. (b) Growth curve showing viable cell numbers in p16^{INK4A}-null Leiden cell populations expressing the control vector (PURO), RE, RE9a or DNHR4 over a 15 day period. Plots show the mean of three independent replicates ±SD.

5.3 Discussion

The data presented here provide evidence that loss of either the NHR3 or NHR4 domain is insufficient to completely oppose RE-induced SLGA and that deletion of both domains is required. Disruption or mutation of NHR3 was permissive for growth and prevented the appearance of senescent cells whereas deletion of NHR4 was accompanied by a weak senescent phenotype characterised by the persistence of fibroblastoid cells within the culture and delayed rather than completely arrested growth. In contrast to RE9a, cell growth and a fibroblast-like morphology was partially restored or intensified in the presence of a p38MAPK inhibitor, suggesting that p38MAPK signalling and growth suppression is at least partially retained by functional deletion of NHR3 or NHR4. Together these results suggest a dominant role for NHR3 in RE-induced SLGA that is potentiated by additional functions of NHR4.

How the NHR3 and NHR4 domains engage senescence signalling pathways is less apparent since mutants of either domain retained the ability to accumulate ROS and activate p38MAPK which are essential for RE-induced SLGA. p16^{INK4A} was not induced, however, supporting the existence of p38MAPK-independent pathways of p16^{INK4A} induction. More surprising was the growth arrest of p16^{INK4A}-null

fibroblasts transduced with DNHR4 despite the persistent sensitivity of all the mutants to p38MAPK inhibition. The data are consistent with alternative $p16^{INK4A}$-independent p38MAPK signalling pathways that are presumably unmasked by loss of the NHR4 domain and to a lesser extent the NHR3 domain, and which contribute growth inhibitory functions to RE. Ablation of these activities is only achieved by complete loss of NHR3 and NHR4 as is observed in the RE9a splice variant.

It is notable that RE9a failed to induce accelerated growth in either Hs68 fibroblasts or $p16^{INK4A}$ null Leiden cells. SLGA was lost in the former cell type but growth was maintained at comparable rates to the controls in both cultures suggesting that NHR3 and NHR4 function to mediate RE growth inhibition and additional domains are required to provide growth-promoting activities revealed in the absence of $p16^{INK4A}$. Although NHR3 was more significant for RE-induced SLGA *in vitro*, NHR4 was identified as the more critical domain *in vivo* with complete restoration of the RE9a leukemic phenotype in mouse models when NHR4 was deleted [95, 97]. It was subsequently shown that NHR4 abrogates leukaemogenesis through interactions with accessory proteins including NCoR and SON [95, 97]. It is notable that another naturally occurring splice variant of RE, RE11a, has been identified in t(8;21) leukaemia which retains NHR1-3 but has lost NHR4 [94]. It will be of considerable interest to determine whether this variant is leukaemogenic *in vivo*. The NHR3 domain was more critical for RE-induced SLGA in Hs68 cells but has been less well characterised *in vivo*. It shares structural homology with AKAPs and interacts with PKA(IIα) but this interaction was demonstrated to have little significance for the anti-leukaemogenic activity of RE [93].

The possibility that both the NHR3 and NHR4 domains are required to induce a robust senescence response is supported by reports that both domains have binding sites for NCoR/SMRT and SON, major co-repressor complexes implicated in RE-mediated gene regulation and cell growth [95, 97]. If effective co-repressor binding requires both domains this may explain the loss of RE-induced SLGA in single-domain mutants. Alternatively, the individual deletion mutants may be sufficient to maintain weak interactions with repressor complexes to promote a partial induction of ROS/p38MAPK signalling that is insufficient for a complete senescence response and/or $p16^{INK4A}$ induction. Interestingly, mNHR3

exhibited maximal p38MAPK activation but failed to induce $p16^{INK4a}$, providing further indirect evidence of p38MAPK independent pathways of $p16^{INK4a}$ activation that require intact NHR3 and NHR4 sequences. To this end it would be informative to immunoprecipitate RE and the NHR mutants and compare their interacting proteins by mass spectrometry. The presence of NCoR/SMRT and SON might not be unexpected but additional components may distinguish between the independent phenotypes exhibited by each mutant and define how each contributes to the RE senescence phenotype.

6 RE and its Mutants Induce Differing Secretory Profiles in Hs68 Cells

6.1 Introduction

This study has identified NHR3 as an essential domain for RE-induced SLGA and NHR4 as an accessory domain that is required for the complete senescence response. In contrast to RE9a which lacks NHR3 and NHR4, all of the NHR mutants displayed ROS accumulation and p38MAPK phosphorylation, which have been associated with activation of NFκB, a master regulator of the SASP [248].

The SASP develops after the appearance of senescent cells and comprises a plethora of inflammatory cytokines and growth factors that can maintain the senescent phenotype of cells or signal clearance of senescent cells by the immune system [249]. However, a persistent SASP can also induce chronic low level inflammation which can have detrimental effects on cells and promote oncogenesis [205]. The SASP is often associated with a persistent DDR [250] and has been reported to be independent of $p16^{INK4A}$ activation [251]. As this study and others have demonstrated that RE-induced senescence in Hs68 cells is dependent on $p16^{INK4A}$ activity and occurs in the absence of significant DNA damage [59, 225], it might be hypothesized that RE-induced senescence is independent of a SASP. Alternatively it has also been demonstrated that RE-induced senescence is dependent on ROS and p38MAPK signalling in Hs68 cells which have been associated with SASP induction particularly in the absence of DNA damage [185, 186].

To determine whether a SASP is a feature of RE-induced SLGA and if so whether it could be used to discriminate between the senescence-inducing functions of NHR3 and NHR4, secretion of IL-6, a prominent SASP marker, was initially examined. The study was then extended to a human cytokine antibody array representing a large panel of secretory markers associated with the SASP [185].

6.1.1 Aims and Objectives

- Determine whether induction of the SASP is a feature of RE-induced senescence.
- Examine how the SASP profile induced by RE compares with those induced by RE9a and the NHR mutants.

6.2 Results

6.2.1 RUNX1-ETO and RUNX1-ETO9a Induce Differing Secretory Profiles in Hs68 Cells.

IL-6 is a major component of SASP and can be induced through p38MAPK activation of IL-1-ß [252] and by NFκB-mediated transcriptional upregulation [253]. To determine whether IL-6 is differentially regulated by RE and RE9a, conditioned medium was collected from cells 6 days post-selection when visible signs of senescence were apparent and assayed for secreted levels of IL-6 using the Human IL-6 Quantikine ELISA kit. Conditioned medium was diluted to account for differences in cell numbers between populations and the IL-6 concentration normalised to the quantity secreted in pLentiPURO-transduced cells which fail to senesce *in vitro*. RUNX1P2 failed to induce IL-6 secretion above background levels (**Figure 6.1a**). In contrast, RE expressing cells secreted high levels of IL-6 consistent with their p38MAPK activation, ROS accumulation and senescence induction. RE9a gave an intermediate level of IL-6 secretion suggesting that NHR3 and NHR4 are necessary but not sufficient for maximal induction of IL-6 by RE.

IL-6 is just one of many factors associated with SASP and cancer [145], but these results encouraged us to examine the SASP profile of RE-expressing cells more closely. To do so a human cytokine array was obtained which detects secretion of 120 cytokines, 100 of which are represented here, and the results compared with those of RE9a and RUNX1P2 which had displayed lower levels of IL-6 secretion by ELISA. Transduced Hs68 cells were selected for puromycin resistance for 5 days and then transferred into complete growth medium. After 4 days, the serum concentration was reduced to 0.2% to minimise the potential cytokine contribution from FCS and the cells were cultured for a further 2 days. The conditioned medium was then harvested and filtered and while cell counts were performed. Samples of conditioned media from independent transductions were diluted to normalise for cell number and applied to the cytokine array chip for final data analysis. OD values were adjusted to exclude background fluorescence and the data normalised to the PURO control. In the heat-maps generated, yellow indicates upregulation, blue indicates downregulation and

grey is used to represent the basal levels of secretion (equivalent to PURO). Heat map gene order was sorted on the values obtained from the RE array.

Conditioned medium from RE expressing cells produced a robust SASP as the majority of secretory markers were increased relative to the PURO control (**Figure 6.1b**). Of these factors, only six were also upregulated by RUNX1P2 (MCP1, Eotaxin, CK beta 8-1, MCP4, GM-CSF and uPAR). Indeed the majority of factors, including IL-6, were unchanged or downregulated by RUNX1P2 which validates the ELISA data and strongly suggests that senescence secretion is either a very limited component of RUNX1P2-induced SLGA or is actually repressed by RUNX1P2. RE9a presented an intermediate profile, failing to induce secretion of many of RE-induced factors and inducing others to a lesser degree. Exceptions include SDF1, BTC, NT3 and IL12 p70 which were secreted at comparable or elevated levels relative to RE. These factors were also strongly repressed by RUNX1P2, suggesting that NHR1 and NHR2 were required for their secretion. Where secretion was not induced by RE9a, distinct patterns emerged. Markers such as IGFBP6, IL-8, Angiogenin and RANTES were repressed to equivalent levels in cells expressing RE9a or RUNX1P2 suggesting that in the absence of NHR3 and NHR4 the effects of RUNX1P2 sequences within RE9a predominate. For one secretory marker, MCP4, expression levels were selectively repressed by RE9a supporting a role for NHR1 and NHR2. A third group was induced by RE9a but not as effectively as by RE. These include MCP1, GRO and IL-6. A final group was represented by TNF-R11, BLC and AXL and appeared to be somewhat refractory to RE9a expression despite significant repression by RUNX1P2 and induction by RE. The remainding factors were repressed by RUNX1P2, RE and RE9a and were presumably regulated by the RUNX1P2 core sequences common to all 3 proteins. Together these data show that RE9a partially antagonises but does not completely invert the SASP driven by RE. The lack of detectable ROS accumulation and p38MAPK signal activation in RE9a expressing cells and the association of these pathways with SASP strongly suggests that they contribute to the SASP induced by RE. The qualitative and quantitative differences in secretory markers generated by RE9a expressing cells are associated with interplay between NHR1, NHR2 and RUNX1 domains resulting in a weakened secretory profile that may account for the ability of RE9a to escape senescence *in vitro*.

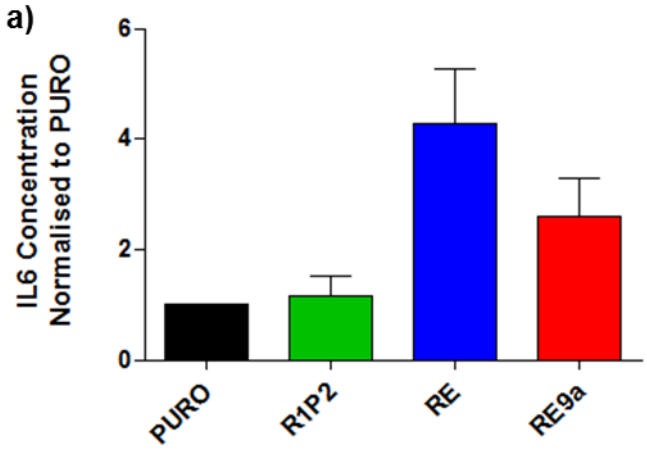

Figure 6.1. RUNX1-ETO induced senescence is accompanied by a robust SASP in Hs68 cells
Hs68 cells were transduced with lentiviral vectors expressing RUNX1P2, RE or RE9a. The empty vector (PURO) was included as a control. (a) Supernatant collected from cells 6 days post-selection was subjected to ELISA for IL-6. Bar chart shows fold change in IL-6 concentration ±SD compared with PURO control. (b) Supernatant collected from cells 6 days post selection was subjected to a human cytokine array. Heat-map generated from data (See Page 100) obtained using a human cytokine array to measure SASP induction by transduced Hs68 cells. Yellow indicates upregulation relative to the PURO control while blue indicates downregulation.

b)

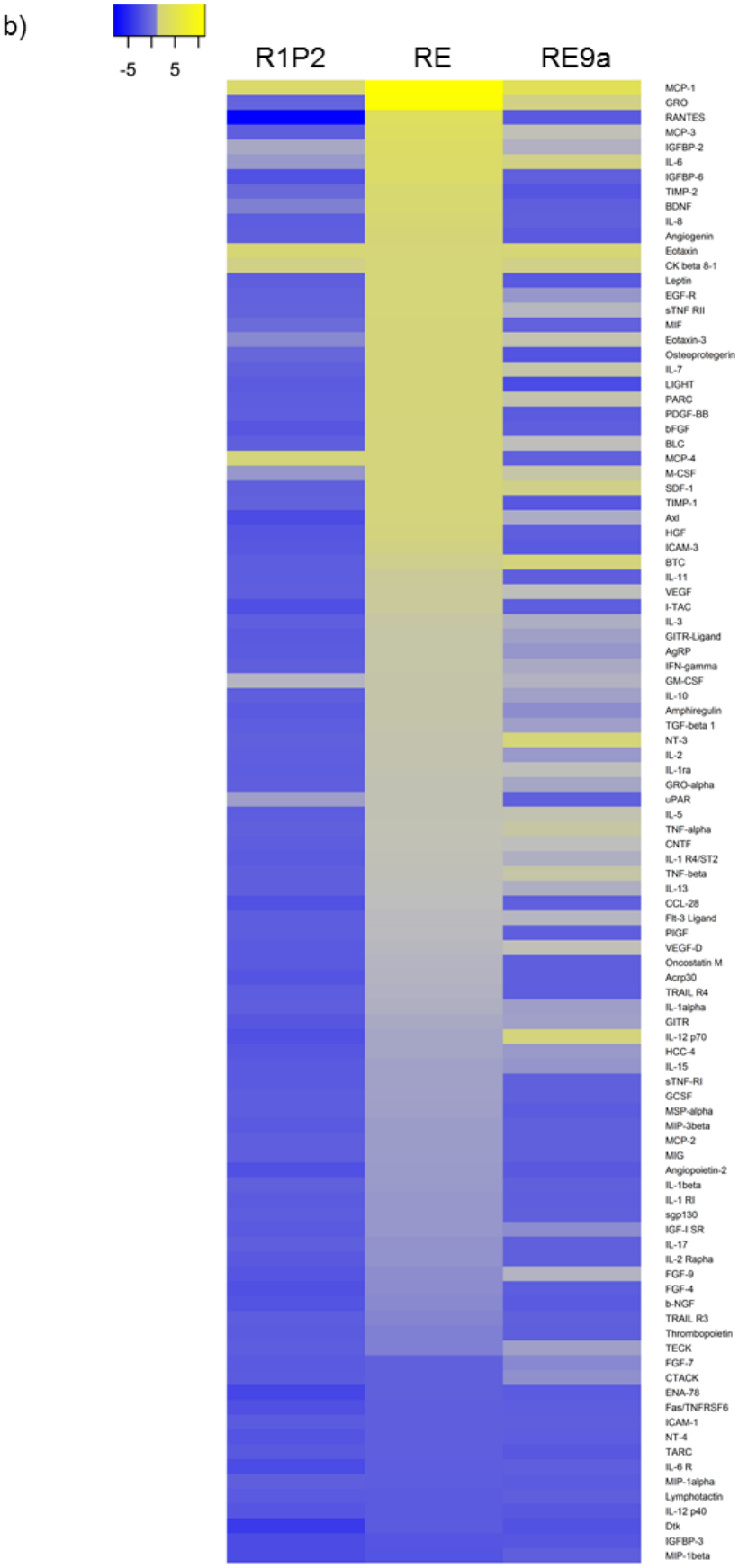
-5
5
R1P2
RE
RE9a
MCP-1
GRO
RANTES
MCP-3
IGFBP-2
IL-6
IGFBP-6
TIMP-2
BDNF
IL-8
Angiogenin
Ecotaxin
CK beta 8-1
Leptin
EGF-R
sTNF RII
MIF
Ecotaxin-3
Osteoprotegerin
IL-7
LIGHT
PARC
PDGF-BB
bFGF
BLC
MCP-4
M-CSF
SDF-1
TIMP-1
Axl
HGF
ICAM-3
BTC
IL-11
VEGF
I-TAC
IL-3
GITR-Ligand
AgRP
IFN-gamma
GM-CSF
IL-10
Amphiregulin
TGF-beta 1
NT-3
IL-2
IL-1ra
GRO-alpha
uPAR
IL-5
TNF-alpha
CNTF
IL-1 R4/ST2
TNF-beta
IL-13
CCL-28
Flt-3 Ligand
PlGF
VEGF-D
Oncostatin M
Acrp30
TRAIL R4
IL-1alpha
GITR
IL-12 p70
HCC-4
IL-15
sTNF-RI
GCSF
MSP-alpha
MIP-3beta
MCP-2
MIG
Angiopoietin-2
IL-1beta
IL-1 RI
sgp130
IGF-I SR
IL-17
IL-2 Rapha
FGF-9
FGF-4
b-NGF
TRAIL R3
Thrombopoietin
TECK
FGF-7
CTACK
ENA-78
Fas/TNFRSF6
ICAM-1
NT-4
TARC
IL-6 R
MIP-1alpha
Lymphotactin
IL-12 p40
Dtk
IGFBP-3
MIP-1beta

6.2.2 Mutation of the NHR3 or NHR4 Domains of RE is Insufficient to Reproduce the RE9a Secretory Phenotype.

To determine whether the SASP profile of RE was dependent on the NHR3 or the NHR4 domain, the NHR mutants were first examined for their ability to induce IL-6 secretion using the Human IL-6 Quantikine ELISA kit. Conditioned media collected from Hs68 cells expressing DNHR3, DNHR4 and mNHR3 revealed levels of IL-6 secretion that were equivalent to RE9a suggesting that both domains are required to fully restore IL-6 secretion by RE (**Figure 6.2 a)**. Since ROS accumulation and p38MAPK activation were present in cells expressing the NHR mutants the data also suggests that these pathways are not sufficient for complete induction of the RE SASP profile.

To investigate whether this pattern was typical over a broader range of SASP markers, the secretory profiles of DNHR3, DNHR4, mNHR3 were compared to RE and RE9a using the human cytokine array described previously. As before, conditioned media were diluted to account for cell number and the OD values normalised to the PURO control cells which fail to senesce. As shown in the heat maps generated in **Figure 6.2 b**, the NHR mutants failed to fully restore the SASP generated by RE, with each inducing a unique secretory profile that diverged less extensively from the RE SASP than RE9a.

A subset of factors including IGFBP6, BDNF and MCP4 were induced to equivalent levels by RE or functional deletion of NHR3 or NHR4, suggesting that retention of either domain is sufficient to induce secretion. Other factors were increased only by mutants retaining NHR4 (PDGF-BB, bFGF) or NHR3 (Angiogenin, MIF) indicating a more specific requirement for one domain or the other. A minority were refractory to either mutant remaining strongly downregulated in the presence of the double (RE9a) or the single (NHR3, NHR4) deletion mutants. These include RANTES, osteoprotegerin and TIMP1 and may depend on the NHR1 and/or NHR2 domains for their downregulation in the absence of an intact RUNX1 C-terminal domain.

To further compare the SASP profiles, the absolute number of upregulated secretory factors shared with RE was expressed as a percentage for RE9a and each of the NHR mutants. RUNX1P2 was also included as it appears to repress

the secretion of numerous SASP components. The list of RE upregulated targets was determined relative to the PURO empty vector control which was arbitrarily given a value of 1.0. As shown in **Figure 6.3a**, RUNX1P2 showed the least similarity, displaying upregulation of only 13% of the secretory factors induced by RE; RE9a expressing cells induced an intermediate profile with 53% similarity to RE whereas mNHR3, DNHR4 and DNHR3 were 77%, 77% and 90% respectively. To examine the relative expression levels of each secreted factor compared to the pLentiPURO control, box-whisker plots were drawn for RE, RE9a and the NHR mutants. As shown in **Figure 6.3b** RUNX1P2 and RE displayed significantly changed secretory profiles compared to pLentiPURO with RE inducing (p=2.8E-5) and RUNX1P2 repressing (p=2.8E-33) the phenotype. RE9a displayed an intermediate phenotype that was induced relative to the pLentiPURO control (p=2.5E-8) but significantly less than RE (p= 3.3E-11). The NHR mutants displayed SASP profiles that were much more equivalent to RE. DNHR3 was not significantly different (p=0.15) whereas mNHR3 and DNHR4 showed relatively weak significance levels when a direct RE comparison was made (mNHR3 p=0.024; DNHR4 p=0.001). Together these data suggest that loss of NHR3 and NHR4 is required to completely restrain the secretory phenotype of RE and that the presence of either domain is sufficient to substantially restore senescence secretion by RE.

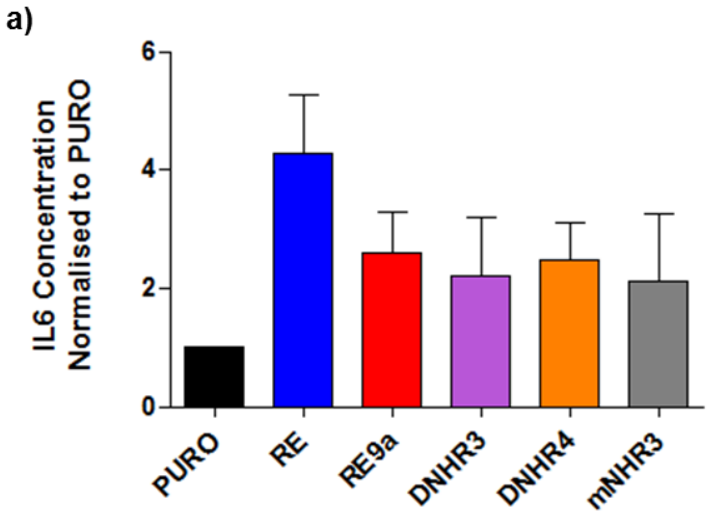

Figure 6.2 Loss of DNHR3 or DNHR4 is insufficient to recapitulate RE9a secretory profile in Hs68 cells

Hs68 cells were transduced with lentiviral vectors expressing RE, RE9a, DNHR3, DNHR4 or mNHR3. The empty vector (PURO) was included as a control. Supernatant was collected from cells 6 days post-selection. (a) IL-6 concentration in supernatants was determined by ELISA. Bar chart shows fold change in IL-6 concentration ±SD compared with the PURO control. (b) Supernatant collected from cells 6 days post selection was subjected to a human cytokine array. Heat-map generated from data (See Page 104) obtained using a human cytokine array to measure SASP induction by transduced Hs68 cells. Yellow indicates upregulation relative to the PURO control while blue indicates downregulation.

b)

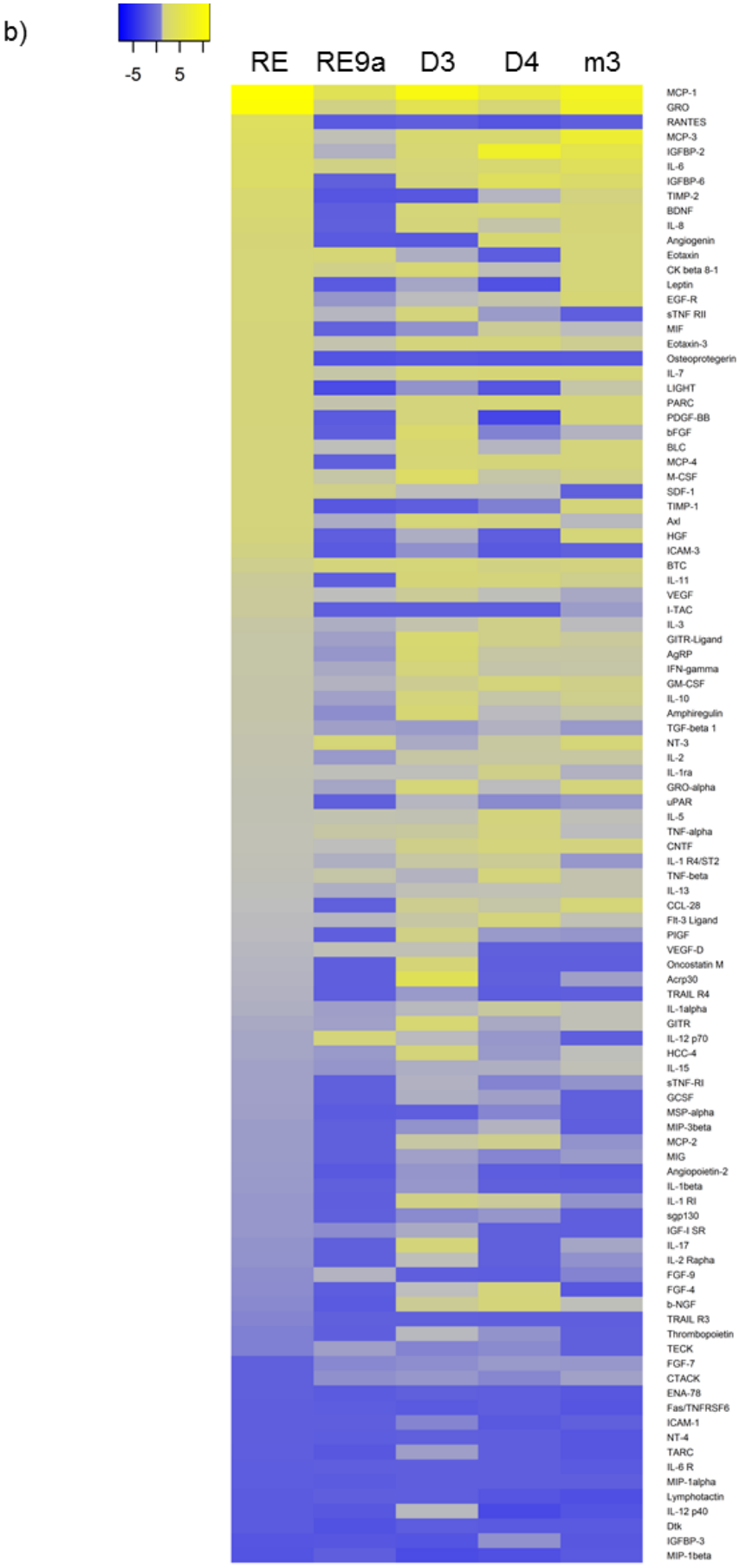
-5
5
RE
RE9a
D3
D4
m3
MCP-1
GRO
RANTES
MCP-3
IGFBP-2
IL-6
IGFBP-6
TIMP-2
BDNF
IL-8
Angiogenin
Eotaxin
CK beta 8-1
Leptin
EGF-R
sTNF RII
MIF
Eotaxin-3
Osteoprotegerin
IL-7
LIGHT
PARC
PDGF-BB
bFGF
BLC
MCP-4
M-CSF
SDF-1
TIMP-1
Axl
HGF
ICAM-3
BTC
IL-11
VEGF
I-TAC
IL-3
GITR-Ligand
AgRP
IFN-gamma
GM-CSF
IL-10
Amphiregulin
TGF-beta 1
NT-3
IL-2
IL-1ra
GRO-alpha
uPAR
IL-5
TNF-alpha
CNTF
IL-1 R4/ST2
TNF-beta
IL-13
CCL-28
Flt-3 Ligand
PlGF
VEGF-D
Oncostatin M
Acrp30
TRAIL R4
IL-1alpha
GITR
IL-12 p70
HCC-4
IL-15
sTNF-RI
GCSF
MSP-alpha
MIP-3beta
MCP-2
MIG
Angiopoietin-2
IL-1beta
IL-1 RI
sgp130
IGF-I SR
IL-17
IL-2 Rapha
FGF-9
FGF-4
b-NGF
TRAIL R3
Thrombopoietin
TECK
FGF-7
CTACK
ENA-78
Fas/TNFRSF6
ICAM-1
NT-4
TARC
IL-6 R
MIP-1alpha
Lymphotactin
IL-12 p40
Dtk
IGFBP-3
MIP-1beta

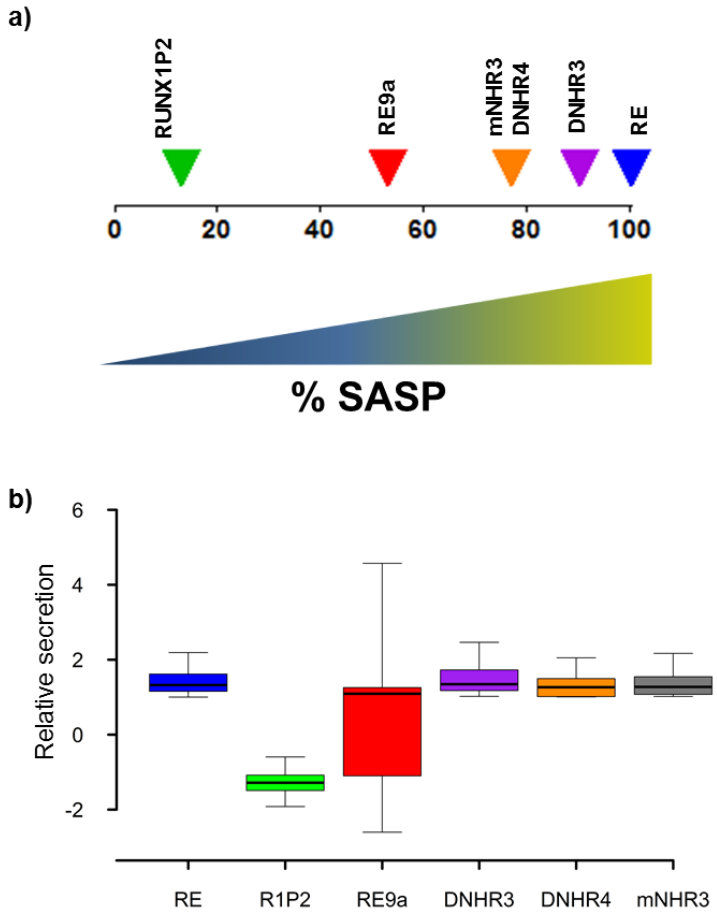

Figure 6.3 Percentage similarity between RE, RE9a and the NHR mutants
The total factors upregulated by RE were denoted as a 100% SASP and compared with upregulated factors from RUNX1P2, RE9a and the NHR mutants. (a) Graphic showing the percentage of similarity of upregulated SASP profiles of Hs68 cells expressing RE9a (53%), DNHR3 (90%), DNHR4 (77%), mNHR3 (77%) and RUNX1P2 (13%) relative to RE (100%). (b) Relative secretion by cells expressing RE, RUNX1P2, RE9a, DNHR3, DNHR4 or mNHR3 expressed as box-whisker plots.

6.3 Discussion

This study demonstrates that RE-induce SLGA is accompanied by increased IL-6 secretion and an extensive SASP in Hs68 cells. In contrast, Hs68 cells expressing RUNX1P2 displayed a marked downregulation of the majority of examined SASP markers, possibly indicating that RUNX1P2 actively represses senescence secretion. RE9a-expressing Hs68 cells displayed an intermediate profile that included a vestigial SASP but appeared largely repressive when compared to RE. Further study of the SASP using the NHR3 and NHR4 mutants demonstrated that

each domain contributes to the SASP phenotype but that none of the mutants fully recapitulate the robust RE SASP or the attenuated RE9a secretory profile. Interestingly, mNHR3 and DNHR4 more closely resemble the RE9a profile than DNHR3. It is possible that the exchange of the TERAKM motif for hydrophobic alanines has more profoundeffects on protein structure than simple deletion of NHR3.

Ectopic expression of RUNX1 in Hs68 cells has been documented to establish a potent senescence-like growth arrest in Hs68 cells [59]. The findings from this study show that RUNX1P2-induced SLGA involves at most a minimal SASP response. This observation may be related to the absence of ROS and p38MAPK activation observed in response to RUNX1P2 which have been associated with the activation of NFκB and induction of the SASP [185, 186, 218, 248, 254]. Furthermore, it has been demonstrated that NFκB-related genes are upregulated in human RUNX1 fusion protein-related leukaemias including t(8;21)-positive AML and that this effect can be recapitulated by knocking down RUNX1, suggesting that RUNX1 may abrogate NFκB signalling *in vivo* [255]. It is notable that RUNX1P2 induced senescence that was dependent on $p16^{INK4A}$ in Hs68 cells. $p16^{INK4A}$ has been reported to induce senescence in the absence of a SASP and may even restrain the SASP in some contexts [251]. Interestingly, expression of $p16^{INK4A}$ was reported to partially inhibit the SASP during replicative senescence in human fibroblasts [251]. This phenomenon was not observed for RE which both induced a $p16^{INK4A}$-dependent SLGA and a robust SASP in Hs68 cells. Indeed, the NHR mutants retained a virtually intact SASP despite failing to induce $p16^{INK4A}$ suggesting that the RE-associated SASP was somewhat refractory to $p16^{INK4A}$ expression. In contrast, ROS accumulation and p38MAPK were features of RE and NHR mutant expression in Hs68 cells and are capable of activating NFκB, a master regulator of the SASP [248]. Since the ROS-p38MAPK signalling pathway was not induced by RE9a and the SASP was severely compromised by this mutant it may be predicted that this pathway represents a significant inducer of the secretory phenotype associated with RE expression in human fibroblasts. Consistent with this interpretation is the observation that NFκB activity was induced in RE-transduced murine haematopoietic cells where it played a critical role in cellular transformation [255]. In this case activation of NFkB was

attributed to the loss of C-terminal domains in RUNX1 which are also absent from the RE constructs described in my study.

The qualitative differences between the secretory phenotype induced by RE and those induced by each of the NHR mutants suggest that particular NHR domains may modify NFkB signalling in some way or even activate alternative signalling pathways. In this respect it is notable that RE9a induced a vestigial SASP that was independent of ROS and p38MAPK activation. Reintroduction of the NHR3 or the NHR4 domain did not completely rescue the secretory profile of RE suggesting that both domains are required for maximal senescence secretion. Cooperation between NHR3 and NHR4 has been noted in the recruitment of corepressor complexes such as SON and NCoR/SMRT to ETO [11] and may be important for a maximal SASP induction by RE. In this respect it is of interest that NCoR/SMRT complexes have also been reported to directly repress transcription of a variety of inflammatory cytokines [256] so their improper recruitment in the context of RE may have consequences for senescence secretion.

The relevance of these findings for t(8;21) leukaemias is illustrated by t(8;21) Kasumi 1 cells that exhibit a dependence on increased levels of NFκB signalling for their cellular proliferation [255]. A SASP is often described as having "antagonistic pleiotropy". As an acute response it may be beneficial protecting against oncogenic transformation and mobilising the immune system to remove senescent cells, but over the longer term its' effects may prove deleterious inducing cellular and tissue damage through chronic inflammation [2]. The opposing effects of a SASP are mediated by individual SASP factors that exert antagonistic effects in different contexts. For example, IL-6, a key SASP component has been identified in a positive feedback signalling pathway with ROS, p38MAPK and NFκB and may consolidate SLGA [257] but IL-6 has also been identified as an important pro-oncogenic factor in numerous cancers and other age-related pathologies [258, 259]. It is of note that IL-6 was identified as a strongly upregulated factor in response to RE in Hs68 cells but was not induced by RUNX1P2. Ectopic expression of RE in primary fibroblasts was immediately repressive for cellular proliferation and therefore represents an acute response. In this case it was associated with a robust and extensive secretory phenotype

that may serve to enhance the SGLA. For the NHR mutants, however the secretory profile was associated with proliferative phenotypes of varying degrees providing clear evidence that the SASP is not necessarily indicative of SLGA but can also be associated with proliferating cells. It is possible that in the context of established t(8;21) leukaemic cells which not only frequently co-express RE and RE9a but also other cooperating mutations, the RE-induced SASP may promote stress and proliferation of pre-malignant and malignant cells which may contribute to their leukaemogenic phenotype *in vivo*.

7 TEL-RUNX1 Expression Promotes Evasion of Premature Senescence in Hs68 Cells

7.1 Introduction

The TR fusion protein generated by the t(12;21) chromosomal translocation is associated with approximately 25% of childhood B-cell ALL [260]. TR alone fails to induce leukaemia in murine models [101] but promotes leukaemogenesis in collaboration with inactivation of $p16^{INK4a}$ or by insertional mutagenesis by a sleeping beauty transposon [103, 104] suggesting that additional mutations are required for TR-mediated transformation *in vivo*.

The TR oncoprotein represents an in-frame fusion between the N-terminus of the TEL transcriptional repressor and the C-terminus of the P1 variant of RUNX1 [261]. The helix-loop-helix (HLH) domain is the only functional domain of TEL that is retained by the fusion protein. The HLH domain is required for protein-protein interactions and has been associated with TEL transcriptional repression and nuclear localisation [112, 262]. Deletion of the HLH domain renders TR unable to drive primary B-cell expansion *in vitro* indicating a pro-proliferative function consistent with a role in B-cell transformation [263]. This group previously reported that TR fails to induce premature senescence in primary human fibroblasts and suggested that this may be important for the leukaemogenicity of the fusion protein [59]. To address whether the P1 variant of RUNX1 or the HLH domain was responsible for escape, RUNX1P1 and a series of TR HLH mutants were introduced into primary human fibroblasts and their ability to induce senescence was examined.

Aims and Objectives

- Compare the proliferative and senescence phenotypes of cells expressing RUNX1P1 and RUNX1P2 to determine whether evasion of senescence by TR could partially be attributed to the presence of the RUNX1P1 isoform in the TR fusion protein.
- Examine mutants affecting the TR HLH domain to determine whether this region of the fusion transcript is important for TR-mediated senescence evasion.
- If the HLH domain is required, determine the mechanism by which it directs senescence evasion.

7.2 Results

7.2.1 Resistance to senescence is not conferred by the P1 isoform of RUNX1

RUNX1P2 induces premature senescence in primary human fibroblasts [59]. To determine whether the P1 variant of RUNX1 displays a similar phenotype, RUNX1P1 was introduced into Hs68 cells on a pLentiPURO vector with RUNX1P2 and pLentiPURO as positive and negative controls respectively. Cultures were then examined for parameters of premature senescence.

Western blot analysis of selected cells revealed slightly higher levels of RUNX1P2 that RUNX1P1 but both proteins were expressed at significantly higher levels than endogenous RUNX1 in the PURO control cultures (**Figure 7.1 a**). Ectopic expression of RUNX1P1 was associated with a profound growth arrest that was essentially indistinguishable from that observed with RUNX1P2 (**Figure 7.1 b**). Moreover, the cells assumed a flattened and enlarged morphology and displayed positive SA-β-Gal staining (**Figure 7.1 c**) consistent with the onset of premature senescence.

Previous studies in primary Hs68 fibroblasts demonstrated association between RUNX1P2-induced SLGA and upregulation of $p16^{INK4a}$ [59]. This study demonstrates phosphorylation of AKT in response to ectopic expression of RUNX1P2 in the same cell background (**Chapter 4, Figure 6.1b**). To determine whether RUNX1P1 shares this phenotype, expression levels of $p16^{INK4a}$ and phosphorylated AKT were assayed in RUNX1P1 transduced Hs68 cells 6 days post-selection when visible signs of senescence were apparent. Although both RUNX1P1 and RUNX1P2 induced expression of $p16^{INK4a}$ and phosphorylated AKT, RUNX1P1 appeared to induce $p16^{INK4a}$ expression more strongly than RUNX1P2 while RUNX1P2 cells displayed greater activation of AKT (**Figure 7.1 d)**. Together these data suggest that the P1 and P2 isoforms of RUNX1 exhibit bias towards specific signalling pathways resulting in quantitative differences in pathway activation.

To further discriminate between the P1 and P2 isoforms of RUNX1, their secretory profiles were examined using a human cytokine array (RayBiotech). Conditioned medium was harvested 6 days after puromycin selection when visible signs of senescence were apparent. In the heat-maps generated, yellow

indicates upregulation, blue indicates downregulation and grey is used to represent the basal levels of secretion (equivalent to PURO). The heat maps were sorted according to magnitude changes induced by RE which was included as a positive control for SASP. A comparison of the heat maps revealed considerable differences between RUNX1P1 and RUNX1P2, with increased levels of secretory markers largely observed in the media harvested from RUNX1P1 expressing cells and only one factor specifically induced by RUNX1P2 (MCP1). Of the upregulated targets, 2 were shared between RUNX1P1 and RUNX1P2 (CK beta 8-1 and Eotaxin) and the remainder were downregulated by RUNX1P2 suggesting that RUNX1P1 is capable of inducing a much more substantial SASP compared to RUNX1P2 (**Figure 7.1 e)**. To quantify the phenotype, the absolute numbers of upregulated secretory factors in each heat map were compared to RE which was used as a positive control for secretion. This study shows that RUNX1P1 induced 73% of the factors upregulated by RE compared to only 13% by RUNX1P2 (**Figure 7.1 f).**

Together these data demonstrate that RUNX1P1 is capable of inducing premature senescence in primary human fibroblasts. The pathways involved are subtly different to RUNX1P2 and include induction of a substantial secretory profile. From this evidence, it could be predicted that the P1 isoform of RUNX1 is not responsible for the escape from senescence observed when TR is introduced into primary human fibroblasts.

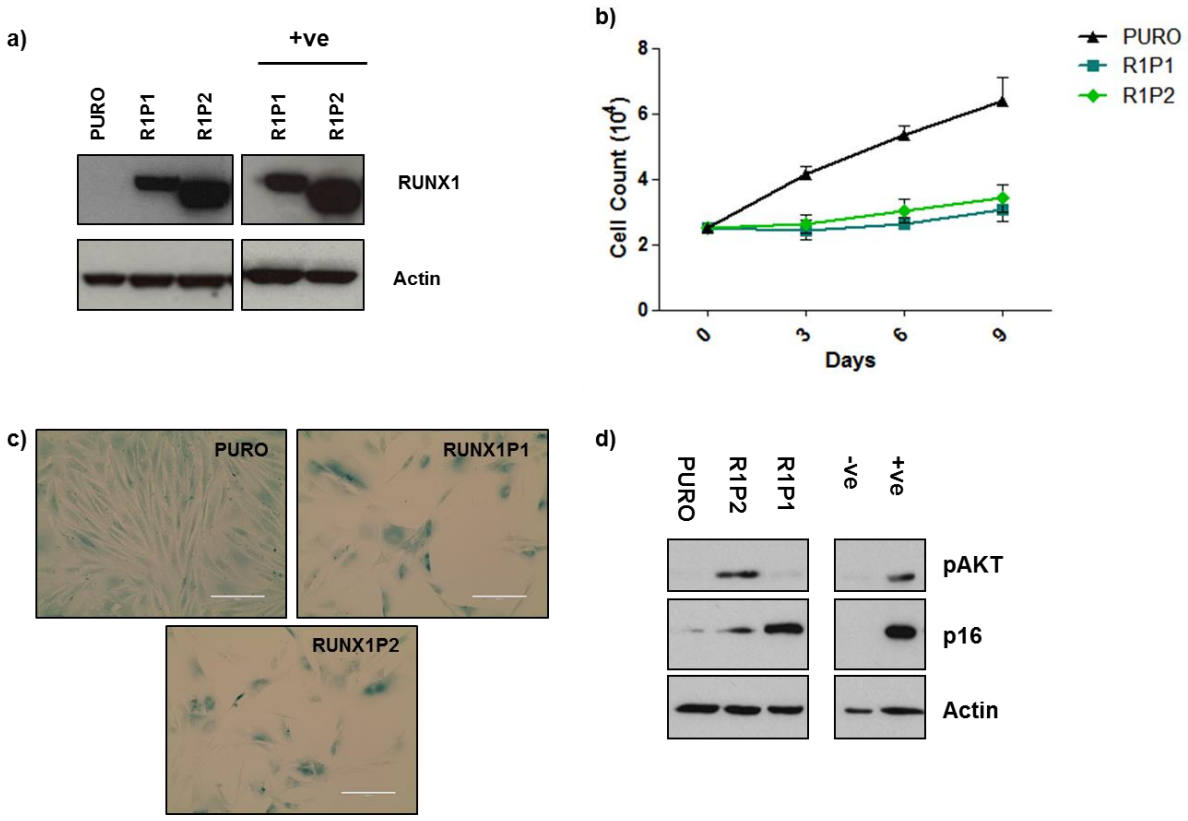

Figure 7.1 RUNX1P1 and RUNX1P2 induce premature senescence in Hs68 cells
Hs68 cells were transduced with lentivirus vectors expressing RUNX1P1 and RUNX1P2. The empty vector was included as a negative control and will be referred to as PURO. Cells were selected in puromycin. (a) Western Blot analysis of RUNX1P1 and RUNX1P2 expression in transduced Hs68 cells using anti-RUNX (D207-3, MBL Ltd). (b) Growth curves of cells expressing PURO, RUNX1P1 or RUNX1P2. Growth was recorded in triplicate over a 9 day period. (c) Transduced cells stained for SA-β-Gal on day 6 post selection. Images were captured using 20x magnification. (d) Western blot analysis of phosphorylated AKT (#9271, Cell Signaling Technology) and $p16^{INK4a}$ (sc-468, Santa Cruz Biotechnology) in transduced Hs68 cells harvested 6 days post-selection. (e) Supernatants harvested from transduced cells on day 6 post-selection were subjected to human cytokine array analysis. Data was normalised to the PURO empty vector control. Heat-map plot generated from data obtained using a human cytokine array to measure the SASP of Hs68 cells expressing RUNX1P1 and RUNX1P2. Yellow indicates upregulation while blue indicates downregulation of secreted factors. RE is included here as a positive control for SASP. (f) Graphic showing the percentage of similarity of SASP profiles of Hs68 cells expressing RUNX1P2 (13%) or RUNX1P1 (73%) relative to RE (100%).

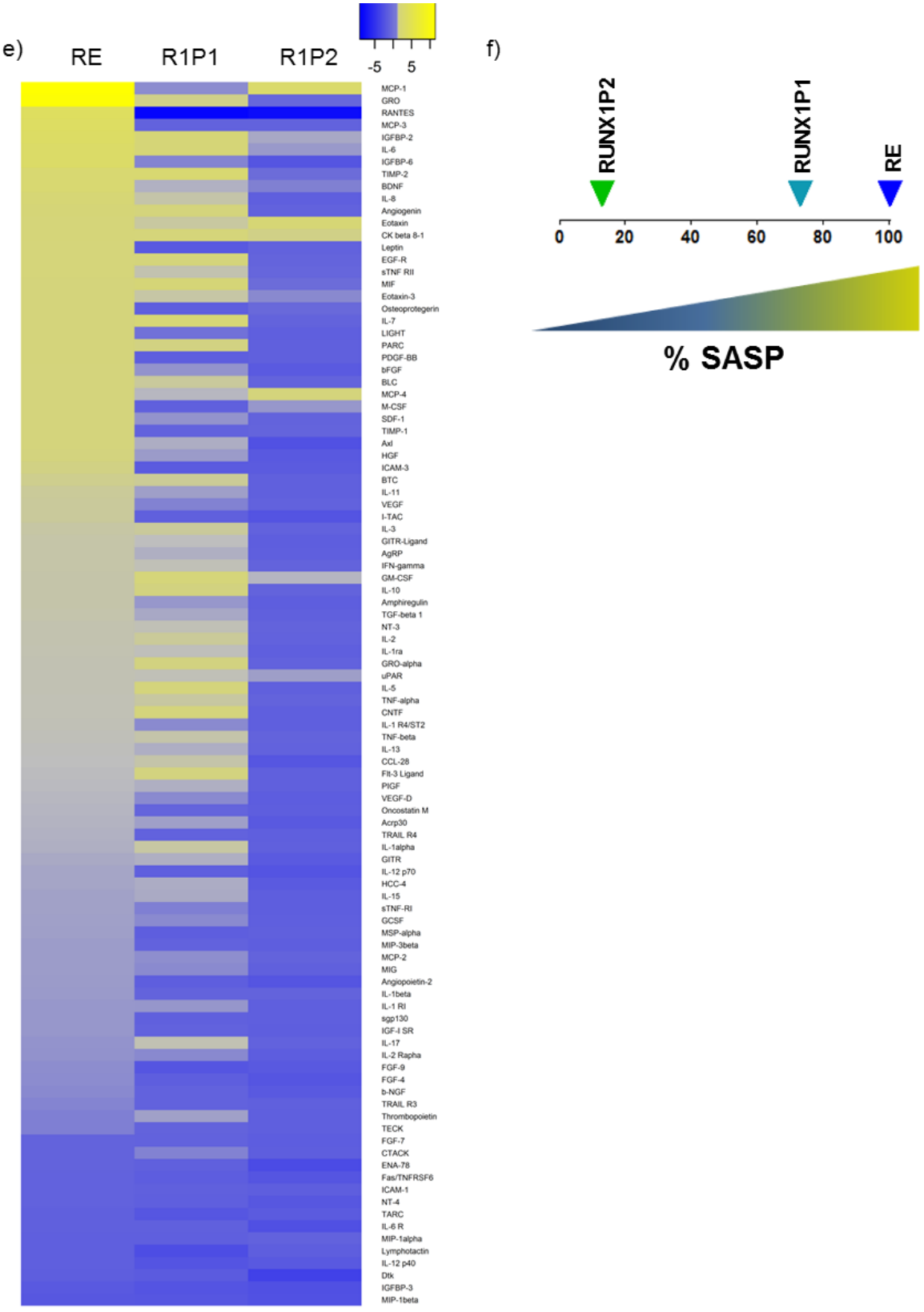
e)
RE
R1P1
R1P2
-5
5
MCP-1
GRO
RANTES
MCP-3
IGFBP-2
IL-6
IGFBP-6
TIMP-2
BDNF
IL-8
Angiogenin
Eotaxin
CK beta 8-1
Leptin
EGF-R
sTNF RII
MIF
Eotaxin-3
Osteoprotegerin
IL-7
LIGHT
PARC
PDGF-BB
bFGF
BLC
MCP-4
M-CSF
SDF-1
TIMP-1
Axl
HGF
ICAM-3
BTC
IL-11
VEGF
I-TAC
IL-3
GITR-Ligand
AgRP
IFN-gamma
GM-CSF
IL-10
Amphiregulin
TGF-beta 1
NT-3
IL-2
IL-1ra
GRO-alpha
uPAR
IL-5
TNF-alpha
CNTF
IL-1 R4/ST2
TNF-beta
IL-13
CCL-28
Flt-3 Ligand
PlGF
VEGF-D
Oncostatin M
Acrp30
TRAIL R4
IL-1alpha
GITR
IL-12 p70
HCC-4
IL-15
sTNF-RI
GCSF
MSP-alpha
MIP-3beta
MCP-2
MIG
Angiopoietin-2
IL-1beta
IL-1 RI
sgp130
IGF-I SR
IL-17
IL-2 Rapha
FGF-9
FGF-4
b-NGF
TRAIL R3
Thrombopoietin
TECK
FGF-7
CTACK
ENA-78
Fas/TNFRSF6
ICAM-1
NT-4
TARC
IL-6 R
MIP-1alpha
Lymphotactin
IL-12 p40
Dtk
IGFBP-3
MIP-1beta
f)
RUNX1P2
RUNX1P1
RE
0
20
40
60
80
100
% SASP

7.2.2 Escape from senescence is mediated by the HLH domain of TEL

To determine whether the inability of TR to induce senescence is a function of the HLH domain, a HLH deletion mutant (**Figure 7.2 a**) (kindly gifted by Professor O. Williams) was subcloned into the pBabe PURO retroviral vector and the cells examined for markers of premature senescence.

As previously reported, Hs68 cells expressing TR continued to divide at a comparable rate to PURO control cultures. In contrast, Hs68 cells expressing TR∆HLH displayed a rapid and dramatic growth arrest (**Figure 7.2 b**) and visible signs of premature senescence (**Figure 7.2 c**) strongly supporting a requirement for the HLH domain for TR-induced evasion of premature senescence. However, data from protein expression analyses revealed markedly reduced levels of TR compared to RUNX1P1 or TR∆HLH and the possibility that TR transduced cells are refractory to premature senescence simply due to insufficient TR protein expression (**Figure 7.2 d**). A similar pattern was observed when expression was driven by a lentiviral vector in human fibroblasts but not when TR was expressed from the same retroviral vectors in murine NIH3T3 cells where the level of ectopic TR was comparable to RUNX1P1 (**Figure 7.2 e**). Together these data exclude a technical problem with the expression vector and rather suggest that TR might be subject to sequestration in a specific cellular compartment in human cells that is less amenable to extraction by conventional techniques.

To address this question, parallel cell pellets of Hs68 cells expressing TR were extracted under increasing denaturing conditions and the lysates examined for expression of TR. As shown in **Figure 7.2 f**, expression of TR was dramatically increased in the presence of 1% SDS. Extraction in lower concentrations of SDS (0.1%) or non-ionic weaker denaturing detergents including Triton (0.4%) and NP40 (0.5%) was less successful suggesting that full length TR was localised to an inaccessible cellular compartment in human cells in a manner dependent on the HLH domain. In support of this hypothesis, subcellular fractionation of the endogenous fusion protein in the t(12;21) positive REH cell line revealed that in contrast to nuclear RUNX1, TR was localised to the membraneous compartment (**Figure 7.2 g**) represented by structures such as the Golgi and the endoplasmic reticulum (ER) and known to require higher levels of detergent for successful

solubilisation [264]. Calnexin was used to delineate the ER-associated membrane fraction as it is a chaperone localised to the ER [265]. Together these data suggest that subcellular localisation of TR is regulated by the HLH domain and may contribute to the failure of TR to induce premature senescence in human fibroblasts.

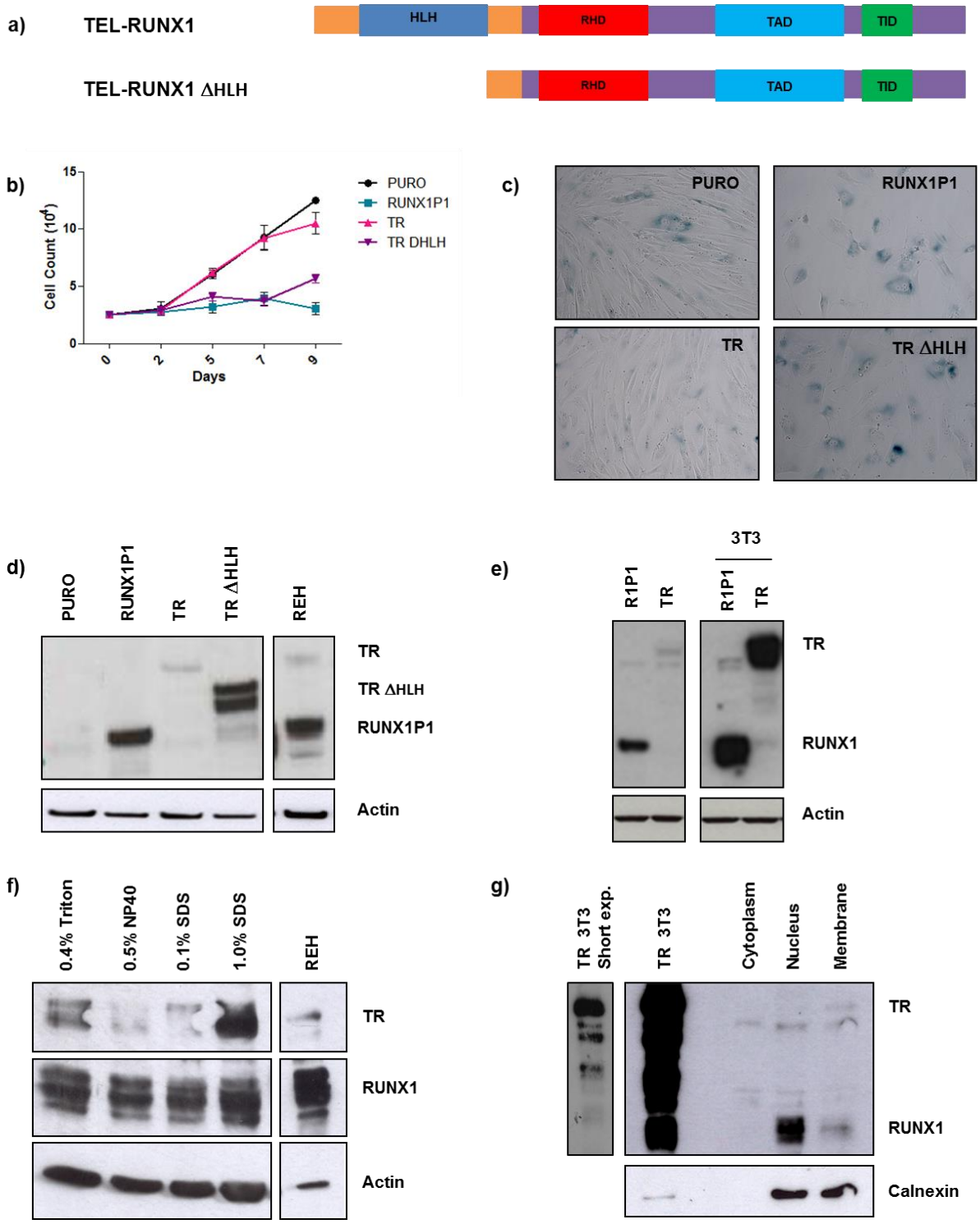

Figure 7.2 The HLH domain of TEL is essential for TR-mediated escape from senescence
Hs68 cells were transduced to express RUNX1P1, TR, and TRΔHLH mutant. (a) Schematic of the TR fusion protein and TRΔHLH. (b) Growth curves of transduced cells taken over a 9 day period. (c) SA-ß-Gal staining performed day 6 post-selection. Images were captured using 20x magnification. (d) Western blot showing RUNX1P1 (53 kDa), TR (98 kDa) and TRΔHLH (80 kDa) expression in Hs68 cells transduced as described above measured using an anti-RUNX antibody (D207-3, MBL Ltd). REH cell lysate was included as a positive control for RUNX1 and TR expression. (e) Western blot analysis comparing RUNX1P1 and TR expression levels Hs68 cells transduced using lentivirus vectors and murine 3T3 cells transduced using retroviral (pBabe) vectors using an anti-RUNX primary antibody (D207-3, MBL, Ltd). (f) Western blot analysis of TR and RUNX1 levels (D207-3, MBL Ltd) after protein extraction in TR-transduced Hs68 cells using

different denaturing detergents. Cells transduced to express TR were lysed using WCL buffer (0.4% Triton), NLT buffer (0.5% NP40), RIPA (0.1% SDS) or RIPA (1% SDS). (g) Western blot analysis of cytoplasmic, nuclear and membraneous fractions of REH cells probed with anti-RUNX antibody (D207-3, MBL Ltd) and anti-calnexin (ab22595, Abcam) to differentiate the membraneous fraction from the cytoplasmic/nuclear fractions.

7.2.3 Lysine 99 of the HLH domain is sufficient to allow TR-induced escape from senescence

Lysine 99 (K99) within the HLH domain of TEL has previously been identified as a critical residue for the subcellular localisation of TR. Indeed mutation of K99 to an arginine (R) residue was sufficient to disrupt the nuclear export of TEL [114]. To determine whether this residue is also sufficient to restore a senescence phenotype in TR expressing cells, a TR K99R mutant was generated by site-directed mutagenesis (with thanks to Dr Anna Kilbey) and sub-cloned into a pLentiPURO lentiviral vector for transduction into Hs68 cells. Transduced cells were harvested after puromycin selection and western blotting performed on extracts prepared under standard conditions (0.4% Triton) for expression of RUNX1P1, TR and TR K99R. As predicted, the apparent expression level of TR was low compared to that of RUNX1P1. In contrast, the TR K99R expression level was high and approximately equivalent to RUNX1P1 (**Figure 7.3 a**). Moreover, Hs68 fibroblasts expressing TR K99R underwent a profound growth arrest (**Figure 7.3 b**) that was accompanied by a flattened and enlarged morphology and positive staining for SA-β-Gal activity that was comparable to that observed for RUNX1P1 (**Figure 7.3 c**) . To determine whether this mutation induced a distinct mode of senescence or simply activated RUNX1 specific senescence pathways transduced Hs68 cells were examined 6 days after selection for $p16^{INK4A}$ expression, which is upregulated during RUNX1-induced SLGA (**Figure 7.1 d**), and ROS, which is not (**Chapter 4, Figure 6.2 a**). As shown in **Figure 7.3 d**, K99R induced increased $p16^{INK4A}$ expression relative to the wildtype fusion protein but not as acutely as RUNX1P1. In contrast ROS production was significantly upregulated by expression of K99R in comparison to the PURO vector control cells (**Figure 7.3 e**). RUNX1P1, like RUNX1P2, failed to upregulate ROS production confirming that this pathway is also not required for RUNX1P1-induced SLGA. $p16^{INK4a}$ and ROS accumulation were refractory to TR expression consistent with the inability of TR to induce senescence. Together these data indicate that mutation of lysine 99 to arginine within the HLH domain of the full length TR fusion protein is sufficient to restore premature senescence in human fibroblasts and suggest that the pathways involved are quantitatively and qualitatively distinguishable from those utilised by RUNX1P1.

To determine whether mutation of K99 alters the subcellular distribution of TR, Hs68 cells were stably transduced with TR and K99R and the proteins visualised by indirect immunofluorescence on a Zeiss LSM 710 confocal microscope. As shown in **Figure 7.3 f**, TR was localised to distinct punctate perinuclear structures whereas TR K99R was predominantly detected in a diffuse pattern in the nucleus co-localising with DAPI. From these data it can be concluded that the K99 residue within the HLH domain regulates the subcellular distribution of TR to the cytoplasm. In this localisation TR supports a proliferative phenotype that may be critical for its pre-leukaemic activity.

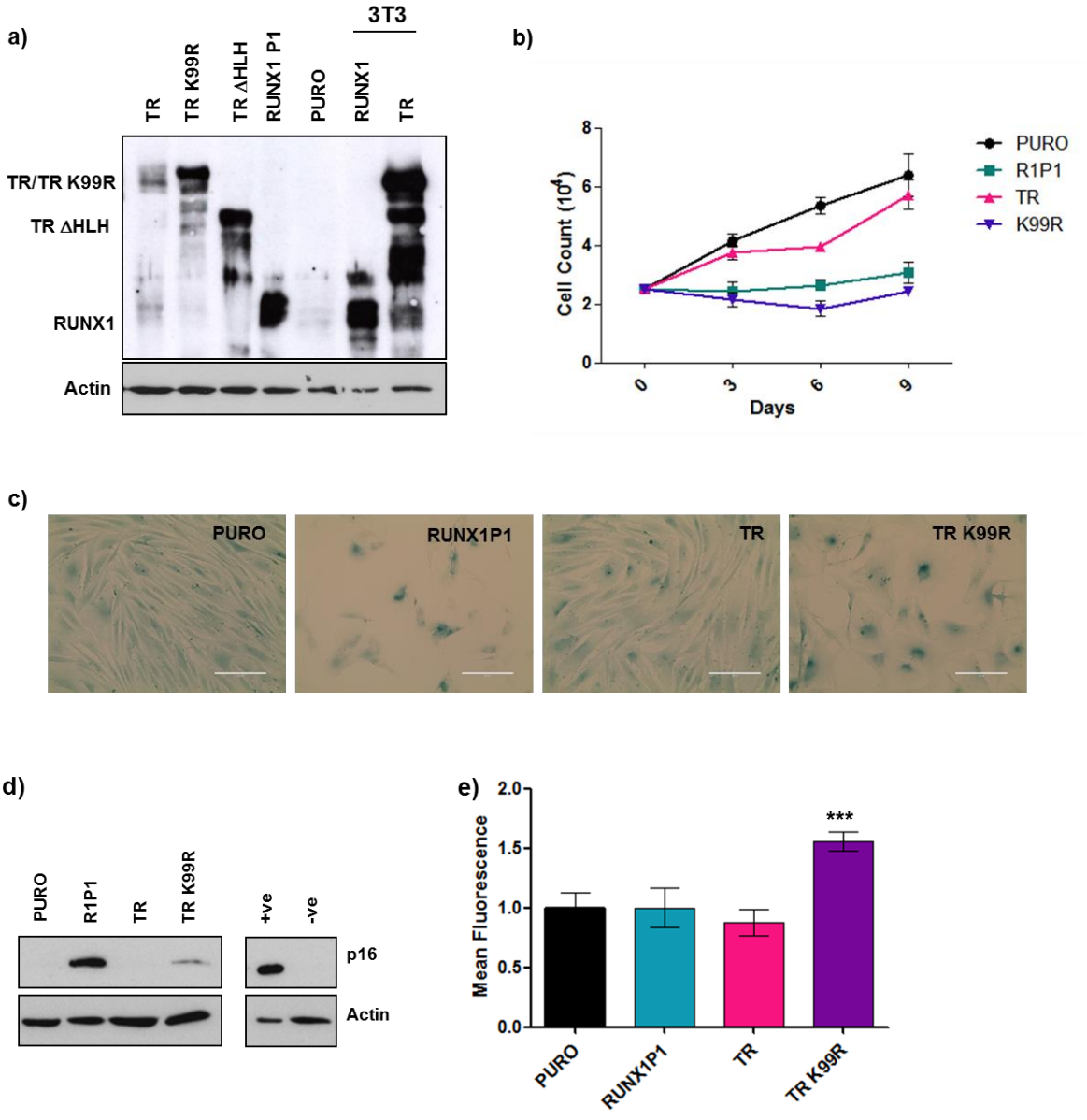
a)
3T3
TR
TR K99R
TR ΔHLH
RUNX1 P1
PURO
RUNX1
TR
TR/TR K99R
TR ΔHLH
RUNX1
Actin
b)
Cell Count (10⁴)
Days
PURO
R1P1
TR
K99R
c)
PURO
RUNX1P1
TR
TR K99R
d)
PURO
R1P1
TR
TR K99R
+ve
-ve
p16
Actin
e)
Mean Fluorescence
***
PURO
RUNX1P1
TR
TR K99R
f)
TEL-RUNX1
TEL-RUNX1 K99R
α-HA-Tag
DAPI + α-HA
FITC 2nd
DAPI + 2nd

Figure 7.3 Lysine 99 of the HLH domain is essential for TR-mediated escape from senescence

Hs68 cells were transduced to express RUNX1P1, TR, TR∆HLH and TR K99R. The PURO empty vector was included as a positive control. (a) Western Blot analysis of expression of RUNX1P1(53 kDa), TR (98 kDa), TR∆HLH (80kDa) and TR K99R (98 kDa) detected with anti-RUNX antibody (D207-3). (b) Growth curve analysis of Hs68 cells expressing RUNX1P1, TR and TR K99R measured proliferation over a 9 day period. (c) Images taken after staining cells for SA-β-Gal on day 6 post-selection. Images were captured using 20x magnification. (d) Western blot analysis of $p16^{INK4a}$ expression levels (sc-468, Santa Cruz Biotechnology) in transduced Hs68 cells. (e) Intracellular ROS levels were measured by FACs-based detection of DCF-DA fluorescence. DCF-DA fluorescence was quantified and normalised to PURO. Significance was determined using students t-test and error bars refer to standard deviation. (f) HA-tagged TR and TR K99R detected by indirect immunofluorescence using an anti-HA antibody and a FITC-conjugated secondary. The nuclei of the cells were stained using DAPI.

7.2.4 Is Lysine 99 of TEL-RUNX1 subject to SUMOylation?

Previous studies suggest that K99 SUMOylation within TEL or the TR fusion protein regulates the subcellular compartmentalisation of both proteins [113, 114]. SUMOylation is a post-translational modification whereby small ubiquitin-like modifier (SUMO) proteins become covalently attached and detached from target proteins in a cyclic manner [266]. Consensus SUMOylation sites can be identified using predictor tools such as SUMOplot™ and consist of a Ψ-K-x-D/E motif where Ψ is a hydrophobic amino acid, K is the Lysine residue to which SUMO becomes conjugated, x is any amino acid and D/E is an acidic amino acid [267]. Interrogation of the sequence around K99 using SUMOplot™ failed to identify K99 as a consensus SUMOylation motif due to the presence of a hydrophilic amino acid (Threonine) rather that a hydrophobic one preceding K99. As previously reported, a second site, K11, was confirmed by SUMOplot™ as being within a consensus SUMOylation motif [115] (**Figure 7.4 a**).

To establish whether TR K99 is a non-consensus SUMOylation site, pLentiNEO lentiviruses expressing TR and TR K99R were introduced into HepaRG cells stably expressing His-tagged SUMO proteins (SUMO-1, SUMO-2 and SUMO-3) under puromycin selection (Kindly gifted by Dr Elizabeth Sloan). Neomycin-resistant cells were harvested after 5-7 days and SUMOylated proteins pulled down by Nickel-Affinity Purification and analysed by western blot (**Figure 7.4 b**). Interrogation of the blots with an anti-RUNT antibody specifically detected TR and TR K99R in cells expressing SUMO1-3 but not in the HIS-only control cells suggesting that both proteins were subject to SUMOylation by SUMO1, 2 and 3. In addition, a ladder of higher molecular weight RUNX reactive bands was detected in His-SUMO1 HepaRG cells expressing either TR or TR K99R which may be consistent with multiple SUMOylations. Reprobing of the blots with an anti-His antibody revealed that free His-SUMO1 was less prevalent than either SUMO2 or SUMO3 but as yet it is not possible to say whether this reflects a greater proportion of SUMO1 existing in the conjugated state or simply lower absolute expression levels of His-SUMO1 in HepaRG cells. As observed in human Hs68 cells, TR was detected at lower levels that TR K99R but both proteins essentially displayed the same pattern of affinity purified bands supporting the conclusion that K99 does not regulate TR subcellular localisation as part of a consensus

SUMOylation site and that TR may be SUMOylated on alternative lysine residues such as K11 which is present in both proteins.

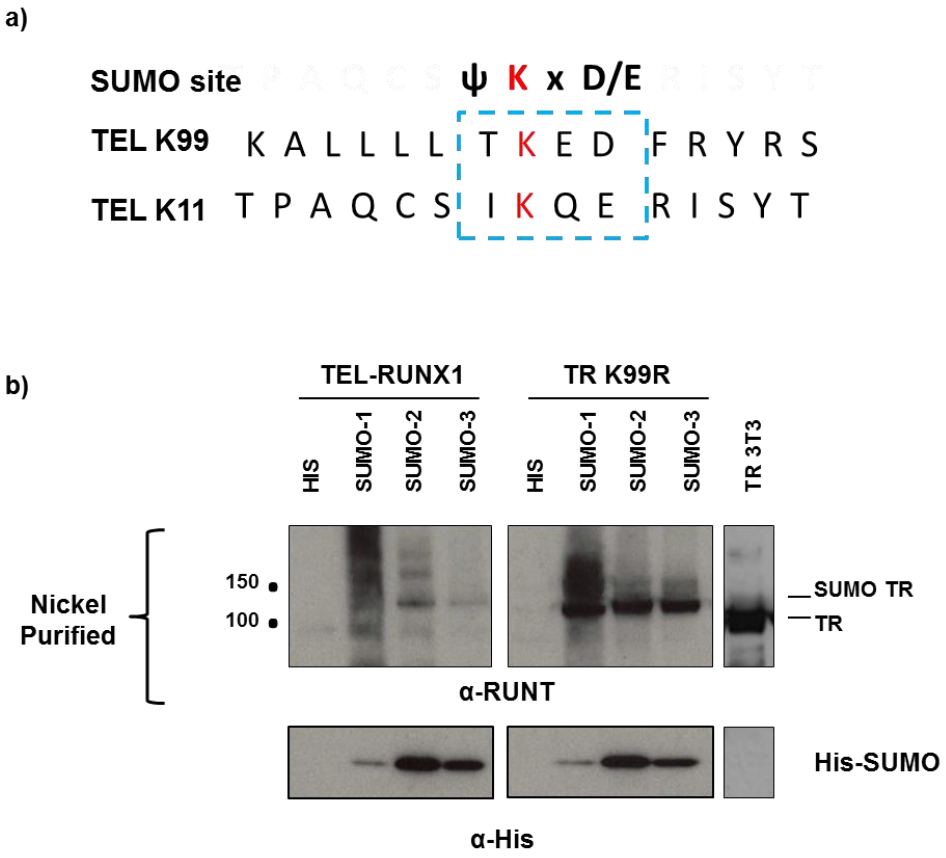

Figure 7.4 Lysine 99 of the HLH domain is not a SUMOylation site
HepaRG cells expressing His-tagged SUMO proteins were transduced with lentivirus vectors encoding TR or TR K99R. (a) Comparison of the consensus SUMOylation sequence, ψKxD/E (ψ= hydrophobic amino acid, K= Lysine, x= any amino acid, D/E= acidic amino acid) to proposed SUMOylation sites at K99 and K11 of TEL/TEL-RUNX1 as determined by SUMOplot. (b) Western Blot analysis of Nickel affinity purified samples taken from HepaRG cells expressing His-tagged SUMO1, SUMO2 or SUMO3. Purified SUMO and interacting TR or TR K99R were detected using an antibody against SUMO.

7.2.5 A t(12;21) Leukaemic Cell-Line is Refractory to TR K99R-Induced SLGA

To determine whether the effects of TR K99R on senescence are restricted to primary cells or can be extended to more physiologically relevant cell backgrounds TR K99R was introduced into REH cells which represent an end stage t(12;21) positive leukaemic line. Using a lentiviral vector delivery system, high levels of ectopic TR K99R were detected compared to the endogenous TR protein in REH cells (**Figure 7.5 a)**. In contrast to primary human fibroblasts expression of TR K99R failed to induce SLGA in REH cells and consistently

promoted their growth relative to the empty vector (PURO) control cultures (**Figure 7.5 b**) REH cells lack expression of the $p16^{INK4A}$ tumour suppressor and also display high levels of endogenous RUNX1 [268]. To determine whether the growth inhibitory properties of RUNX1 are silenced by loss of $p16^{INK4A}$ RUNX1P2 was introduced into $p16^{INK4A}$-null primary human diploid fibroblasts (Leiden cells) and examined their growth. As shown in **Figure 7.5 c,** RUNX1 promoted growth in this cell background suggesting that loss of $p16^{INK4A}$ reveals pro-oncogenic functions of RUNX1 that render end stage leukaemic cells refractory to premature senescence.

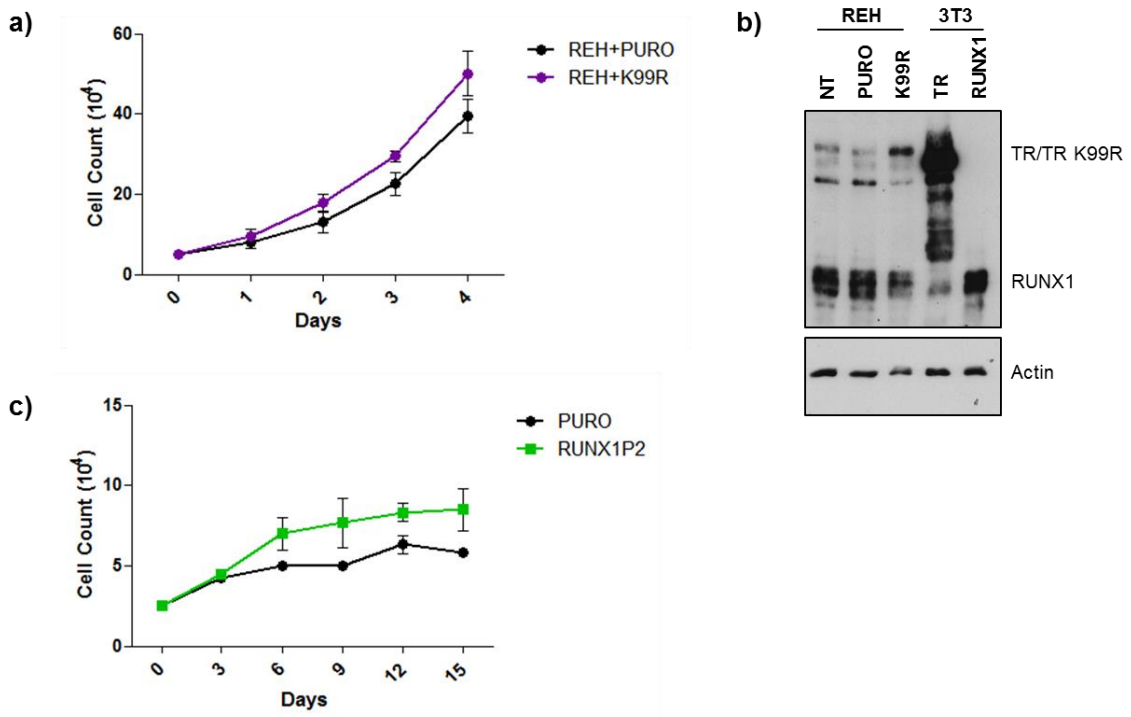

Figure 7.5 A t(12;21) leukaemic cell-line is refractory to TR K99R-induced senescence
REH cells were transduced with a lentivirus vector encoding TR K99R or the PURO empty vector control. (a) Growth curves showing proliferation of PURO and TR K99R-expressing REH cells over a 4-day period. (b) Western blot analysis of TR, TR K99R and RUNX1 expression in transduced and non-transduced REH cells using an anti-RUNX antibody (D207-3, MBL Ltd). Leiden fibroblasts ($p16^{INK4A}$-null) were transduced with a lentivirus vector encoding RUNX1P2 or the PURO empty vector control. (c) Growth curves showing proliferation of PURO and RUNX1-expressing Leiden cells measured over a 15-day period.

7.3 Discussion

In line with a previous report, this study has shown that despite retention of an almost intact RUNX1 sequence, TR fails to induce senescence in Hs68 cells [59]. The possibility that RUNX1P1 sequences are responsible can now be excluded and Lysine 99 within the TEL HLH domain was identified as a critical residue responsible for the subcellular localisation of TR and escape from premature senescence.

I have shown that RUNX1P1 SLGA is visually indistinguishable from RUNX1P2 but unique with respect to senescence secretion which is robust and largely restricted to RUNX1P1. It has previously been reported that RUNX1 attenuates NFκB activation through a direct interaction with the IκB Kinase (IKK) complex [255]. While this may account for the weak SASP associated with RUNX1P2, our data suggest that RUNX1P1 is capable of inducing a SASP, possibly as a less effective attenuator of NFκB activity or through alternative signalling pathways. It is notable that sequences outwith the RHD and C-terminus of RUNX1 were also required to attenuate NFκB activity in murine haematopoietic cells [255]. Furthermore, a failure of RUNX1P1 to accumulate intracellular ROS was observed in human fibroblasts. Elevated ROS is reported to activate p38MAPK, a major inducer of NFκB and the secretory phenotype, supporting the existence of an alternative pathway. Finally, RUNX1P1 and RUNX1P2 induced SLGA through subtly different signalling pathways, confirming that these isoforms do not behave identically in human fibroblasts.

A SASP can be beneficial or deleterious depending on cellular context [205]. As an acute response to oncogene expression, the SASP can reinforce SLGA in senescent lesions and the surrounding cells via autocrine and paracrine mechanisms thereby contributing to tumour suppression. However, persistent SASP signalling can promote malignant phenotypes through chronic inflammation [145, 186, 205, 206, 209]. It is therefore interesting that RUNX1P1 and not RUNX1P2 was identified as a collaborating oncogene in a CD2-Myc retroviral insertional model of murine lymphoma [58]. Moreover, RUNX1P1 is the predominant isoform expressed in childhood B-cell ALL (M. Stewart, Unpublished data) where RUNX1 is frequently amplified [269-273], all suggesting that RUNX1P1 may be the more oncogenic isoforms of RUNX1 in lymphoid leukaemia

[274]. The t(12;21) chromosomal translocation encodes almost the entire P1 isoform of RUNX1 fused to the TEL HLH domain [105]. From the data presented here, it seems unlikely that P1 sequences are responsible for TR-induced evasion of SLGA but they may none-the-less contribute to the oncogenicity of the fusion protein in the context of leukaemia development.

The HLH domain is the only functional domain of TEL retained by the TR fusion and is required for the preleukaemic activity of TR in haematopoietic stem cell models of B-cell ALL [112]. Early B cells derived from these models display enhanced colony formation *in vitro* and an advantage over normal haematopoietic progenitors when reconstituted *in vivo* [102, 263, 275]. Furthermore, it has been reported that TR positive murine pre-B cells display reduced sensitivity to growth inhibitory signalling by TGF-β which was hypothesized to result in preferential pre-leukaemic cell expansion [229]. These observations have now been extended to primary human fibroblasts, showing that TR expression is consistent with a proliferative phenotype that essentially evades SLGA and is entirely dependent on Lysine 99 within the HLH domain. The biological significance of this result is realised by the fact that the TR fusion alone is insufficient to drive leukaemia in murine haematopoietic models supporting a requirement for secondary cooperating mutations [101, 103, 263]. Consistent with this interpretation is the high incidence of t(12;21) chromosomal translocations in newborns that far exceeds the occurrence of childhood B-ALL [276], and retrospective analyses of Guthrie Spots showing that the TR preleukaemic clone arises in utero and persists for several years before developing into ALL [277]. My data shows that TR evades SLGA and sustains the proliferation of human fibroblasts through a mechanism of cytoplasmic sequestration regulated by Lysine 99. Lysine 99 was previously reported as a site of SUMOylation in TEL and TR that regulates nuclear export [114]. It was not possible to confirm Lysine 99 as a perfect SUMO consensus sequence or indeed a specific site of SUMOylation in TR, but mutation of Lysine 99 to an arginine residue was sufficient to redistribute TR to the nucleus and induce SGLA. TR K99R has not been described as a naturally occurring mutant but localisation of TR to the membraneous compartment in the REH B-ALL cell line strongly suggests that cytoplasmic sequestration is not simply a feature of overexpression in fibroblasts and may be relevant in a leukaemic context. Moreover this study

shows that TR resisted extraction in human fibroblasts which is consistent with membrane localisation. Nuclear import of TR K99R was confirmed by immunofluorescence. It has been proposed that nuclear TR functions as a negative repressor of RUNX1 activity [109]. As a nuclear transcription factor, the TEL HLH domain interacts with a number of co-repressor complexes including KAP1, NCoR/SMRT, mSin3A and HDACs [278-280]. It is believed that TEL recruitment of co-repressors to RUNX1 responsive gene promoters via the RUNX1 RHD results in constitutive transcriptional repression of RUNX1 targets [110]. While this is an attractive model it has also been reported that TR expression derepressed a number of RUNX1 dependent promoters in murine fibroblasts [75] and that TR can sequester co-factors in the cytoplasm including RUNX1 co-activators such as p300 [262]. Together these reports suggest that TR is more than just a constitutive repressor of RUNX1 function and support findings from this study, showing that TR K99R-induced SLGA was distinct from RUNX1P1 in human fibroblasts. Although the cultures were visually indistinguishable they were biochemically distinct, particularly with respect to the dramatic accumulation of intracellular ROS associated with TR K99R, suggesting that TR K99R is capable of directing a unique senescence phenotype from RUNX1P1.

Contrary to the effects of TR K99R in human fibroblasts this mutant was unable to induce premature senescence in REH cells suggesting that these end stage leukaemic cells have become refractory to senescence failsafe mechanisms. Consistent with this argument is the amplification and/or overexpression of RUNX1 commonly associated with childhood B-cell ALL and B-cell ALL cell lines that is apparently compatible with cellular proliferation **[274, 281]**. Since RUNX1 and TR K99R are sufficient to induce SLGA in primary human fibroblasts it may be predicted that end stage leukaemia cells have acquired secondary mutations that mask this activity. In this respect it is notable that RUNX1P1 [59] and RUNX1P2 promoted the growth of $p16^{INK4A}$ null Leiden cells supporting the existence of RUNX1 oncogenic functions revealed only in the absence of $p16^{INK4A}$. Moreover REH cells harbour deletions affecting the *CDKN2A* gene which encodes $p16^{INK4A}$ and $p14^{ARF}$ [282]. Finally TR, unlike RUNX1P1 or TR K99R failed to induce $p16^{INK4A}$ or SLGA in human fibroblasts providing a strong causative link between $p16^{INK4A}$ and RUNX1-induced SLGA *in vitro*. From the evidence presented here it may be predicted that suppression of RUNX1-induced growth arrest by the TEL

fusion moiety is critical for leukaemia initiation but is dispensable for end-stage leukaemias that have become refractory to this failsafe mechanism.

8 General Discussion

8.1 What is the Biological Significance of SLGA?

As discussed in chapter 1, OIS was initially described in murine and human fibroblasts in response to H-Ras^{V12} and attributed to a DDR triggered by hyper-replication [130, 169, 170]. It has since been described by us and others in response to a wide range of oncogenes but does not necessarily involve DNA damage [59, 225, 226]. Rather, the common factor appears to be the induction of major tumour suppressor pathways including p53 and p16^{INK4A} to induce SLGA. p53 activation was a feature of Runx-induced senescence in primary MEFS and associated with a rapid and profound SLGA in the absence of DNA damage [224]. This study has demonstrated a similar phenotype in response to RUNX1ETO, albeit through the engagement of distinct tumour suppressor pathways, lending credence to the hypothesis that immediate inhibition of cell cycle transit is achievable in the absence of hyper-replication and DNA damage.

Potential inducers of cell cycle arrest independently of serum restriction include the CDK inhibitors p21^{CIP1} and p16^{INK4A}. These effectors are activated in response to multiple senescence-inducing agents including oncogenes such as RUNX1 and RUNX1ETO [59, 225]. It is notable that CDK inhibitors also induce reversible quiescence following growth factor withdrawal suggesting that the defining feature of premature senescence is not the cell cycle inhibition *per se* but the persistence of growth promoting pathway activity that continues even after a stable proliferative arrest [283]. In this respect oncogenes not only induce CDK inhibitors and SLGA but also regulate growth promoting signals that facilitate cellular transformation when barriers to cell cycle progression such as p53 and p16^{INK4a} are removed. The biological significance of premature senescence is indicated by the observation of SLGA in premalignant lesions of multiple human tumours *in vivo* [132-134]. Indeed it has been proposed that senescence acts as a failsafe mechanism to restrict cancer development [131, 284, 285]. In this regard it is notable that RUNX1 and RE induce leukaemia *in vivo* but are associated with a rapid and profound SLGA *in vitro* [59, 225]. The findings that SLGA potential is masked in TR by fusion to TEL and attenuated by the leukaemogenic isoform of RE, RE9a, argues strongly in favour of SLGA as a cancer failsafe response rather than an artefact of *in vitro* culture conditions or ectopic expression of proteins at non-physiological levels. Together the data

suggest that oncogenic stress represents a potent inducer of SLGA that can restrict leukaemia development *in vivo* when cell cycle inhibition is maintained.

8.2 The Inflammatory Secretome and SLGA

Senescence represents a metabolically active, stable growth arrest associated with an inflammatory secretome or SASP enriched for pro-inflammatory cytokines and chemokines, growth factors, cell surface molecules and survival factors [205]. Since the SASP is wide ranging in multiple cell types and a feature of replicative and premature senescence different inducers of SLGA were compared for senescence secretion and revealed marked differences between RUNX1 isoforms and between RUNX1 and its fusion derivatives. Specifically, RUNX1P2 actively repressed secretion whereas RUNX1P1 induced a robust secretory phenotype that was exceeded only by RE. The minimal SASP response evoked by RUNX1P2 raises the question as to whether this SASP has any biological function. Indeed does a SASP-deficient SLGA simply represent normal physiological growth arrest? This seems unlikely since RUNX1 expression was associated with the typical cellular hypertrophy and SA-β-Gal activity characteristic of senescent cells. Moreover $p16^{INK4A}$ activation was induced by RUNX1 in the presence of continuous growth stimulation, providing a profile of "active" cell cycle arrest that is commonly used to distinguish between senescent and quiescent cells [283].

When considering whether SASP repression by RUNX1P2 has biological function it is relevant to consider the tumour-promoting activities of senescence-associated secretion. In general, a pro-inflammatory tissue environment is pro-tumourigenic [286]. The SASP encompasses a plethora of growth factors and other effectors that can modify the microenvironment to facilitate metastasis and promotes secretion or shedding of cytokine receptors to allow neighbouring pre-malignant and malignant cells to evade immune surveillance. Any repression of the secretory phenotype might therefore be regarded as tumour suppressive so it is notable that the p53 tumour suppressor, in addition to suppressing cancer by inhibiting cell growth also does so through restraint of the secretory phenotype, earning it the title of "super suppressor" [127]. This study has shown that RUNX1P2-induced SLGA is dependent on $p16^{INK4A}$ which fails to influence the SASP and indeed is not required for its development [251]. Others have reported

that RUNX1 functions as a cytoplasmic attenuator of NFκB signalling, which is a major regulator of the secretory phenotype [255]. From the evidence presented here it may be predicted that RUNX1 controls senescence secretion through downregulation of NFκB signalling which, in collaboration with $p16^{INK4A}$-induced growth arrest, sustains RUNX1-induced SLGA. The biological significance of this model for tumour development is evident in the myeloid system where RUNX1 is generally considered to act as a tumour suppressor and to repress myeloid tumour development through attenuation of NFκB signalling [255]. For lymphoid malignancies the consequences of RUNX1 expression are quite different. Evidence from this group supports an oncogenic function for RUNX1 in this lineage with Runx1P1 and c-Myc cooperating in the development of murine lymphoma [287] and over-expression and/or amplification of *RUNX1P1* reported in a subgroup of ALL. Moreover RUNX1P1 is the isoform expressed from the t(12;21) translocation [288] further emphasizing the significance of RUNX1P1 oncogenic functions in the lymphoid lineage. Results from this study demonstrate a robust secretory phenotype in human fibroblasts in response to ectopic RUNX1P1 consistent with oncogenic activity. The dramatic difference between RUNX1P1 and RUNX1P2 expression for senescence secretion in this cell background supports further investigation of NFκB signalling pathways. It will be of interest to determine how the activity of NFκB affects senescence secretion and whether it relates to the oncogenic and tumour suppressor functions of RUNX1 in the lymphoid and myeloid lineages respectively.

The most robust secretory phenotype observed in human fibroblasts was in response to ectopic expression of RE and was accompanied by a rapid and dramatic SLGA. RE9a, in contrast, failed to induce SLGA but was much less effective at restraining the SASP suggesting that these represent independent functions. In support of this hypothesis, p53 inhibition in cells where $p16^{INK4A}$ is only weakly expressed is sufficient to reverse the SLGA but not the SASP [127]. Moreover, relatively similar SASP profiles were noted in response to the NHR mutants despite their disparate effects on cell growth. Together these data suggest that senescence secretion is compatible with proliferative phenotypes, raising the possibility that a SASP has very different effects on proliferating and non-proliferating cell populations. The apparent paradox may be explained by the antagonistic functions of senescence secretion to both reinforce senescence

growth arrest and promote degenerative and hyperproliferative effects in neighbouring cells to promote tumour cell growth. The dual potential has parallels with the theory of antagonistic pleiotropy that was proposed to explain the evolutionary selection for gene functions that promote senescence [289]. Moreover, it may provide an explanation for why the acute repose to RE in primary human fibroblasts was an SLGA reinforced by a robust SASP, whereas in end stage AML and t(8;21) AML patient samples high levels of ROS and NFκB activity have been directly associated with cellular proliferation [255, 290]. In this respect it is noteworthy that RE and RE9a are co-expressed in t(8;21) leukaemias and RE and RE9a have been shown to cooperate in the development of myeloid leukaemia in mouse models [80]. It was shown that RE9a sustained a proliferative population in human fibroblasts which may prove more susceptible to the transforming effects of senescence secretion than a non-proliferating population. It is not possible to conclude whether RE9a opposed cell cycle arrest directly or indirectly through partial restraint of the SASP, but cellular proliferation is essential for the acquisition of secondary mutations and is likely to provide a critical component of the cooperation between RE and RE9a *in vivo*. A similar conclusion may be drawn from studies involving the TR fusion oncoprotein. While sustained proliferation was demonstrated in TR-expressing human fibroblasts, others have reported a similar phenotype in pre-leukaemic B cells [291]. In the study mentioned, proliferation was accompanied by high levels of ROS and DNA damage both of which have been associated with senescence secretion and suggested to contribute to the acquisition of secondary mutations required for tumour development [291]. Together these results suggest that overcoming the senescence failsafe represents a genuine mechanism for leukaemia development. However they also provide evidence that elements of the senescent phenotype persist and modulate the response *in vivo*. In this respect it is notable that knockdown of endogenous RUNX1 expression induced apoptosis in t(8;21) positive Kasumi 1 cells [292]. It would be of interest to determine whether RUNX1 opposition of senescence secretion acts to modulate the dramatic effects of RE on this pathway and thereby promote survival of the leukaemic cell.

8.3 How is RUNX1-Induced SLGA Overcome in Natural Tumourigenesis?

I have demonstrated that RUNX1 and RE induce SLGA *in vitro* despite their strong association with leukaemia *in vivo* and that the senescence failsafe is evaded by RE9a and TR. Moreover RE9a is associated with a more leukaemogenic phenotype in animal models suggesting that cooperating mutations that evade SLGA promote tumourigenesis.

8.3.1 RUNX1 Leukaemogenesis

Animal models have facilitated the identification of cooperating genes required for Runx1 tumourigenicity and include loss of p53 and overexpression of Myc. A previous report from this laboratory demonstrated escape from Runx1-induced senescence and cellular transformation in p53-null primary MEFs suggesting that loss of p53 releases cells from Runx1-induced proliferative arrest [230]. A similar conclusion was drawn for the Runx/Myc collaboration in murine T cell lymphoma where Myc overexpression rescued a Runx2 induced differentiation block to promote T cell proliferation [287]. Growth arrest represents a critical component of senescence. It is accompanied by an active metabolism that is only revealed as tumour-promoting when cell cycle arrest is overcome [283]. In this respect it is notable that p53 loss induces inflammatory secretion in human fibroblasts and c-Myc modulation of protein synthesis is both critical for Myc oncogenicity and associated with senescence metabolism pathways such as mTOR and PI3K/AKT [127, 293, 294]. From this evidence it may be predicted that RUNX1 collaborators not only overcome cell cycle arrest but are also important for tumour cell growth, making them ideally suited to overcome Runx1-induced senescence and to promote cellular transformation. Further evidence to support this is provided by the cooperation between RUNX1 and loss of p53 or overexpression of MYC in human leukaemias. Gene expression profiling of precursor B-cell ALL revealed overexpression of *RUNX1* and *cMyc* while in rare cases of *RUNX1* amplification in therapy related myelodysplasia (AML or myelodysplastic syndrome (MDS)) inactivating mutations of p53 were consistently described [295, 296]. The role of RUNX1 in these cases is not well defined but animal models suggest that cell survival may be the key. Depletion of Runx1-induced Fas ligand in a p53-null mouse model of thymic lymphoma and Runx2-dependent inhibition of Myc-induced apoptosis was described in Runx2/Myc

thymic lymphomas [287, 297]. Moreover addiction to Runx1 was also observed in a floxed *Runx1* model of primary EμMyc lymphomas with *Runx1*-expressing cell lines derived from the lymphomas displaying an increased resistance to DNA damaging agents compared to their *Runx1*-excised counterparts [298]. In this respect it is of note that senescence secretion includes a number of survival factors and was induced by the P1 isoform of RUNX1 which was also expressed in precursor B-ALL (Monica Stewart pers comm) and identified by retroviral insertion in a CD2Myc model of thymic lymphoma. Moreover tumour suppressors implicated in premature senescence such as PML and FOXO have been shown to play important survival roles in leukaemic stem cells [299, 300] and experiments to reintroduce a survival signal into *Runx1*-deleted leukaemic cells derived from a mouse model of MLL-ENL partially rescued the Runx1 growth phenotype all suggesting that features of the senescence failsafe can be exploited to promote survival of tumour cells when proliferative arrest is overcome [301].

8.3.2 TEL-RUNX1 Leukaemogenesis

The t(12;21) translocation is present in approximately 25% of childhood B cell precursor ALL but fails to induce leukaemia in mouse models suggesting that secondary events are required [103]. It was shown that TEL masks RUNX1 activity in the TR fusion protein to evade SLGA *in vitro* thereby maintaining a proliferative phenotype that may be important for the acquisition of secondary mutations. Although p53 mutation is observed at relapse and is associated with poor outcome, loss of p53 function has not been observed in primary t(12;21) leukaemias suggesting that it is unlikely to be a major TR cooperating event [302]. An analysis of genetic abnormalities in newly diagnosed ALL revealed c-Myc translocations in 5 out of 1346 cases. All were in cases of childhood B-cell ALL but it was unclear whether these overlapped with the t(12;21) translocation [303]. Cooperation between Myc and TR was supported by another study, however, that reported Myc overexpression in patient-derived cells addicted to the t(12;21) fusion oncoprotein and apoptotic cell death when Myc activity is inhibited in t(12;21) REH cells [304]. It would therefore be of interest to determine whether c-Myc transcription was specifically upregulated in response to TR in human fibroblasts and required to maintain cellular proliferation. One of the most frequent genetic events in childhood ALL is loss of heterozygocity (LOH) in chromosome arm 9p including the *CDKN2A* locus encoding $p16^{INK4A}$ and

p14^{ARF}. For childhood precursor B-ALL the occurrence of 9p LOH is approximately 21% whereas for the t(12;21) subgroup it is around 15% [305]. The importance of this gene locus for tumour suppression is evidenced by the increased incidence of t(12;21) leukaemias in retroviral transduction transplantation models where *CDK2NA* is deleted [103]. p14^{ARF} was not detected in Hs68 fibroblasts but a requirement for 16^{INK4A} was demonstrated in RUNX1-induced SLGA with loss of p16^{INK4A} associated with accelerated growth in response to RUNX1P1 [59], RUNX1P2 or the TR K99R mutant. Together these data support the hypothesis that loss of the second allele or haploinsufficiency of *CDKN2A* is an important collaborating event in B-ALL. TR expression sustained proliferation of Hs68 fibroblasts and, in contrast to RUNX1 and TR K99R had no apparent effect on p16^{INK4A} expression levels. It seems unlikely that *CDKN2A* haploinsufficiency was responsible for TR-induced evasion of senescence in such a short time frame experiment. Instead, the lack of p16^{INK4A} expression may either reflect a dominant negative suppressor activity of TR towards a RUNX1 gene target [306] or the cytoplasmic distribution of TR observed in Hs68 fibroblasts. In this respect it is noteworthy that REH end stage t(12;21) leukaemic cells maintain high levels of endogenous RUNX1 expression but are genetically null for *CDKN2A* suggesting that loss of p16^{INK4A} may be more relevant to later progression stages where increased RUNX1 copy number is selected for and the requirement to evade RUNX1-induced senescence more significant. Moreover silencing of TR in t(12;21)-positive B-ALL cell lines abrogates PI3K/AKT/mTOR signalling to reduce cellular proliferation and survival suggesting that TR exploits this metabolic senescence-inducing pathway to expose tumour promoting functions when obstacles favouring proliferative arrest are removed [307]. From the evidence presented here it may be predicted that suppression of RUNX1-induced growth arrest by the TEL fusion moiety is critical for leukaemia initiation but dispensable for end-stage leukaemias that have become refractory to this failsafe mechanism.

8.3.3 RUNX1-ETO Leukaemogenesis

RE is atypical in that it is associated with a high proportion of M2 AML but, unlike TR and RE9a, induces an intense SLGA in human fibroblasts. The pathways involved are distinct from RUNX1 and include ROS-p38MAPK signalling and robust senescence secretion. The significance of RE-induced senescence is realised by

the inability of RE to induce leukaemia in mouse models [80] and suggests a requirement for secondary mutations to overcome the senescence failsafe. This hypothesis is supported by the leukaemogenicity of the RE9a isoform [80] that evades senescence *in vitro*, and has provided the impetus to identify the secondary cooperating events in t(8;21) leukaemias. From such studies it has been shown that while p53 mutation is not a general feature of t(8;21) leukaemias, trisomy 8 with amplification of *c-Myc* at 8q24 is represented in approximately 15-20% and 10-15% of MDS and AML respectively [308, 309]. Moreover the increase in *c-MYC* copy number appears to be important for disease progression suggesting that Myc may cooperate with RE *in vivo*. MYC has also been shown to overcome cell cycle inhibition by CBFβ-SMMHC which, like RE, is associated with a CBF leukaemia and induces SLGA *in vitro* suggesting that this collaboration may represent a more widespread feature of CBF transformation [225, 310]. It was shown that RE-induced SGLA was dependent on $p16^{INK4A}$ in primary human fibroblasts. Moreover, $p16^{INK4A}$ was not induced by RE9a, which also evaded SLGA, suggesting a critical role in the senescence failsafe in response to RE. Deletions or intragenic mutations of $p16^{INK4A}$ are infrequently observed in AML [308]. However, t(8;21) patients are reported to show high levels of hypermethylation of the *p15* and adjacent *p16* gene that at least for *p15* show excellent concordance with disease progression [311]. Hypermethylation may suppress expression of these CDK inhibitors as well as the overlapping *ARF* gene that governs the activity of MDM2 and thence the activity of p53. In this respect it is notable that t(8;21) patient samples revealed markedly lower levels of $p14^{ARF}$ mRNA when compared with AMLs lacking this translocation [312].

If secondary mutations play a role in escape from the senescence failsafe when and how do they occur *in vivo*? Retroviral transduction of RE into human $CD34^{+}$ stem cells was associated with an early and robust growth arrest that persisted for 4-6 weeks before the emergence of a RE-expressing proliferative population exhibiting a down regulation of DNA repair enzymes [82]. It is notable that p53 response pathways were also activated in this population. A similar pattern was observed in t(8;21) compared to other AML patient samples and hypothesised to contribute to their favourable response to chemotherapy in the clinic [313]. Since germline p53 mutations are rare in AML and p53 restrains the activities of

ROS and the SASP [127, 314], the data suggests that other secondary mutations are required to overcome the initial RE-induced growth arrest. We hypothesise that additional events, such as loss of p53, determine how quickly that proliferating population progresses to full-blown leukaemia. It is therefore notable that RE9a and RE cooperate to induce a more aggressive leukaemic phenotype *in vivo* [80] and it is possible that the toxic combination of cellular proliferation with ROS and senescence secretion is responsible. It should also be noted that RE9a was capable of inducing a vestigial SASP that was qualitatively distinct from RE and for this reason cannot be excluded as a contributing factor in the RE and RE9a cooperation.

8.4 Conclusions

Oncogene-induced-senescence is recognised as a physiological mechanism that limits the progression of premalignant lesions and is associated with a number of leukaemic fusion oncoproteins including RE, BCR-ABL and CBFB-MYH11 [59, 225]. For initiated cells to progress to a tumour the profound growth arrest that accompanies OIS must be overcome and secondary mutations acquired. However it now seems likely that some survival signals characterising the senescence phenotype may actually persist in cancer development and promote survival within a different cellular context. In this respect it is notable that two tumour suppressors implicated in premature senescence, PML and FOXO, were also reported to have important survival roles in leukaemic stem cells [299, 300]. Furthermore, RUNX1 has been demonstrated as an essential survival factor in a murine model of MLL-ENL and yet is an inducer of premature senescence in primary fibroblasts [230, 301]. The survival of preleukaemic proliferating cells is now considered crucial for leukaemogenesis. The TR translocation occurs in utero in early B cell progenitors establishing a pre-leukaemic clone that can persist for up to several years [52, 276, 277]. Similar observations have been made for RE and MLL-AF4 [315] suggesting that this may represent a more general phenomenon of leukaemogenesis.

This study shows that the initial response to nuclear expression of TR (K99R) or RE in human primary fibroblasts is a profound SLGA. It is significant that the expansion of human CD34+ cells in response to RE infection was preceded by an

early and persistent growth restriction suggesting that acquisition of a proliferative phenotype is essential for emergence of the pre-leukaemic clone [82]. Both ROS and SASP were observed in response to expression of RE in primary human fibroblasts and both have been directly or indirectly implicated in AML. Elevated ROS promotes proliferation of AML cell lines and primary AML blasts and was observed in over 60% of AML patient samples whereas PKD1 was identified as a poor prognosis factor in AML and has been linked to overexpression of NFkB, a master regulator of the SASP [186, 290, 316]. ROS was also a feature of TR-induced senescence when TR (K99R) was redistributed to the nucleus. Although ROS accumulation was not observed with wild-type TR, high ROS and a DNA damage response have been reported in TR expressing pre-leukaemic pro-B cell lines and proposed to underlie the mechanism for acquisition of secondary mutations [291]. In this regard it is interesting that the proliferative capacity of t(8;21) positive leukaemias was opposed by ROS scavengers [290] and NFκB inhibitors [255], supporting a critical requirement for specific features of the senescent phenotype to preserve the proliferation of pre-leukaemic cells and favour leukaemia development.

Chronic inflammatory stimulation may also provide an explanation for the more aggressive leukaemic phenotype observed when RE and RE9a were combined in a retroviral transduction transplantation mouse model [80]It is possible that RE provides additional paracrine stimuli in the form of ROS and chronic inflammatory factors to increase the likelihood of secondary mutations in the proliferating RE9a compartment thereby facilitating leukaemia progression. In this regard it is interesting that RE9a shares over 30% of the gene signature expressed by RE particularly favouring genes involved in cell survival and proliferation [317]. A similar mechanism may be exploited by TR since it also maintains rather than promotes the proliferation of in Hs68 fibroblasts. In this case the factors responsible for driving secondary mutation are less clear but it is interesting that TR expressing pro-B-cells are characterised by a positive signature for cellular stress and immune function genes with potential for inducing the opportunity for secondary mutations [318]. A requirement for secondary mutations was also observed in this study when TR K99R and RE were introduced into $p16^{INK4A}$ null cell backgrounds. Loss of $p16^{INK4A}$ revealed novel

oncogenic functions in both fusion proteins that promoted the growth of REH and Leiden fibroblasts respectively.

Persisting RUNX1 expression is a feature of many fusion leukaemias including TR and RE. It is rarely mutated and cases of compensation by other RUNX family members have been reported where RUNX1 expression was experimentally reduced in vitro [301]. An essential proliferative role is evidenced by the requirement for proper RUNX1 function for the efficient growth of RE, MLL-AF9 and MLL-AF4 leukaemic cells [301, 319]. Moreover t(12;21) leukaemias invariably express RUNX1 without mutation and recurrent copy number changes involving the 21q22 amplicon encoding RUNX1 are commonly observed [295, 320, 321]. Our results may initially seem to contrast with these observations since both isoforms of RUNX1 were associated with a rapid and robust SLGA in primary human fibroblasts. However as these cells were non-leukaemic and engineered to induce ectopic RUNX1 proteins it is conceivable that cellular background and expression levels are critical. In this regard it is notable that high levels of RUNX1 arrested growth in human CD34+ cells but maintained the proliferation of MLL-AF4 leukaemic cells [82, 319]. In contrast, more modest levels of RUNX1 were necessary to support the growth of myeloid leukaemic lines expressing RE or MLL-AF9 [301]. Similarly, an intolerance of high ectopic RUNX1 protein expression was observed in murine thymic lymphoma cell lines but lower levels of the endogenous protein equip murine B-cell lymphoma cell lines with a greater proliferative capacity than their floxed Runx1 counterparts [298].

The decision to promote or restrict growth by RUNX1 may operate at the transcriptional level. Introduction of a series of naturally occurring RUNX1 mutants into RE and MLL-AFN leukaemic cell lines revealed that the RUNT homology domain was critical for both accelerated and restricted growth suggesting that specific transcriptional programmes are directed through RUNX1 recruitment of particular co-factors associated with growth suppression or growth activation [301]. In addition to an essential role for growth, RUNX1 may also be required for the survival of fusion leukaemias. Runx1 has been associated with upregulation of the Bcl-2 survival factor in MLL fusion leukaemia and addiction to RUNX1 was demonstrated in t(8;21) and inv(16) myeloid leukaemic cell lines [292]. In this respect it is noteworthy that addiction to Runx1 was also a feature of a floxed Runx1 model of primary EμMyc lymphomas

with in vitro lines displaying an increased resistance to DNA damaging agents compared to their excised counterparts [298]. Enhanced survival is an essential feature of the leukaemic initiating cell. RUNX1 expression conveys a survival phenotype and crucially does so in the absence of ROS or SASP thereby reducing the opportunity for acquisition of secondary mutations. It is possible that the stability of RUNX1 compared to RE mediated growth arrest in human CD34+ cells is a consequence of this and a crucial component of RUNX1 addiction in fusion leukaemias [82].

From the evidence presented it may be predicted that senescence represents an important failsafe that is relevant to leukaemia development *in vivo*. Signalling pathways invoked in leukaemogenesis commonly reverse proliferative growth arrest or enhance metabolic growth-promoting pathways associated with premature senescence. The pattern enforces the current dogma that senescence pathways have antagonistic functions in survival and tumour progression, both of which appear to be exploited in leukaemia. RUNX1 and its fusion oncoproteins do not disappoint in this respect with roles in growth and survival that present as SLGA or uncontrolled proliferation depending on cooperating mutations and the microenvironment. Treatment failure in acute leukaemia is believed to be caused by the persistence of leukaemia-initiating cells after conventional therapy and is a major prognostic factor for disease relapse. Genes that are essential for their growth and survival could present promising targets to selectively eradicate cancer cells while preserving normal stem cells. The finding that RUNX1 fusion oncoproteins promote ROS and SASP signalling is encouraging for ongoing efforts to specifically target SASP signalling in leukaemic cells. Moreover, the requirement for endogenous RUNX1 for the viability and growth of fusion-containing leukaemic cells supports the possibility of combination therapy between conventional therapeutics and RUNX1 inhibition for greater efficacy.

8.5 Future work

RE and RE9a induce more rapid leukaemogenesis than RE9a alone [80] suggesting that RE9a functions to inhibit RE-dependent anti-cancer mechanisms such as cellular senescence. To address this it would be informative to co-express RE and RE9a in Hs68 cells which give a well-defined senescence profile, and determine whether RE-induced senescence is opposed by RE9a. Such studies could also be extended to include co-expression of TR and RUNX1 which also show opposing effects on cellular senescence and are co-expressed in acute leukaemia.

Fibroblasts do not represent a physiologically relevant target cell for RUNX1 or its fusion oncoproteins with respect to leukaemia. To determine whether the results achieved in this study are reproduced in more biologically relevant cell backgrounds it will be of interest to express RUNX1 and its fusion oncoproteins in CD34+ haematopoietic stem cells and examine them for signs of premature senescence. For reasons described above these studies could be extended to include combinations of RE and RE9a or TR and RUNX1 to more closely mimic the pathologies they are associated with human leukaemia.

The SASP has been identified as having both pro-senescence and pro-oncogenic properties depending on the cellular context [205]. To address the particular functions of the SASP induced in response to RE, conditioned media could be collected and applied to parallel cultures expressing the RE9a construct or the vector only control. If the conditioned media was senescence promoting in these cell backgrounds it would be of interest to examine the effects of NFκB inhibitors on RE-induced senescence as this treatment would be expected to reverse the SASP. Alternatively, if the conditioned media accelerated the growth of RE9a expressing fibroblasts this might provide an explanation for the observed synergy between RE and RE9a in acute leukaemias [80] and a rationale for extending these studies into a more physiologically relevant target cell.

Pro-senescence therapies have been suggested as an approach to oppose cancer progression [322]. However as expression of RE and TR K99R in $p16^{INK4A}$-null Leiden and REH cells resulted in accelerated proliferation, it is reasonable to suggest that established leukaemia cells will have acquired secondary mutations that render them refractory to pro-senescence therapies that target the cell cycle. An alternative approach may be to target the chronic inflammatory SASP that we have described in response to RE. NFκB activity and ROS are important for SASP development [186, 248] and have previously been identified as poor prognostic factors in AML [255, 290] supporting the importance of the SASP in RE mediated leukaemogenicity. To understand the SASP more fully and to identify potential drugable targets it will be important to define the phenotype in a more physiologically relevant target cell line such as $CD34^+$ stem cells. The functional consequences of particular components could then be tested on RE9a expressing cells to determine their oncogenic potential and significance for leukaemia development.

References

1. Kagoshima, H., et al., *The Runt domain identifies a new family of heteromeric transcriptional regulators.* Trends Genet, 1993. **9**(10): p. 338-41.
2. Ogawa, E., et al., *PEBP2/PEA2 represents a family of transcription factors homologous to the products of the Drosophila runt gene and the human AML1 gene.* Proc Natl Acad Sci U S A, 1993. **90**(14): p. 6859-63.
3. Ghozi, M.C., et al., *Expression of the human acute myeloid leukemia gene AML1 is regulated by two promoter regions.* Proc Natl Acad Sci U S A, 1996. **93**(5): p. 1935-40.
4. Meyers, S., J.R. Downing, and S.W. Hiebert, *Identification of AML-1 and the (8;21) translocation protein (AML-1/ETO) as sequence-specific DNA-binding proteins: the runt homology domain is required for DNA binding and protein-protein interactions.* Mol Cell Biol, 1993. **13**(10): p. 6336-45.
5. Friedman, A.D., *Cell cycle and developmental control of hematopoiesis by Runx1.* J Cell Physiol, 2009. **219**(3): p. 520-4.
6. Growney, J.D., et al., *Loss of Runx1 perturbs adult hematopoiesis and is associated with a myeloproliferative phenotype.* Blood, 2005. **106**(2): p. 494-504.
7. Cohen, M.M., Jr., *RUNX genes, neoplasia, and cleidocranial dysplasia.* Am J Med Genet, 2001. **104**(3): p. 185-8.
8. Blyth, K., E.R. Cameron, and J.C. Neil, *The RUNX genes: gain or loss of function in cancer.* Nat Rev Cancer, 2005. **5**(5): p. 376-87.
9. Lund, A.H. and M. van Lohuizen, *RUNX: a trilogy of cancer genes.* Cancer Cell, 2002. **1**(3): p. 213-5.
10. Miyoshi, H., et al., *Alternative splicing and genomic structure of the AML1 gene involved in acute myeloid leukemia.* Nucleic Acids Res, 1995. **23**(14): p. 2762-9.
11. Tanaka, T., et al., *An acute myeloid leukemia gene, AML1, regulates hemopoietic myeloid cell differentiation and transcriptional activation antagonistically by two alternative spliced forms.* EMBO J, 1995. **14**(2): p. 341-50.
12. Bowers, S.R., et al., *Runx1 binds as a dimeric complex to overlapping Runx1 sites within a palindromic element in the human GM-CSF enhancer.* Nucleic Acids Res, 2010. **38**(18): p. 6124-34.
13. Golemis, E.A., N.A. Speck, and N. Hopkins, *Alignment of U3 region sequences of mammalian type C viruses: identification of highly conserved motifs and implications for enhancer design.* J Virol, 1990. **64**(2): p. 534-42.
14. Melnikova, I.N., et al., *Sequence specificity of the core-binding factor.* J Virol, 1993. **67**(4): p. 2408-11.
15. Speck, N.A. and S. Terryl, *A new transcription factor family associated with human leukemias.* Crit Rev Eukaryot Gene Expr, 1995. **5**(3-4): p. 337-64.
16. Otto, F., M. Lubbert, and M. Stock, *Upstream and downstream targets of RUNX proteins.* J Cell Biochem, 2003. **89**(1): p. 9-18.
17. Speck, N.A. and D.G. Gilliland, *Core-binding factors in haematopoiesis and leukaemia.* Nat Rev Cancer, 2002. **2**(7): p. 502-13.
18. Frank, R.C., et al., *The t(8;21) fusion protein, AML1/ETO, transforms NIH3T3 cells and activates AP-1.* Oncogene, 1999. **18**(9): p. 1701-10.

19. Hernandez-Munain, C. and M.S. Krangel, *Regulation of the T-cell receptor delta enhancer by functional cooperation between c-Myb and core-binding factors.* Mol Cell Biol, 1994. **14**(1): p. 473-83.
20. Petrovick, M.S., et al., *Multiple functional domains of AML1: PU.1 and C/EBPalpha synergize with different regions of AML1.* Mol Cell Biol, 1998. **18**(7): p. 3915-25.
21. Zhang, D.E., et al., *CCAAT enhancer-binding protein (C/EBP) and AML1 (CBF alpha2) synergistically activate the macrophage colony-stimulating factor receptor promoter.* Mol Cell Biol, 1996. **16**(3): p. 1231-40.
22. Fowler, M., et al., *RUNX1 (AML-1) and RUNX2 (AML-3) cooperate with prostate-derived Ets factor to activate transcription from the PSA upstream regulatory region.* J Cell Biochem, 2006. **97**(1): p. 1-17.
23. Elagib, K.E., et al., *RUNX1 and GATA-1 coexpression and cooperation in megakaryocytic differentiation.* Blood, 2003. **101**(11): p. 4333-41.
24. Howcroft, T.K., et al., *A T lymphocyte-specific transcription complex containing RUNX1 activates MHC class I expression.* J Immunol, 2005. **174**(4): p. 2106-15.
25. Kitabayashi, I., et al., *Interaction and functional cooperation of the leukemia-associated factors AML1 and p300 in myeloid cell differentiation.* EMBO J, 1998. **17**(11): p. 2994-3004.
26. Zhao, X., et al., *Methylation of RUNX1 by PRMT1 abrogates SIN3A binding and potentiates its transcriptional activity.* Genes Dev, 2008. **22**(5): p. 640-53.
27. Lutterbach, B., et al., *A mechanism of repression by acute myeloid leukemia-1, the target of multiple chromosomal translocations in acute leukemia.* J Biol Chem, 2000. **275**(1): p. 651-6.
28. Reed-Inderbitzin, E., et al., *RUNX1 associates with histone deacetylases and SUV39H1 to repress transcription.* Oncogene, 2006. **25**(42): p. 5777-86.
29. Durst, K.L. and S.W. Hiebert, *Role of RUNX family members in transcriptional repression and gene silencing.* Oncogene, 2004. **23**(24): p. 4220-4.
30. Aronson, B.D., et al., *Groucho-dependent and -independent repression activities of Runt domain proteins.* Mol Cell Biol, 1997. **17**(9): p. 5581-7.
31. Kawazu, M., et al., *Functional domains of Runx1 are differentially required for CD4 repression, TCRbeta expression, and CD4/8 double-negative to CD4/8 double-positive transition in thymocyte development.* J Immunol, 2005. **174**(6): p. 3526-33.
32. Arce, L., K.T. Pate, and M.L. Waterman, *Groucho binds two conserved regions of LEF-1 for HDAC-dependent repression.* BMC Cancer, 2009. **9**: p. 159.
33. Wang, Q., et al., *Disruption of the Cbfa2 gene causes necrosis and hemorrhaging in the central nervous system and blocks definitive hematopoiesis.* Proc Natl Acad Sci U S A, 1996. **93**(8): p. 3444-9.
34. Okuda, T., et al., *AML1, the target of multiple chromosomal translocations in human leukemia, is essential for normal fetal liver hematopoiesis.* Cell, 1996. **84**(2): p. 321-30.
35. Niki, M., et al., *Hematopoiesis in the fetal liver is impaired by targeted mutagenesis of a gene encoding a non-DNA binding subunit of the transcription factor, polyomavirus enhancer binding protein 2/core binding factor.* Proc Natl Acad Sci U S A, 1997. **94**(11): p. 5697-702.

36. Sasaki, K., et al., *Absence of fetal liver hematopoiesis in mice deficient in transcriptional coactivator core binding factor beta.* Proc Natl Acad Sci U S A, 1996. **93**(22): p. 12359-63.
37. Wang, Q., et al., *The CBFbeta subunit is essential for CBFalpha2 (AML1) function in vivo.* Cell, 1996. **87**(4): p. 697-708.
38. Bee, T., et al., *Nonredundant roles for Runx1 alternative promoters reflect their activity at discrete stages of developmental hematopoiesis.* Blood, 2010. **115**(15): p. 3042-50.
39. Ichikawa, M., et al., *AML-1 is required for megakaryocytic maturation and lymphocytic differentiation, but not for maintenance of hematopoietic stem cells in adult hematopoiesis.* Nat Med, 2004. **10**(3): p. 299-304.
40. Lorsbach, R.B., et al., *Role of RUNX1 in adult hematopoiesis: analysis of RUNX1-IRES-GFP knock-in mice reveals differential lineage expression.* Blood, 2004. **103**(7): p. 2522-9.
41. Cameron, E.R. and J.C. Neil, *The Runx genes: lineage-specific oncogenes and tumor suppressors.* Oncogene, 2004. **23**(24): p. 4308-14.
42. Chiorazzi, N., K.R. Rai, and M. Ferrarini, *Chronic lymphocytic leukemia.* N Engl J Med, 2005. **352**(8): p. 804-15.
43. Inaba, H., M. Greaves, and C.G. Mullighan, *Acute lymphoblastic leukaemia.* Lancet, 2013. **381**(9881): p. 1943-55.
44. Hehlmann, R., et al., *Chronic myeloid leukaemia.* Lancet, 2007. **370**(9584): p. 342-50.
45. Dohner, H., D.J. Weisdorf, and C.D. Bloomfield, *Acute Myeloid Leukemia.* N Engl J Med, 2015. **373**(12): p. 1136-52.
46. Look, A.T., *Oncogenic transcription factors in the human acute leukemias.* Science, 1997. **278**(5340): p. 1059-64.
47. Shimizu, K., et al., *Molecular assignment of a translocation breakpoint in acute myeloid leukemia with t(8;21).* Genes Chromosomes Cancer, 1991. **3**(3): p. 163-7.
48. Miyoshi, H., et al., *t(8;21) breakpoints on chromosome 21 in acute myeloid leukemia are clustered within a limited region of a single gene, AML1.* Proc Natl Acad Sci U S A, 1991. **88**(23): p. 10431-4.
49. Friedman, A.D., *Leukemogenesis by CBF oncoproteins.* Leukemia, 1999. **13**(12): p. 1932-42.
50. Kundu, M. and P.P. Liu, *Function of the inv(16) fusion gene CBFB-MYH11.* Curr Opin Hematol, 2001. **8**(4): p. 201-5.
51. Le Beau, M.M., et al., *Clinical and cytogenetic correlations in 63 patients with therapy-related myelodysplastic syndromes and acute nonlymphocytic leukemia: further evidence for characteristic abnormalities of chromosomes no. 5 and 7.* J Clin Oncol, 1986. **4**(3): p. 325-45.
52. Ford, A.M., et al., *Fetal origins of the TEL-AML1 fusion gene in identical twins with leukemia.* Proc Natl Acad Sci U S A, 1998. **95**(8): p. 4584-8.
53. Greaves, M.F. and J. Wiemels, *Origins of chromosome translocations in childhood leukaemia.* Nat Rev Cancer, 2003. **3**(9): p. 639-49.
54. Fong, C.T. and G.M. Brodeur, *Down's syndrome and leukemia: epidemiology, genetics, cytogenetics and mechanisms of leukemogenesis.* Cancer Genet Cytogenet, 1987. **28**(1): p. 55-76.
55. Bishop, J.F., *The treatment of adult acute myeloid leukemia.* Semin Oncol, 1997. **24**(1): p. 57-69.
56. Cooper, S.L. and P.A. Brown, *Treatment of pediatric acute lymphoblastic leukemia.* Pediatr Clin North Am, 2015. **62**(1): p. 61-73.

57. Stewart, M., et al., *Proviral insertions induce the expression of bone-specific isoforms of PEBP2alphaA (CBFA1): evidence for a new myc collaborating oncogene.* Proc Natl Acad Sci U S A, 1997. **94**(16): p. 8646-51.
58. Wotton, S., et al., *Proviral insertion indicates a dominant oncogenic role for Runx1/AML-1 in T-cell lymphoma.* Cancer Res, 2002. **62**(24): p. 7181-5.
59. Wolyniec, K., et al., *RUNX1 and its fusion oncoprotein derivative, RUNX1-ETO, induce senescence-like growth arrest independently of replicative stress.* Oncogene, 2009. **28**(27): p. 2502-12.
60. Silva, F.P., et al., *Identification of RUNX1/AML1 as a classical tumor suppressor gene.* Oncogene, 2003. **22**(4): p. 538-47.
61. Fijneman, R.J., et al., *Runx1 is a tumor suppressor gene in the mouse gastrointestinal tract.* Cancer Sci, 2012. **103**(3): p. 593-9.
62. Perez-Vera, P., et al., *Multiple copies of RUNX1: description of 14 new patients, follow-up, and a review of the literature.* Cancer Genet Cytogenet, 2008. **180**(2): p. 129-34.
63. Harrison, C.J., et al., *An international study of intrachromosomal amplification of chromosome 21 (iAMP21): cytogenetic characterization and outcome.* Leukemia, 2014. **28**(5): p. 1015-21.
64. Yanagida, M., et al., *Increased dosage of Runx1/AML1 acts as a positive modulator of myeloid leukemogenesis in BXH2 mice.* Oncogene, 2005. **24**(28): p. 4477-85.
65. Song, W.J., et al., *Haploinsufficiency of CBFA2 causes familial thrombocytopenia with propensity to develop acute myelogenous leukaemia.* Nat Genet, 1999. **23**(2): p. 166-75.
66. Michaud, J., et al., *In vitro analyses of known and novel RUNX1/AML1 mutations in dominant familial platelet disorder with predisposition to acute myelogenous leukemia: implications for mechanisms of pathogenesis.* Blood, 2002. **99**(4): p. 1364-72.
67. Grossmann, V., et al., *Prognostic relevance of RUNX1 mutations in T-cell acute lymphoblastic leukemia.* Haematologica, 2011. **96**(12): p. 1874-7.
68. Zhang, J., et al., *The genetic basis of early T-cell precursor acute lymphoblastic leukaemia.* Nature, 2012. **481**(7380): p. 157-63.
69. Della Gatta, G., et al., *Reverse engineering of TLX oncogenic transcriptional networks identifies RUNX1 as tumor suppressor in T-ALL.* Nat Med, 2012. **18**(3): p. 436-40.
70. Wildonger, J. and R.S. Mann, *The t(8;21) translocation converts AML1 into a constitutive transcriptional repressor.* Development, 2005. **132**(10): p. 2263-72.
71. Yergeau, D.A., et al., *Embryonic lethality and impairment of haematopoiesis in mice heterozygous for an AML1-ETO fusion gene.* Nat Genet, 1997. **15**(3): p. 303-6.
72. Okuda, T., et al., *Expression of a knocked-in AML1-ETO leukemia gene inhibits the establishment of normal definitive hematopoiesis and directly generates dysplastic hematopoietic progenitors.* Blood, 1998. **91**(9): p. 3134-43.
73. Meyers, S., N. Lenny, and S.W. Hiebert, *The t(8;21) fusion protein interferes with AML-1B-dependent transcriptional activation.* Mol Cell Biol, 1995. **15**(4): p. 1974-82.
74. Frank, R., et al., *The AML1/ETO fusion protein blocks transactivation of the GM-CSF promoter by AML1B.* Oncogene, 1995. **11**(12): p. 2667-74.

75. Wotton, S., et al., *Gene array analysis reveals a common Runx transcriptional programme controlling cell adhesion and survival.* Oncogene, 2008. **27**(44): p. 5856-66.
76. Rhoades, K.L., et al., *Analysis of the role of AML1-ETO in leukemogenesis, using an inducible transgenic mouse model.* Blood, 2000. **96**(6): p. 2108-15.
77. Yuan, Y., et al., *AML1-ETO expression is directly involved in the development of acute myeloid leukemia in the presence of additional mutations.* Proc Natl Acad Sci U S A, 2001. **98**(18): p. 10398-403.
78. Higuchi, M., et al., *Expression of a conditional AML1-ETO oncogene bypasses embryonic lethality and establishes a murine model of human t(8;21) acute myeloid leukemia.* Cancer Cell, 2002. **1**(1): p. 63-74.
79. Buchholz, F., et al., *Inducible chromosomal translocation of AML1 and ETO genes through Cre/loxP-mediated recombination in the mouse.* EMBO Rep, 2000. **1**(2): p. 133-9.
80. Yan, M., et al., *A previously unidentified alternatively spliced isoform of t(8;21) transcript promotes leukemogenesis.* Nat Med, 2006. **12**(8): p. 945-9.
81. Fenske, T.S., et al., *Stem cell expression of the AML1/ETO fusion protein induces a myeloproliferative disorder in mice.* Proc Natl Acad Sci U S A, 2004. **101**(42): p. 15184-9.
82. Mulloy, J.C., et al., *The AML1-ETO fusion protein promotes the expansion of human hematopoietic stem cells.* Blood, 2002. **99**(1): p. 15-23.
83. Chou, F.S., et al., *N-Ras(G12D) induces features of stepwise transformation in preleukemic human umbilical cord blood cultures expressing the AML1-ETO fusion gene.* Blood, 2011. **117**(7): p. 2237-40.
84. Erickson, P.F., et al., *The ETO portion of acute myeloid leukemia t(8;21) fusion transcript encodes a highly evolutionarily conserved, putative transcription factor.* Cancer Res, 1994. **54**(7): p. 1782-6.
85. Kozu, T., et al., *Significance of MTG8 in leukemogenesis.* Leukemia, 1997. **11 Suppl 3**: p. 297-8.
86. Lutterbach, B., et al., *The MYND motif is required for repression of basal transcription from the multidrug resistance 1 promoter by the t(8;21) fusion protein.* Mol Cell Biol, 1998. **18**(6): p. 3604-11.
87. Gelmetti, V., et al., *Aberrant recruitment of the nuclear receptor corepressor-histone deacetylase complex by the acute myeloid leukemia fusion partner ETO.* Mol Cell Biol, 1998. **18**(12): p. 7185-91.
88. Lutterbach, B., et al., *ETO, a target of t(8;21) in acute leukemia, interacts with the N-CoR and mSin3 corepressors.* Mol Cell Biol, 1998. **18**(12): p. 7176-84.
89. Zhang, J., et al., *Oligomerization of ETO is obligatory for corepressor interaction.* Mol Cell Biol, 2001. **21**(1): p. 156-63.
90. Hildebrand, D., et al., *Multiple regions of ETO cooperate in transcriptional repression.* J Biol Chem, 2001. **276**(13): p. 9889-95.
91. Amann, J.M., et al., *ETO, a target of t(8;21) in acute leukemia, makes distinct contacts with multiple histone deacetylases and binds mSin3A through its oligomerization domain.* Mol Cell Biol, 2001. **21**(19): p. 6470-83.
92. Bartel, Y., M. Grez, and C. Wichmann, *Interference with RUNX1/ETO leukemogenic function by cell-penetrating peptides targeting the NHR2 oligomerization domain.* Biomed Res Int, 2013. **2013**: p. 297692.
93. Corpora, T., et al., *Structure of the AML1-ETO NHR3-PKA(RIIalpha) complex and its contribution to AML1-ETO activity.* J Mol Biol, 2010. **402**(3): p. 560-77.

94. Kozu, T., et al., *MYND-less splice variants of AML1-MTG8 (RUNX1-CBFA2T1) are expressed in leukemia with t(8;21).* Genes Chromosomes Cancer, 2005. **43**(1): p. 45-53.
95. Ahn, E.Y., et al., *Disruption of the NHR4 domain structure in AML1-ETO abrogates SON binding and promotes leukemogenesis.* Proc Natl Acad Sci U S A, 2008. **105**(44): p. 17103-8.
96. Ahn, E.Y., et al., *SON controls cell-cycle progression by coordinated regulation of RNA splicing.* Mol Cell, 2011. **42**(2): p. 185-98.
97. DeKelver, R.C., et al., *Attenuation of AML1-ETO cellular dysregulation correlates with increased leukemogenic potential.* Blood, 2013. **121**(18): p. 3714-7.
98. Yan, M., et al., *Deletion of an AML1-ETO C-terminal NcoR/SMRT-interacting region strongly induces leukemia development.* Proc Natl Acad Sci U S A, 2004. **101**(49): p. 17186-91.
99. McLean, T.W., et al., *TEL/AML-1 dimerizes and is associated with a favorable outcome in childhood acute lymphoblastic leukemia.* Blood, 1996. **88**(11): p. 4252-8.
100. Greaves, M., *In utero origins of childhood leukaemia.* Early Hum Dev, 2005. **81**(1): p. 123-9.
101. Andreasson, P., et al., *The expression of ETV6/CBFA2 (TEL/AML1) is not sufficient for the transformation of hematopoietic cell lines in vitro or the induction of hematologic disease in vivo.* Cancer Genet Cytogenet, 2001. **130**(2): p. 93-104.
102. Fischer, M., et al., *Defining the oncogenic function of the TEL/AML1 (ETV6/RUNX1) fusion protein in a mouse model.* Oncogene, 2005. **24**(51): p. 7579-91.
103. Bernardin, F., et al., *TEL-AML1, expressed from t(12;21) in human acute lymphocytic leukemia, induces acute leukemia in mice.* Cancer Res, 2002. **62**(14): p. 3904-8.
104. van der Weyden, L., et al., *Modeling the evolution of ETV6-RUNX1-induced B-cell precursor acute lymphoblastic leukemia in mice.* Blood, 2011. **118**(4): p. 1041-51.
105. Romana, S.P., et al., *The t(12;21) of acute lymphoblastic leukemia results in a tel-AML1 gene fusion.* Blood, 1995. **85**(12): p. 3662-70.
106. Raynaud, S., et al., *The 12;21 translocation involving TEL and deletion of the other TEL allele: two frequently associated alterations found in childhood acute lymphoblastic leukemia.* Blood, 1996. **87**(7): p. 2891-9.
107. Kim, D.H., et al., *TEL-AML1 translocations with TEL and CDKN2 inactivation in acute lymphoblastic leukemia cell lines.* Blood, 1996. **88**(3): p. 785-94.
108. Poirel, H., et al., *Analysis of TEL proteins in human leukemias.* Oncogene, 1998. **16**(22): p. 2895-903.
109. Gunji, H., et al., *TEL/AML1 shows dominant-negative effects over TEL as well as AML1.* Biochem Biophys Res Commun, 2004. **322**(2): p. 623-30.
110. Fenrick, R., et al., *Both TEL and AML-1 contribute repression domains to the t(12;21) fusion protein.* Mol Cell Biol, 1999. **19**(10): p. 6566-74.
111. Guidez, F., et al., *Recruitment of the nuclear receptor corepressor N-CoR by the TEL moiety of the childhood leukemia-associated TEL-AML1 oncoprotein.* Blood, 2000. **96**(7): p. 2557-61.
112. Morrow, M., et al., *TEL-AML1 preleukemic activity requires the DNA binding domain of AML1 and the dimerization and corepressor binding domains of TEL.* Oncogene, 2007. **26**(30): p. 4404-14.

113. Chakrabarti, S.R., et al., *Posttranslational modification of TEL and TEL/AML1 by SUMO-1 and cell-cycle-dependent assembly into nuclear bodies.* Proc Natl Acad Sci U S A, 2000. **97**(24): p. 13281-5.
114. Wood, L.D., et al., *Small ubiquitin-like modifier conjugation regulates nuclear export of TEL, a putative tumor suppressor.* Proc Natl Acad Sci U S A, 2003. **100**(6): p. 3257-62.
115. Roukens, M.G., et al., *Identification of a new site of sumoylation on Tel (ETV6) uncovers a PIAS-dependent mode of regulating Tel function.* Mol Cell Biol, 2008. **28**(7): p. 2342-57.
116. Hay, R.T., *SUMO: a history of modification.* Mol Cell, 2005. **18**(1): p. 1-12.
117. Elmore, S., *Apoptosis: a review of programmed cell death.* Toxicol Pathol, 2007. **35**(4): p. 495-516.
118. Riedl, S.J. and Y. Shi, *Molecular mechanisms of caspase regulation during apoptosis.* Nat Rev Mol Cell Biol, 2004. **5**(11): p. 897-907.
119. Jiang, X. and X. Wang, *Cytochrome c promotes caspase-9 activation by inducing nucleotide binding to Apaf-1.* J Biol Chem, 2000. **275**(40): p. 31199-203.
120. Bratton, S.B. and G.S. Salvesen, *Regulation of the Apaf-1-caspase-9 apoptosome.* J Cell Sci, 2010. **123**(Pt 19): p. 3209-14.
121. Waring, P. and A. Mullbacher, *Cell death induced by the Fas/Fas ligand pathway and its role in pathology.* Immunol Cell Biol, 1999. **77**(4): p. 312-7.
122. Micheau, O. and J. Tschopp, *Induction of TNF receptor I-mediated apoptosis via two sequential signaling complexes.* Cell, 2003. **114**(2): p. 181-90.
123. Hayflick, L. and P.S. Moorhead, *The serial cultivation of human diploid cell strains.* Exp Cell Res, 1961. **25**: p. 585-621.
124. Chen, Q.M., et al., *Involvement of Rb family proteins, focal adhesion proteins and protein synthesis in senescent morphogenesis induced by hydrogen peroxide.* J Cell Sci, 2000. **113 (Pt 22)**: p. 4087-97.
125. Dimri, G.P., et al., *A biomarker that identifies senescent human cells in culture and in aging skin in vivo.* Proc Natl Acad Sci U S A, 1995. **92**(20): p. 9363-7.
126. Shay, J.W., O.M. Pereira-Smith, and W.E. Wright, *A role for both RB and p53 in the regulation of human cellular senescence.* Exp Cell Res, 1991. **196**(1): p. 33-9.
127. Coppe, J.P., et al., *Senescence-associated secretory phenotypes reveal cell-nonautonomous functions of oncogenic RAS and the p53 tumor suppressor.* PLoS Biol, 2008. **6**(12): p. 2853-68.
128. Levy, M.Z., et al., *Telomere end-replication problem and cell aging.* J Mol Biol, 1992. **225**(4): p. 951-60.
129. Rossiello, F., et al., *Irreparable telomeric DNA damage and persistent DDR signalling as a shared causative mechanism of cellular senescence and ageing.* Curr Opin Genet Dev, 2014. **26**: p. 89-95.
130. Serrano, M., et al., *Oncogenic ras provokes premature cell senescence associated with accumulation of p53 and p16INK4a.* Cell, 1997. **88**(5): p. 593-602.
131. Braig, M., et al., *Oncogene-induced senescence as an initial barrier in lymphoma development.* Nature, 2005. **436**(7051): p. 660-5.
132. Chen, Z., et al., *Crucial role of p53-dependent cellular senescence in suppression of Pten-deficient tumorigenesis.* Nature, 2005. **436**(7051): p. 725-30.

133. Collado, M., et al., *Tumour biology: senescence in premalignant tumours.* Nature, 2005. **436**(7051): p. 642.
134. Michaloglou, C., et al., *BRAFE600-associated senescence-like cell cycle arrest of human naevi.* Nature, 2005. **436**(7051): p. 720-4.
135. Courtois-Cox, S., et al., *A negative feedback signaling network underlies oncogene-induced senescence.* Cancer Cell, 2006. **10**(6): p. 459-72.
136. Dankort, D., et al., *A new mouse model to explore the initiation, progression, and therapy of BRAFV600E-induced lung tumors.* Genes Dev, 2007. **21**(4): p. 379-84.
137. Sarkisian, C.J., et al., *Dose-dependent oncogene-induced senescence in vivo and its evasion during mammary tumorigenesis.* Nat Cell Biol, 2007. **9**(5): p. 493-505.
138. d'Adda di Fagagna, F., *Living on a break: cellular senescence as a DNA-damage response.* Nat Rev Cancer, 2008. **8**(7): p. 512-22.
139. Rodier, F. and J. Campisi, *Four faces of cellular senescence.* J Cell Biol, 2011. **192**(4): p. 547-56.
140. Zhu, J., et al., *Senescence of human fibroblasts induced by oncogenic Raf.* Genes Dev, 1998. **12**(19): p. 2997-3007.
141. Kato, D., et al., *Features of replicative senescence induced by direct addition of antennapedia-p16INK4A fusion protein to human diploid fibroblasts.* FEBS Lett, 1998. **427**(2): p. 203-8.
142. Ogryzko, V.V., et al., *Human fibroblast commitment to a senescence-like state in response to histone deacetylase inhibitors is cell cycle dependent.* Mol Cell Biol, 1996. **16**(9): p. 5210-8.
143. Beausejour, C.M., et al., *Reversal of human cellular senescence: roles of the p53 and p16 pathways.* EMBO J, 2003. **22**(16): p. 4212-22.
144. Dirac, A.M. and R. Bernards, *Reversal of senescence in mouse fibroblasts through lentiviral suppression of p53.* J Biol Chem, 2003. **278**(14): p. 11731-4.
145. Kuilman, T., et al., *Oncogene-induced senescence relayed by an interleukin-dependent inflammatory network.* Cell, 2008. **133**(6): p. 1019-31.
146. Lee, B.Y., et al., *Senescence-associated beta-galactosidase is lysosomal beta-galactosidase.* Aging Cell, 2006. **5**(2): p. 187-95.
147. Hirama, T. and H.P. Koeffler, *Role of the cyclin-dependent kinase inhibitors in the development of cancer.* Blood, 1995. **86**(3): p. 841-54.
148. Lane, D.P., *Cancer. p53, guardian of the genome.* Nature, 1992. **358**(6381): p. 15-6.
149. Maltzman, W. and L. Czyzyk, *UV irradiation stimulates levels of p53 cellular tumor antigen in nontransformed mouse cells.* Mol Cell Biol, 1984. **4**(9): p. 1689-94.
150. Momand, J., et al., *The mdm-2 oncogene product forms a complex with the p53 protein and inhibits p53-mediated transactivation.* Cell, 1992. **69**(7): p. 1237-45.
151. Oliner, J.D., et al., *Oncoprotein MDM2 conceals the activation domain of tumour suppressor p53.* Nature, 1993. **362**(6423): p. 857-60.
152. Thut, C.J., J.A. Goodrich, and R. Tjian, *Repression of p53-mediated transcription by MDM2: a dual mechanism.* Genes Dev, 1997. **11**(15): p. 1974-86.
153. Giaccia, A.J. and M.B. Kastan, *The complexity of p53 modulation: emerging patterns from divergent signals.* Genes Dev, 1998. **12**(19): p. 2973-83.

154. Agarwal, M.L., et al., *p53 controls both the G2/M and the G1 cell cycle checkpoints and mediates reversible growth arrest in human fibroblasts.* Proc Natl Acad Sci U S A, 1995. **92**(18): p. 8493-7.
155. Meek, D.W., *The p53 response to DNA damage.* DNA Repair (Amst), 2004. **3**(8-9): p. 1049-56.
156. Gartel, A.L. and S.K. Radhakrishnan, *Lost in transcription: p21 repression, mechanisms, and consequences.* Cancer Res, 2005. **65**(10): p. 3980-5.
157. Rayess, H., M.B. Wang, and E.S. Srivatsan, *Cellular senescence and tumor suppressor gene p16.* Int J Cancer, 2012. **130**(8): p. 1715-25.
158. Krimpenfort, P., et al., *Loss of p16Ink4a confers susceptibility to metastatic melanoma in mice.* Nature, 2001. **413**(6851): p. 83-6.
159. Dannenberg, J.H., et al., *Ablation of the retinoblastoma gene family deregulates G(1) control causing immortalization and increased cell turnover under growth-restricting conditions.* Genes Dev, 2000. **14**(23): p. 3051-64.
160. Sage, J., et al., *Targeted disruption of the three Rb-related genes leads to loss of G(1) control and immortalization.* Genes Dev, 2000. **14**(23): p. 3037-50.
161. Itahana, K., J. Campisi, and G.P. Dimri, *Mechanisms of cellular senescence in human and mouse cells.* Biogerontology, 2004. **5**(1): p. 1-10.
162. Rogakou, E.P., et al., *Megabase chromatin domains involved in DNA double-strand breaks in vivo.* J Cell Biol, 1999. **146**(5): p. 905-16.
163. Huang, X., H.D. Halicka, and Z. Darzynkiewicz, *Detection of histone H2AX phosphorylation on Ser-139 as an indicator of DNA damage (DNA double-strand breaks).* Curr Protoc Cytom, 2004. **Chapter 7**: p. Unit 7 27.
164. Canman, C.E., *Activation of the ATM Kinase by Ionizing Radiation and Phosphorylation of p53.* Science, 1998. **281**(5383): p. 1677-1679.
165. Canman, C.E. and D.S. Lim, *The role of ATM in DNA damage responses and cancer.* Oncogene, 1998. **17**(25): p. 3301-8.
166. Ogrunc, M., et al., *Oncogene-induced reactive oxygen species fuel hyperproliferation and DNA damage response activation.* Cell Death Differ, 2014. **21**(6): p. 998-1012.
167. Sheu, J.J., et al., *Mutant BRAF induces DNA strand breaks, activates DNA damage response pathway, and up-regulates glucose transporter-1 in nontransformed epithelial cells.* Am J Pathol, 2012. **180**(3): p. 1179-88.
168. Liang, Y., et al., *DNA damage response pathways in tumor suppression and cancer treatment.* World J Surg, 2009. **33**(4): p. 661-6.
169. Di Micco, R., et al., *Oncogene-induced senescence is a DNA damage response triggered by DNA hyper-replication.* Nature, 2006. **444**(7119): p. 638-42.
170. Bartkova, J., et al., *DNA damage response as a candidate anti-cancer barrier in early human tumorigenesis.* Nature, 2005. **434**(7035): p. 864-70.
171. Bertwistle, D. and A. Ashworth, *BRCA1 and BRCA2.* Curr Biol, 2000. **10**(16): p. R582.
172. Jacinto, F.V. and M. Esteller, *Mutator pathways unleashed by epigenetic silencing in human cancer.* Mutagenesis, 2007. **22**(4): p. 247-53.
173. Holmstrom, K.M. and T. Finkel, *Cellular mechanisms and physiological consequences of redox-dependent signalling.* Nat Rev Mol Cell Biol, 2014. **15**(6): p. 411-21.
174. Murphy, M.P., *How mitochondria produce reactive oxygen species.* Biochem J, 2009. **417**(1): p. 1-13.

175. Truong, T.H. and K.S. Carroll, *Redox regulation of epidermal growth factor receptor signaling through cysteine oxidation.* Biochemistry, 2012. **51**(50): p. 9954-65.
176. Aguirre, J. and J.D. Lambeth, *Nox enzymes from fungus to fly to fish and what they tell us about Nox function in mammals.* Free Radic Biol Med, 2010. **49**(9): p. 1342-53.
177. Hampton, M.B., A.J. Kettle, and C.C. Winterbourn, *Inside the neutrophil phagosome: oxidants, myeloperoxidase, and bacterial killing.* Blood, 1998. **92**(9): p. 3007-17.
178. Hempel, S.L., et al., *Dihydrofluorescein diacetate is superior for detecting intracellular oxidants: comparison with 2',7'-dichlorodihydrofluorescein diacetate, 5(and 6)-carboxy-2',7'-dichlorodihydrofluorescein diacetate, and dihydrorhodamine 123.* Free Radic Biol Med, 1999. **27**(1-2): p. 146-59.
179. Belousov, V.V., et al., *Genetically encoded fluorescent indicator for intracellular hydrogen peroxide.* Nat Methods, 2006. **3**(4): p. 281-6.
180. Murphy, M.P., et al., *Unraveling the biological roles of reactive oxygen species.* Cell Metab, 2011. **13**(4): p. 361-6.
181. Colavitti, R. and T. Finkel, *Reactive oxygen species as mediators of cellular senescence.* IUBMB Life, 2005. **57**(4-5): p. 277-81.
182. Wright, W.E. and J.W. Shay, *Telomere dynamics in cancer progression and prevention: fundamental differences in human and mouse telomere biology.* Nat Med, 2000. **6**(8): p. 849-51.
183. Parrinello, S., et al., *Oxygen sensitivity severely limits the replicative lifespan of murine fibroblasts.* Nat Cell Biol, 2003. **5**(8): p. 741-7.
184. Takahashi, A., et al., *Mitogenic signalling and the p16INK4a-Rb pathway cooperate to enforce irreversible cellular senescence.* Nat Cell Biol, 2006. **8**(11): p. 1291-7.
185. Freund, A., C.K. Patil, and J. Campisi, *p38MAPK is a novel DNA damage response-independent regulator of the senescence-associated secretory phenotype.* EMBO J, 2011. **30**(8): p. 1536-48.
186. Wang, P., et al., *Protein kinase D1 is essential for Ras-induced senescence and tumor suppression by regulating senescence-associated inflammation.* Proc Natl Acad Sci U S A, 2014. **111**(21): p. 7683-8.
187. Coulthard, L.R., et al., *p38(MAPK): stress responses from molecular mechanisms to therapeutics.* Trends Mol Med, 2009. **15**(8): p. 369-79.
188. Ito, K., et al., *Reactive oxygen species act through p38 MAPK to limit the lifespan of hematopoietic stem cells.* Nat Med, 2006. **12**(4): p. 446-51.
189. Harada, G., et al., *Molecular mechanisms for the p38-induced cellular senescence in normal human fibroblast.* J Biochem, 2014. **156**(5): p. 283-90.
190. Usatyuk, P.V., et al., *Redox regulation of reactive oxygen species-induced p38 MAP kinase activation and barrier dysfunction in lung microvascular endothelial cells.* Antioxid Redox Signal, 2003. **5**(6): p. 723-30.
191. Sato, A., et al., *Pivotal role for ROS activation of p38 MAPK in the control of differentiation and tumor-initiating capacity of glioma-initiating cells.* Stem Cell Res, 2014. **12**(1): p. 119-31.
192. Lee, M.W., et al., *The involvement of reactive oxygen species (ROS) and p38 mitogen-activated protein (MAP) kinase in TRAIL/Apo2L-induced apoptosis.* FEBS Lett, 2002. **512**(1-3): p. 313-8.
193. Chen, C.L., et al., *Ceramide induces p38 MAPK and JNK activation through a mechanism involving a thioredoxin-interacting protein-mediated pathway.* Blood, 2008. **111**(8): p. 4365-74.

194. Fujino, G., et al., *Thioredoxin and TRAF family proteins regulate reactive oxygen species-dependent activation of ASK1 through reciprocal modulation of the N-terminal homophilic interaction of ASK1.* Mol Cell Biol, 2007. **27**(23): p. 8152-63.
195. Kamata, H., et al., *Reactive oxygen species promote TNFalpha-induced death and sustained JNK activation by inhibiting MAP kinase phosphatases.* Cell, 2005. **120**(5): p. 649-61.
196. Raman, M., et al., *TAO kinases mediate activation of p38 in response to DNA damage.* EMBO J, 2007. **26**(8): p. 2005-14.
197. Borodkina, A., et al., *Interaction between ROS dependent DNA damage, mitochondria and p38 MAPK underlies senescence of human adult stem cells.* Aging (Albany NY), 2014. **6**(6): p. 481-95.
198. Wang, W., et al., *Sequential activation of the MEK-extracellular signal-regulated kinase and MKK3/6-p38 mitogen-activated protein kinase pathways mediates oncogenic ras-induced premature senescence.* Mol Cell Biol, 2002. **22**(10): p. 3389-403.
199. Xu, Y., et al., *Emerging roles of the p38 MAPK and PI3K/AKT/mTOR pathways in oncogene-induced senescence.* Trends Biochem Sci, 2014. **39**(6): p. 268-76.
200. Bulavin, D.V., et al., *Inactivation of the Wip1 phosphatase inhibits mammary tumorigenesis through p38 MAPK-mediated activation of the p16(Ink4a)-p19(Arf) pathway.* Nat Genet, 2004. **36**(4): p. 343-50.
201. Bulavin, D.V., et al., *Phosphorylation of human p53 by p38 kinase coordinates N-terminal phosphorylation and apoptosis in response to UV radiation.* EMBO J, 1999. **18**(23): p. 6845-54.
202. Fujikawa, M., et al., *ESE-3, an Ets family transcription factor, is up-regulated in cellular senescence.* Cancer Sci, 2007. **98**(9): p. 1468-75.
203. Krishnamurthy, J., et al., *Ink4a/Arf expression is a biomarker of aging.* J Clin Invest, 2004. **114**(9): p. 1299-307.
204. Naka, K., et al., *Stress-induced premature senescence in hTERT-expressing ataxia telangiectasia fibroblasts.* J Biol Chem, 2004. **279**(3): p. 2030-7.
205. Coppe, J.P., et al., *The senescence-associated secretory phenotype: the dark side of tumor suppression.* Annu Rev Pathol, 2010. **5**: p. 99-118.
206. Acosta, J.C., et al., *A complex secretory program orchestrated by the inflammasome controls paracrine senescence.* Nat Cell Biol, 2013. **15**(8): p. 978-90.
207. Das, G., B.V. Shravage, and E.H. Baehrecke, *Regulation and function of autophagy during cell survival and cell death.* Cold Spring Harb Perspect Biol, 2012. **4**(6).
208. Narita, M., A.R. Young, and M. Narita, *Autophagy facilitates oncogene-induced senescence.* Autophagy, 2009. **5**(7): p. 1046-7.
209. Krtolica, A., et al., *Senescent fibroblasts promote epithelial cell growth and tumorigenesis: a link between cancer and aging.* Proc Natl Acad Sci U S A, 2001. **98**(21): p. 12072-7.
210. Rodier, F., et al., *Persistent DNA damage signalling triggers senescence-associated inflammatory cytokine secretion.* Nat Cell Biol, 2009. **11**(8): p. 973-9.
211. Acosta, J.C., et al., *Chemokine signaling via the CXCR2 receptor reinforces senescence.* Cell, 2008. **133**(6): p. 1006-18.

212. Chien, Y., et al., *Control of the senescence-associated secretory phenotype by NF-kappaB promotes senescence and enhances chemosensitivity.* Genes Dev, 2011. **25**(20): p. 2125-36.
213. Crescenzi, E., et al., *NF-kappaB-dependent cytokine secretion controls Fas expression on chemotherapy-induced premature senescent tumor cells.* Oncogene, 2011. **30**(24): p. 2707-17.
214. Rovillain, E., et al., *Activation of nuclear factor-kappa B signalling promotes cellular senescence.* Oncogene, 2011. **30**(20): p. 2356-66.
215. Lawrence, T., *The nuclear factor NF-kappaB pathway in inflammation.* Cold Spring Harb Perspect Biol, 2009. **1**(6): p. a001651.
216. Storz, P. and A. Toker, *Protein kinase D mediates a stress-induced NF-kappaB activation and survival pathway.* EMBO J, 2003. **22**(1): p. 109-20.
217. Vermeulen, L., et al., *Transcriptional activation of the NF-kappaB p65 subunit by mitogen- and stress-activated protein kinase-1 (MSK1).* EMBO J, 2003. **22**(6): p. 1313-24.
218. Saccani, S., S. Pantano, and G. Natoli, *p38-Dependent marking of inflammatory genes for increased NF-kappa B recruitment.* Nat Immunol, 2002. **3**(1): p. 69-75.
219. Burd, C.E., et al., *Monitoring tumorigenesis and senescence in vivo with a p16(INK4a)-luciferase model.* Cell, 2013. **152**(1-2): p. 340-51.
220. Xue, W., et al., *Senescence and tumour clearance is triggered by p53 restoration in murine liver carcinomas.* Nature, 2007. **445**(7128): p. 656-60.
221. Baker, D.J., et al., *Naturally occurring p16(Ink4a)-positive cells shorten healthy lifespan.* Nature, 2016. **530**(7589): p. 184-9.
222. Chang, J., et al., *Clearance of senescent cells by ABT263 rejuvenates aged hematopoietic stem cells in mice.* Nat Med, 2016. **22**(1): p. 78-83.
223. Davalos, A.R., et al., *Senescent cells as a source of inflammatory factors for tumor progression.* Cancer Metastasis Rev, 2010. **29**(2): p. 273-83.
224. Kilbey, A., et al., *Runx2 disruption promotes immortalization and confers resistance to oncogene-induced senescence in primary murine fibroblasts.* Cancer Res, 2007. **67**(23): p. 11263-71.
225. Wajapeyee, N., et al., *Senescence induction in human fibroblasts and hematopoietic progenitors by leukemogenic fusion proteins.* Blood, 2010. **115**(24): p. 5057-60.
226. Astle, M.V., et al., *AKT induces senescence in human cells via mTORC1 and p53 in the absence of DNA damage: implications for targeting mTOR during malignancy.* Oncogene, 2012. **31**(15): p. 1949-62.
227. Rubnitz, J.E., et al., *Characteristics and outcome of t(8;21)-positive childhood acute myeloid leukemia: a single institution's experience.* Leukemia, 2002. **16**(10): p. 2072-7.
228. Viale, A., et al., *Cell-cycle restriction limits DNA damage and maintains self-renewal of leukaemia stem cells.* Nature, 2009. **457**(7225): p. 51-6.
229. Ford, A.M., et al., *The TEL-AML1 leukemia fusion gene dysregulates the TGF-beta pathway in early B lineage progenitor cells.* J Clin Invest, 2009. **119**(4): p. 826-36.
230. Wotton, S.F., et al., *RUNX1 transformation of primary embryonic fibroblasts is revealed in the absence of p53.* Oncogene, 2004. **23**(32): p. 5476-86.
231. Todaro, G.J. and H. Green, *Quantitative studies of the growth of mouse embryo cells in culture and their development into established lines.* J Cell Biol, 1963. **17**: p. 299-313.

232. Morgenstern, J.P. and H. Land, *A series of mammalian expression vectors and characterisation of their expression of a reporter gene in stably and transiently transfected cells.* Nucleic Acids Res, 1990. **18**(4): p. 1068.
233. Erickson, P., et al., *Identification of breakpoints in t(8;21) acute myelogenous leukemia and isolation of a fusion transcript, AML1/ETO, with similarity to Drosophila segmentation gene, runt.* Blood, 1992. **80**(7): p. 1825-31.
234. Brookes, S., et al., *INK4a-deficient human diploid fibroblasts are resistant to RAS-induced senescence.* EMBO J, 2002. **21**(12): p. 2936-45.
235. Kim, S.J. and P.K. Wong, *ROS upregulation during the early phase of retroviral infection plays an important role in viral establishment in the host cell.* J Gen Virol, 2013. **94**(Pt 10): p. 2309-17.
236. Larue, R.S., et al., *Lentiviral Vif degrades the APOBEC3Z3/APOBEC3H protein of its mammalian host and is capable of cross-species activity.* J Virol, 2010. **84**(16): p. 8193-201.
237. Zhang, F., et al., *Lentiviral vectors containing an enhancer-less ubiquitously acting chromatin opening element (UCOE) provide highly reproducible and stable transgene expression in hematopoietic cells.* Blood, 2007. **110**(5): p. 1448-57.
238. Boehm, J.S., et al., *Transformation of human and murine fibroblasts without viral oncoproteins.* Mol Cell Biol, 2005. **25**(15): p. 6464-74.
239. Lee, A.C., et al., *Ras proteins induce senescence by altering the intracellular levels of reactive oxygen species.* J Biol Chem, 1999. **274**(12): p. 7936-40.
240. Saitoh, M., et al., *Mammalian thioredoxin is a direct inhibitor of apoptosis signal-regulating kinase (ASK) 1.* EMBO J, 1998. **17**(9): p. 2596-606.
241. Pan, J.-S., *Reactive oxygen species: A double-edged sword in oncogenesis.* World Journal of Gastroenterology, 2009. **15**(14): p. 1702.
242. Jenkins, N.C., et al., *The p16(INK4A) tumor suppressor regulates cellular oxidative stress.* Oncogene, 2011. **30**(3): p. 265-74.
243. Cuenda, A. and S. Rousseau, *p38 MAP-kinases pathway regulation, function and role in human diseases.* Biochim Biophys Acta, 2007. **1773**(8): p. 1358-75.
244. Lin, A.W., et al., *Premature senescence involving p53 and p16 is activated in response to constitutive MEK/MAPK mitogenic signaling.* Genes Dev, 1998. **12**(19): p. 3008-19.
245. Liu, Y., et al., *The tetramer structure of the Nervy homology two domain, NHR2, is critical for AML1/ETO's activity.* Cancer Cell, 2006. **9**(4): p. 249-60.
246. Lowe, S.W., E. Cepero, and G. Evan, *Intrinsic tumour suppression.* Nature, 2004. **432**(7015): p. 307-15.
247. Hackanson, B., et al., *NHR4 domain mutations of ETO are probably very infrequent in AML1-ETO positive myeloid leukemia cells.* Leukemia, 2010. **24**(4): p. 860-1.
248. Salminen, A., A. Kauppinen, and K. Kaarniranta, *Emerging role of NF-kappaB signaling in the induction of senescence-associated secretory phenotype (SASP).* Cell Signal, 2012. **24**(4): p. 835-45.
249. Sagiv, A. and V. Krizhanovsky, *Immunosurveillance of senescent cells: the bright side of the senescence program.* Biogerontology, 2013. **14**(6): p. 617-28.
250. Fumagalli, M. and F. d'Adda di Fagagna, *SASPense and DDRama in cancer and ageing.* Nat Cell Biol, 2009. **11**(8): p. 921-3.

251. Coppe, J.P., et al., *Tumor suppressor and aging biomarker p16(INK4a) induces cellular senescence without the associated inflammatory secretory phenotype.* J Biol Chem, 2011. **286**(42): p. 36396-403.
252. Patil, C., et al., *p38 MAPK regulates IL-1beta induced IL-6 expression through mRNA stability in osteoblasts.* Immunol Invest, 2004. **33**(2): p. 213-33.
253. Libermann, T.A. and D. Baltimore, *Activation of interleukin-6 gene expression through the NF-kappa B transcription factor.* Mol Cell Biol, 1990. **10**(5): p. 2327-34.
254. Duan, W.J., et al., *Silibinin activated ROS-p38-NF-kappaB positive feedback and induced autophagic death in human fibrosarcoma HT1080 cells.* J Asian Nat Prod Res, 2011. **13**(1): p. 27-35.
255. Nakagawa, M., et al., *AML1/RUNX1 functions as a cytoplasmic attenuator of NF-kappaB signaling in the repression of myeloid tumors.* Blood, 2011. **118**(25): p. 6626-37.
256. Ghisletti, S., et al., *Cooperative NCoR/SMRT interactions establish a corepressor-based strategy for integration of inflammatory and anti-inflammatory signaling pathways.* Genes Dev, 2009. **23**(6): p. 681-93.
257. Wang, X., F. Luo, and H. Zhao, *Paraquat-induced reactive oxygen species inhibit neutrophil apoptosis via a p38 MAPK/NF-kappaB-IL-6/TNF-alpha positive-feedback circuit.* PLoS One, 2014. **9**(4): p. e93837.
258. Guo, Y., et al., *Interleukin-6 signaling pathway in targeted therapy for cancer.* Cancer Treat Rev, 2012. **38**(7): p. 904-10.
259. Maggio, M., et al., *Interleukin-6 in aging and chronic disease: a magnificent pathway.* J Gerontol A Biol Sci Med Sci, 2006. **61**(6): p. 575-84.
260. Golub, T.R., et al., *Fusion of the TEL gene on 12p13 to the AML1 gene on 21q22 in acute lymphoblastic leukemia.* Proc Natl Acad Sci U S A, 1995. **92**(11): p. 4917-21.
261. Romana, S.P., M. Le Coniat, and R. Berger, *t(12;21): a new recurrent translocation in acute lymphoblastic leukemia.* Genes Chromosomes Cancer, 1994. **9**(3): p. 186-91.
262. Lee, Y.J., et al., *Mechanism of transcriptional repression by TEL/RUNX1 fusion protein.* Mol Cells, 2004. **17**(2): p. 217-22.
263. Morrow, M., et al., *TEL-AML1 promotes development of specific hematopoietic lineages consistent with preleukemic activity.* Blood, 2004. **103**(10): p. 3890-6.
264. Holden, P. and W.A. Horton, *Crude subcellular fractionation of cultured mammalian cell lines.* BMC Res Notes, 2009. **2**: p. 243.
265. Ho, S.C., et al., *Membrane anchoring of calnexin facilitates its interaction with its targets.* Mol Immunol, 1999. **36**(1): p. 1-12.
266. Wang, Y. and M. Dasso, *SUMOylation and deSUMOylation at a glance.* J Cell Sci, 2009. **122**(Pt 23): p. 4249-52.
267. Gareau, J.R. and C.D. Lima, *The SUMO pathway: emerging mechanisms that shape specificity, conjugation and recognition.* Nat Rev Mol Cell Biol, 2010. **11**(12): p. 861-71.
268. Drexler, H.G., *Review of alterations of the cyclin-dependent kinase inhibitor INK4 family genes p15, p16, p18 and p19 in human leukemia-lymphoma cells.* Leukemia, 1998. **12**(6): p. 845-59.
269. Streubel, B., et al., *Amplification of the AML1(CBFA2) gene on ring chromosomes in a patient with acute myeloid leukemia and a constitutional ring chromosome 21.* Cancer Genet Cytogenet, 2001. **124**(1): p. 42-6.

270. Mikhail, F.M., et al., *AML1 gene over-expression in childhood acute lymphoblastic leukemia.* Leukemia, 2002. **16**(4): p. 658-68.
271. Robinson, H.M., et al., *Amplification of AML1 in acute lymphoblastic leukemia is associated with a poor outcome.* Leukemia, 2003. **17**(11): p. 2249-50.
272. Harewood, L., et al., *Amplification of AML1 on a duplicated chromosome 21 in acute lymphoblastic leukemia: a study of 20 cases.* Leukemia, 2003. **17**(3): p. 547-53.
273. Kirschnerova, G., A. Tothova, and O. Babusikova, *Amplification of AML1 gene in association with karyotype, age and diagnosis in acute leukemia patients.* Neoplasma, 2006. **53**(2): p. 150-4.
274. Reichard, K.K., H. Kang, and S. Robinett, *Pediatric B-lymphoblastic leukemia with RUNX1 amplification: clinicopathologic study of eight cases.* Mod Pathol, 2011. **24**(12): p. 1606-11.
275. Tsuzuki, S., et al., *Modeling first-hit functions of the t(12;21) TEL-AML1 translocation in mice.* Proc Natl Acad Sci U S A, 2004. **101**(22): p. 8443-8.
276. Lausten-Thomsen, U., et al., *Prevalence of t(12;21)[ETV6-RUNX1]-positive cells in healthy neonates.* Blood, 2011. **117**(1): p. 186-9.
277. Mori, H., et al., *Chromosome translocations and covert leukemic clones are generated during normal fetal development.* Proc Natl Acad Sci U S A, 2002. **99**(12): p. 8242-7.
278. Nakamura, Y., et al., *TEL/ETV6 binds to corepressor KAP1 via the HLH domain.* Int J Hematol, 2006. **84**(4): p. 377-80.
279. Chakrabarti, S.R. and G. Nucifora, *The leukemia-associated gene TEL encodes a transcription repressor which associates with SMRT and mSin3A.* Biochem Biophys Res Commun, 1999. **264**(3): p. 871-7.
280. Wang, L. and S.W. Hiebert, *TEL contacts multiple co-repressors and specifically associates with histone deacetylase-3.* Oncogene, 2001. **20**(28): p. 3716-25.
281. Niini, T., et al., *AML1 gene amplification: a novel finding in childhood acute lymphoblastic leukemia.* Haematologica, 2000. **85**(4): p. 362-6.
282. Taniguchi, T., et al., *Expression of p16INK4A and p14ARF in hematological malignancies.* Leukemia, 1999. **13**(11): p. 1760-9.
283. Blagosklonny, M.V., *Cell cycle arrest is not senescence.* Aging (Albany NY), 2011. **3**(2): p. 94-101.
284. Bartkova, J., et al., *Oncogene-induced senescence is part of the tumorigenesis barrier imposed by DNA damage checkpoints.* Nature, 2006. **444**(7119): p. 633-7.
285. Courtois-Cox, S., S.L. Jones, and K. Cichowski, *Many roads lead to oncogene-induced senescence.* Oncogene, 2008. **27**(20): p. 2801-9.
286. Mantovani, A., et al., *Cancer-related inflammation.* Nature, 2008. **454**(7203): p. 436-44.
287. Blyth, K., et al., *Runx2 and MYC collaborate in lymphoma development by suppressing apoptotic and growth arrest pathways in vivo.* Cancer Res, 2006. **66**(4): p. 2195-201.
288. Brady, G., et al., *Downregulation of RUNX1 by RUNX3 requires the RUNX3 VWRPY sequence and is essential for Epstein-Barr virus-driven B-cell proliferation.* J Virol, 2009. **83**(13): p. 6909-16.
289. Williams, G.C., *Pleiotropy, Natural Selection, and the Evolution of Senescence.* Evolution, 1957. **11**(4): p. 398-411.

290. Hole, P.S., et al., *Overproduction of NOX-derived ROS in AML promotes proliferation and is associated with defective oxidative stress signaling.* Blood, 2013. **122**(19): p. 3322-30.
291. Kantner, H.P., et al., *ETV6/RUNX1 induces reactive oxygen species and drives the accumulation of DNA damage in B cells.* Neoplasia, 2013. **15**(11): p. 1292-300.
292. Ben-Ami, O., et al., *Addiction of t(8;21) and inv(16) acute myeloid leukemia to native RUNX1.* Cell Rep, 2013. **4**(6): p. 1131-43.
293. Pourdehnad, M., et al., *Myc and mTOR converge on a common node in protein synthesis control that confers synthetic lethality in Myc-driven cancers.* Proc Natl Acad Sci U S A, 2013. **110**(29): p. 11988-93.
294. Zhu, J., J. Blenis, and J. Yuan, *Activation of PI3K/Akt and MAPK pathways regulates Myc-mediated transcription by phosphorylating and promoting the degradation of Mad1.* Proc Natl Acad Sci U S A, 2008. **105**(18): p. 6584-9.
295. Niini, T., et al., *Expression of myeloid-specific genes in childhood acute lymphoblastic leukemia - a cDNA array study.* Leukemia, 2002. **16**(11): p. 2213-21.
296. Andersen, M.K., D.H. Christiansen, and J. Pedersen-Bjergaard, *Amplification or duplication of chromosome band 21q22 with multiple copies of the AML1 gene and mutation of the TP53 gene in therapy-related MDS and AML.* Leukemia, 2005. **19**(2): p. 197-200.
297. Shimizu, K., et al., *Roles of AML1/RUNX1 in T-cell malignancy induced by loss of p53.* Cancer Sci, 2013. **104**(8): p. 1033-8.
298. Borland, G., et al., *Addiction to Runx1 is partially attenuated by loss of p53 in the Emicro-Myc lymphoma model.* Oncotarget, 2016.
299. Sykes, S.M., et al., *AKT/FOXO signaling enforces reversible differentiation blockade in myeloid leukemias.* Cell, 2011. **146**(5): p. 697-708.
300. Ito, K., et al., *PML targeting eradicates quiescent leukaemia-initiating cells.* Nature, 2008. **453**(7198): p. 1072-8.
301. Goyama, S., et al., *Transcription factor RUNX1 promotes survival of acute myeloid leukemia cells.* J Clin Invest, 2013. **123**(9): p. 3876-88.
302. Stengel, A., et al., *TP53 mutations occur in 15.7% of ALL and are associated with MYC-rearrangement, low hypodiploidy, and a poor prognosis.* Blood, 2014. **124**(2): p. 251-8.
303. Chen, B., et al., *Newly diagnosed acute lymphoblastic leukemia in China (I): abnormal genetic patterns in 1346 childhood and adult cases and their comparison with the reports from Western countries.* Leukemia, 2012. **26**(7): p. 1608-16.
304. Mangolini, M., et al., *STAT3 mediates oncogenic addiction to TEL-AML1 in t(12;21) acute lymphoblastic leukemia.* Blood, 2013. **122**(4): p. 542-9.
305. Sulong, S., et al., *A comprehensive analysis of the CDKN2A gene in childhood acute lymphoblastic leukemia reveals genomic deletion, copy number neutral loss of heterozygosity, and association with specific cytogenetic subgroups.* Blood, 2009. **113**(1): p. 100-7.
306. Hiebert, S.W., et al., *The t(12;21) translocation converts AML-1B from an activator to a repressor of transcription.* Mol Cell Biol, 1996. **16**(4): p. 1349-55.
307. Fuka, G., et al., *Silencing of ETV6/RUNX1 abrogates PI3K/AKT/mTOR signaling and impairs reconstitution of leukemia in xenografts.* Leukemia, 2012. **26**(5): p. 927-33.
308. Licht, J.D., *AML1 and the AML1-ETO fusion protein in the pathogenesis of t(8;21) AML.* Oncogene, 2001. **20**(40): p. 5660-79.

309. Angelova, S., et al., *IS THE AMPLIFICATION OF c-MYC, MLL AND RUNX1 GENES IN AML AND MDS PATIENTS WITH TRISOMY 8, 11 AND 21 A FACTOR FOR A CLONAL EVOLUTION IN THEIR KARYOTYPE?* Tsitol Genet, 2015. **49**(3): p. 25-32.
310. Bernardin, F., et al., *c-Myc overcomes cell cycle inhibition by CBFbeta-SMMHC, a myeloid leukemia oncoprotein.* Cancer Biol Ther, 2002. **1**(5): p. 492-6.
311. Wong, I.H., et al., *Aberrant p15 promoter methylation in adult and childhood acute leukemias of nearly all morphologic subtypes: potential prognostic implications.* Blood, 2000. **95**(6): p. 1942-9.
312. Linggi, B., et al., *The t(8;21) fusion protein, AML1 ETO, specifically represses the transcription of the p14(ARF) tumor suppressor in acute myeloid leukemia.* Nat Med, 2002. **8**(7): p. 743-50.
313. Krejci, O., et al., *p53 signaling in response to increased DNA damage sensitizes AML1-ETO cells to stress-induced death.* Blood, 2008. **111**(4): p. 2190-9.
314. Sablina, A.A., et al., *The antioxidant function of the p53 tumor suppressor.* Nat Med, 2005. **11**(12): p. 1306-13.
315. Wiemels, J.L., et al., *In utero origin of t(8;21) AML1-ETO translocations in childhood acute myeloid leukemia.* Blood, 2002. **99**(10): p. 3801-5.
316. Zabkiewicz, J., et al., *The PDK1 master kinase is over-expressed in acute myeloid leukemia and promotes PKC-mediated survival of leukemic blasts.* Haematologica, 2014. **99**(5): p. 858-64.
317. Lo, M.C., et al., *Combined gene expression and DNA occupancy profiling identifies potential therapeutic targets of t(8;21) AML.* Blood, 2012. **120**(7): p. 1473-84.
318. Linka, Y., et al., *The impact of TEL-AML1 (ETV6-RUNX1) expression in precursor B cells and implications for leukaemia using three different genome-wide screening methods.* Blood Cancer J, 2013. **3**: p. e151.
319. Wilkinson, A.C., et al., *RUNX1 is a key target in t(4;11) leukemias that contributes to gene activation through an AF4-MLL complex interaction.* Cell Rep, 2013. **3**(1): p. 116-27.
320. Lilljebjorn, H., et al., *Whole-exome sequencing of pediatric acute lymphoblastic leukemia.* Leukemia, 2012. **26**(7): p. 1602-7.
321. Lilljebjorn, H., et al., *The correlation pattern of acquired copy number changes in 164 ETV6/RUNX1-positive childhood acute lymphoblastic leukemias.* Hum Mol Genet, 2010. **19**(16): p. 3150-8.
322. Nardella, C., et al., *Pro-senescence therapy for cancer treatment.* Nat Rev Cancer, 2011. **11**(7): p. 503-11.